



Budapest University of Technology and Economics

PhD School in Psychology – Cognitive Science

Mariann Füzesiné Hudák

**UNDERSTANDING BASIC VISUAL MECHANISMS THROUGH
VISUAL ILLUSIONS**

PhD Thesis

Supervisor: Dr. Ilona Kovács

Budapest, 2013

‘There is no harm in doubt and skepticism, for it is through these that new discoveries are made.’

(Richard Feynman, Letter to Armando Garcia J, December 11, 1985)

1	Acknowledgements.....	3
2	Abstract.....	4
3	Kivonat.....	4
4	Summary.....	4
5	Összefoglaló.....	5
6	Introduction.....	7
6.1	Looking into the ‘black box’ through illusions - An alternative to physiological studies	7
6.2	Theories of lightness-brightness perception.....	12
6.2.1	The roots.....	12
6.2.2	Lateral inhibition – the classical textbook explanation	14
6.2.3	Recent lateral inhibition-based models	17
6.2.3.1	Filtering and symbolic description.....	17
6.2.3.2	High-pass filtering.....	18
6.2.3.3	Multiple-scale filtering – natural image statistics.....	19
6.2.3.4	Multiple-scale filtering – the oriented DoG model	21
6.2.4	Mid-level theories: Intrinsic image models.....	24
6.2.5	Mid-level theories: Anchoring	30
6.2.5.1	The original anchoring theory	30
6.2.5.2	Double anchoring theory	37
6.2.6	A low-level alternative: activation spreading alias filling-in	40
6.2.7	Filling-in brightness modelling vs. anchoring: not mutually excluding concepts.....	55

6.3	Chromatic illusions – the potential application of a good brightness model to chromatic stimuli	58
6.4	Dynamic illusions	62
6.4.1	Dynamic illusions elicited by static images: where filling-in gets confused	62
6.4.1.1	The Scintillating grid illusion	62
6.4.1.2	Kitaoka’s induced movement illusions	65
6.4.1.3	Stabilized retinal images	67
6.4.2	Afterimages elicited by short presentation: the temporal dynamics of filling-in vs. adaptation	68
6.4.3	Adaptation and temporal integration	72
6.4.4	A dynamic illusion for the two eyes: binocular rivalry and the role of adaptation in it ...	73
6.5	Developmental aspects of visual illusions	76
7	The aims and synopses of the thesis	81
8	References	86
6.	Studies	95
6.1	Study I	95
6.2	Study II	109
6.3	Study III	118
6.4	Study IV	122

1 Acknowledgements

I would like to thank my supervisor, Ilona Kovács for guiding me during my work on this thesis and during the years as her student at the PhD school.

I am very grateful to János Geier, with whom I have been working together since my undergraduate years and who has been supporting me both as an advisor, colleague and as a friend. His generous help in teaching me computer programming and many other skills that a good scientist needs is also invaluable.

I am also indebted to my co-authors with whom I have worked during the years, Stuart Anstis, Jochen Braun, Björn Friedrich, Patrícia Gerván, Zoltán Jakab, Bernd Lingelbach and Alexander Pastukhov.

I also would like to thank Orsolya Jánosházi and Nóra Szelényi for their comments on earlier drafts of this work, and all observers for participating in our experiments.

2 Abstract

The aim of my research is to investigate basic visual mechanisms by means of various visual illusions. The main focus is on brightness perception, where we tested the plausibility of several models, including a long-standing textbook explanation, by varying the physical characteristics of images eliciting brightness illusions and comparing the resulting perceptual experience with the predictions of the models. We refuted the textbook explanation of classical illusions and supported the filling-in approach of brightness modelling. We also investigated the temporal integration of monocular and binocular vision by means of dynamic illusions, after-effects and binocular rivalry. In the latter case, developmental changes were also found.

3 Kivonat

Kutatásom célja a látás alapfolyamatainak megismerése különféle vizuális illúziók segítségével. A leghangsúlyosabb ezek közül a világosságészlelés, amelynek számos modelljét teszteltük, beleértve a régóta elfogadott tankönyvi magyarázatot is. Ehhez a világosságillúziókat kiváltó képek paramétereit variáltuk, és összehasonlítottuk a modellek jóslatait az emberek által észlelt világosságprofillal. Így klasszikus illúziók tankönyvi magyarázatát cáfoltuk meg. Eredményeink a kitöltés alapú modelleket támasztják alá. Dinamikus illúziók, utóképek és a binokuláris rivalizáció jelenségének segítségével a látórendszer téri integrációját is vizsgáltuk, mind az egyszemes, mind a két szemmel történő látás esetén. Utóbbi esetben a fejlődés során fellépő változásokat is találtunk.

4 Summary

Visual illusions provide ample opportunities to investigate the basic working mechanisms of the visual system. Such illusions, in which the perceived pattern of light differs from its physical distribution, are systematic “errors” produced by normal visual information processing. If the overall pattern of errors are systematically mapped by psychophysical methods and captured by a single unified explanatory theory in the particular domain (such as brightness or colour), then that theory is likely to account for veridical perception as well, since the pattern of errors indicate how the underlying mechanism works.

Our first goal was to investigate whether the generally accepted explanation of numerous lightness-brightness phenomena, the concept of lateral inhibition was indeed suitable to

explain classical brightness illusions. For this aim, we used the two textbook strongholds of this long-standing theory. First, we curved the Hermann grid, which eliminated the illusory spots. Second, we modified the background of the Chevreul staircase, which significantly altered the illusion. In both cases, the conditions of the lateral inhibition-based explanation remained untouched. Therefore, it failed to predict the elicited perceptual changes. On this basis, we rejected lateral inhibition as an explanatory principle for brightness phenomena. In the introduction, the limitations of current theories, including low-level filtering models and mid-level theories are also analysed and probed with modifications of illusions they are supposed to account for.

Our second goal was to find a unified explanation for the investigated brightness phenomena. We showed that edges played a crucial role in brightness perception. In the Hermann grid, the illusion persisted if one side of the streets remained straight. In the Chevreul illusion, we found that the change of the upper and lower boundary edges of the staircase caused the perceptual changes. Other data from the literature are also reviewed, proving that the most important factor in brightness and colour perception is the edge-structure of the image, and homogeneous surfaces are filled-in based on the signals originating from edges.

Besides the spatial integration of brightness and colour signals, we examined some characteristics of temporal integration as well. We found that brightness and colour integration over time takes place in the visual system even without high-level cues such as form. Randomly flickering squares elicited an afterimage of a meaningful shape.

To understand the system level, it is necessary to investigate binocular vision, too. We touched upon this issue by means of a binocular illusion: binocular rivalry. Our results were interpreted in Pastukhov and Braun's (2011) framework, assuming a temporal integration process behind bistable perceptual phenomena. We found significant developmental differences within this framework: children alternated and adapted more quickly and showed a stronger adaptation effect than adults.

5 Összefoglaló

A vizuális illúziók számtalan lehetőséget nyújtanak a vizuális rendszer alapvető mechanizmusainak vizsgálatára. Az ilyen illúziók, amelyek esetén az észlelt fénymintázat eltér a fizikai fényeloszlástól, a látórendszer szisztematikus „hibázásainak” tekinthetőek,

amelyek a látórendszer normál információfeldolgozási folyamataiból adódnak. Ha pszichofizikai módszerek segítségével felderítjük ezen hibázások mintázatát, és ezeket egységes magyarázóelméletbe tudjuk foglalni egy adott területen belül (mint például a világosság-vagy színészlelés), akkor ez az elmélet nagy valószínűséggel jól fogja magyarázni a természetes látvány feldolgozását is, mivel az illúziók esetén vétett „hibázások” pontosan azt jelzik, hogy hogyan működnek a látórendszer mögöttes mechanizmusai.

Az első célunk az volt, hogy megvizsgáljuk, hogy számos világosságillúzió általánosan elfogadott magyarázata, a laterális gátlás elve valóban elfogadható magyarázatként szolgál-e klasszikus világosságillúziókra. Ennek érdekében e régóta elismert magyarázat két tankönyvi alapkövét használtuk fel. Először meggömbítettük a Hermann rácsot, ami megszüntette az illuzórikus foltokat. Ezután a Chevreul illúzió lépcsősorának háttérét módosítottuk, ami jelentősen megváltoztatta az illúziót. Ezekre a jelenségekre alapozva cáfoltuk, hogy a laterális gátlás elve alkalmas lenne világosságészlelési jelenségek magyarázatára. Disszertációm bevezetőjében napjaink magyarázóelméleteinek korlátait is bemutatom, ide értve az alacsony szintű szűrőmodelleket, valamint a középszintű elméleteket is. Próbára tételük éppen azon illúziók módosításaival történik, amelyek magyarázatára ezen elméletek megszülettek.

Második célunk az volt, hogy a vizsgált világosságészlelési jelenségekre egy új, egységes magyarázóelvet találjunk. Megmutattuk, hogy az élek kritikus szerepet játszanak a világosságészlelésben. A Hermann rács illúzió nem szűnt meg abban az esetben, ha a meggömbített utcáknak az egyik éle mégis egyenes maradt. A Chevreul illúzió esetében azt találtuk, hogy az illúzió módosulását a lépcsősor alsó és felső határelének megváltozása okozza. Továbbá bevezetőmben szakirodalomból számos bizonyítékot bemutatok arra, hogy a világosság-és színészlelés legfontosabb tényezője a látott kép élstruktúrája, és a nagyobb homogén területek kitöltése az élekből induló neurális jelek által történik.

A világosság-és színszignálok téri integrációja mellett az idői integráció néhány sajátosságát is vizsgáltuk. Azt találtuk, hogy a látórendszerben a világosság-és színszignálok idői integrációja még olyan magasabb szintű támpontok nélkül is létrejön, mint például a forma. Kísérletünkben véletlenszerűen villódzó négyzetek értelmes forma utóképet váltották ki.

A látás rendszerszintű megértéséhez a kétszemes látást is szükséges tanulmányozni. Ezt a kérdéskört is érintettük egy kétszemes illúzió, a binokuláris rivalizáció segítségével. Eredményeinket Pastukhov és Braun's (2011) elméleti keretében értelmeztük, akik egy idői

integrációs mechanizmust feltételeznek a bistabil perceptuális jelenségek mögött. Jelentős különbségeket találtunk a fejlődés különböző szakaszaiban ezen értelmezési keret szerint: a gyermekek gyorsabban alternáltak, valamint gyorsabban és erősebben adaptálódtak binokuláris rivalizációs kísérletünk során, mint a felnőtt résztvevők.

6 Introduction

6.1 Looking into the ‘black box’ through illusions - An alternative to physiological studies

Visual illusions reveal much about the mechanisms of information processing in the visual system. Though the only contact of our visual system with the external world is the distribution of light projected on our retinas, it builds up a chromatic, 3-D model, which makes orientation and action possible. However, our visual system makes certain errors during this process: our perception is often different from that of the physical light distribution. As Richard L. Gregory (1968) adequately raises the point, ‘to read reality from images is to solve a problem: a running set of very difficult problems throughout active life. Errors are illusions. Certain situations present special difficulty, giving rise to systematic errors: can these serve as clues to how the brain generally solves the problem of what objects are represented by which images?’ (p. 1).

During my research, I aim to discover the main characteristics of the basic visual mechanisms by means of the systematic investigation of these “errors”: visual illusions. On the basis of the regularities of these errors, consequences can be drawn with regards to the basic mechanisms of perception. Hereby, as an alternative of physiological experiments, we can gain insight into the working mode of the visual system by means of revealing the regularities of psychophysically measurable illusory phenomena and by modelling them. This approach is comparable to that of Julesz’s “psychoanatomy” or “cyclopean perception”: ‘The experimental methodology of cyclopean perception is purely psychological, yet its background and quest are neurophysiological. This is exactly what is traditionally regarded as physiological psychology. But whereas physiological psychology is usually a passive discipline that tries to explain psychological findings by physiological evidence, cyclopean perception is an active discipline that can tell the neurophysiologist where to search (or not search) for a certain perceptual process’ (Julesz, 1971/2006, p. 7-8).

Julesz, by generating a patent set of stimuli, showed that stereopsis occurred earlier in the visual system than object recognition, contrary to the generally accepted view prior to his work. By means of his Random Dot Stereograms (RDS), he did not need any invasive physiological or brain imaging technique to draw this conclusion unequivocally with regards to the build-up of processes inside the “black box” of the brain. This conclusion was merely based on the input (RDS stimuli) that contained no recognisable shape, and the perceptual output, yielding a definite shape, such as a square, located unambiguously in front of, or behind, a background, in the 3D space.

Our aim with regards to the systematic study of illusions is similar to that of Julesz’s. We should agree with his claim that the way to discover the visual system is not always to take physiological evidence as ready explanations for perceptual phenomena. Rather, we should use perceptual phenomena actively to discover what lies inside the “black box”.

Early experts of physiology also agreed that explanations of perceptual phenomena based on physiological measurements should be treated with care. Even the pioneer of extracellular recordings of the mammalian retina and the discoverer of antagonistic retinal receptive fields in the cat (serving as the physiological basis of the explanatory principle of lateral inhibition, which will be described later in detail), Steven Kuffler (1953) himself was sceptical with regards to the perceptual information carried by single-cell responses he measured. He rather opted for a system-level approach: ‘it is difficult to think of information content in terms of single unit contributions. One may rather have to consider that groups of fibers modulate activity levels and patterns by superposition and subtraction.’ (Kuffler, 1953, p. 65). He also added that ‘such fibers then merely signal change, but not necessarily the direction of change, such as brightness or darkness.’ (p. 65). According to Barlow et al (1957), in order to explain perceptual phenomena such as the simultaneous brightness contrast illusion by the principle of lateral inhibition measured in retinal receptive fields, two additional assumptions, which are not confirmed by the physiological measurements themselves, should be made. The first is that high firing rate in the ON centres gives rise directly to perceiving white, whereas in OFF centres, it initiates the perception of black. The second assumption is that this experience of black or white is limited to the area of the centre, while the surround only modulates the percept in the centre. Therefore, the authors conclude that lateral inhibition in single-units should not necessarily be regarded as the explanation for the simultaneous brightness contrast illusion. The causal relation between single cell responses measured in animal studies and human perceptual experience is difficult to confirm.

Moreover, according to Enroth-Cugell and Robson (1966), the very rationale for these single-cell measurements is right that these single-cell inhibitory responses do not manifest themselves in the human perceptual experience, since they are obscured by central processes.

Recent studies on retinal single-cell responses, on the other hand, do not even address the issue of relating physiologically measured cell responses to human perceptual phenomena. By the 2000s, even at such a low level as the retina, physiologists have discovered a range of receptive fields of great variety with regards to their shape, size, sensitivity profile and functional organization (see e.g. DeVries and Baylor, 1997; Brown et al, 2000; Rockhill et al. 2002; Dacey, 2004). These more recent findings (such as C-shaped, footprint-shaped or orientation-selective retinal receptive fields, etc., just to mention a few) obtained by means of modern physiological techniques are so diverse that it would be difficult to trace visual (in this case, brightness) illusions back to such a great diversity of receptive field profiles.

On this basis, an approach that is in principle similar to Julesz's "psychoanatomy", seems rather useful in order to gain some insight into the "black box" from the other side of the coin. In line with Julesz's approach, we think that through illusions, one can capture the algorithm of the particular brain area(s) or the particular processes that might be related to a particular perceptual phenomenon or function. In Marr's (1982) terms, central to our approach is the level of algorithm, and the level of implementation is a next step to be discovered by physiologists. As Gilchrist (2006) aptly notes, 'the overall pattern of errors is the signature of the human visual software' (Gilchrist, 2006, p. 24).

Gilchrist (2006) also points out that it is much more difficult to imagine two different models that predict the same pattern of errors than two others that predict veridical perception equally well. I interpret this claim so that if a model can correctly predict the pattern of e.g. brightness errors, which can be reliably studied by psychophysical experiments, then that model will probably predict veridical brightness perception as well, since in this case, the model is likely to have captured the essential algorithm of the software of the particular visual domain, e.g. brightness perception. On the other hand, if a model predicts more or less correctly what we see in real-scene images, we cannot be sure that the overall pattern of errors is also predicted well by this model. This is because the tiny inaccuracies of a model are not necessarily recognized when applied only to real-scene images. In other words, images eliciting illusions are more suitable for testing a model since they highlight errors produced by the visual system much more evidently than real-scene images do.

The existence of illusions clearly indicate that the human visual software has a certain mode of processing, whose output, the perceived pattern of brightness, is somewhat different from the physical light distribution that can be measured by photometers. This deviation does not occur to anyone when looking at real scenes. Images eliciting visual illusions, however, provoke the visual system so that they also reveal the circumstances when it errs, and a good model of the visual system should commit the same errors as the modelled system. Therefore, a good model of a certain domain of vision, such as brightness or lightness perception, must account for the pattern of errors (such as lightness-brightness illusions), as well as for the perception of real-scene greyscale images, by means of the same process, using the same parameters. Gilchrist (2006), however, claims that this excellent tool, the systematic study of visual illusions and their comprehensive modelling have not been utilized systematically to date. As he notes, ‘theories have attempted to explain lightness illusions largely in a piecemeal manner (but see Gregory, 1997). The overall pattern of lightness errors has never been surveyed in a single publication.’ (Gilchrist, 2006, p. 266).

Gregory (1997, 2009) attempts to classify visual illusions based on their supposed cause or explanation, searching for a somewhat common background for illusions in each class. The main distinction he makes is between “physical” and “cognitive” illusions. However, although he regards illusions as basic phenomena on which science should focus in order to reveal *how* the brain works, which is an essential point in our approach as well, he seems to have a different focus. His main basis of classification is as follows: ‘The first [class] (physical) is the result of an optical disturbance intervening between the object and the retina; the second (physical) is due to disturbed physiological signals in the eyes or the brain; the third (cognitive) is the application of misleading knowledge of objects; the fourth (cognitive) is the application of misleading general rules.’ (Gregory, 1997, p. 190).

The first point at which we must disagree with these principles is that he regards perceptions due to some optical disturbance of light as visual illusions. In my point of view, those can be termed as “optical” illusions but not visual ones. Such optical illusions that are caused by the refraction of light (e.g. fata morgana, projected or mirror images, or the apparent deflection of a straight stick at the surface of water into which it is immersed, etc) occur outside our visual system, therefore, they tell nothing about its working mode, and should not even be considered in studies on visual illusions.

The second point at which our approach differs from that of Gregory’s is that while he regards bottom-up illusions as being ‘due to disturbed physiological signals in the eyes or the

brain' (p.190), I do not regard these as 'disturbances': the occurrence of these low-level illusions are generated by the normal way of processing visual signals in the brain; these are the result of the normal algorithm of processing the external light distribution and converting it into perceived images. Still, Gregory (1997, 2009) devotes little emphasis to these so-called "physical" illusions and analyses "cognitive" ones in much more detail. The focus of this thesis, however, is on illusions that are generally considered as low-or mid-level phenomena.

In order to understand basic visual mechanisms by means of studying visual illusions, the three levels of understanding a system established by David Marr (1982) provide useful guidelines. In his system, the computational theory of a device lies at the highest level. At this level, the theorist should set the goals of the computation and should characterise the abstract properties of transforming the input information (in our case, physical light distribution) into the other (percept), accounting for the appropriateness of the assumed logic.

Visual illusions help establishing the computational aim, and allow for checking the appropriateness of the theory. If only a small portion of the known illusions occurring in a particular domain (e.g. brightness, colour, size, etc) are accounted for by a certain theory, then that theory should be further refined until it predicts all of them, otherwise another theory should be sought. The computational aim is therefore to establish a theoretical framework which comprehensively accounts for the overall pattern of (brightness, lightness, colour, size, etc) errors. Such a computational theory will inherently be able to account for perceiving real-world images as well as illusions.

At such a low-level visual domain as brightness perception, computers allow us to test the concrete algorithm that implements our computational theory. The level of the algorithm itself and its input and output comprise the second level that Marr describes. In our approach, which proceeds from illusions, the input should be an image that elicits a particular illusion in humans. The computer simulation of the theorised working mode of the particular domain of the visual system using the hypothesised algorithm should transform this input image into an output image that corresponds to the human perceptual experience. The adequacy of the model can be confirmed by comparing the output with the results of psychophysical experiments.

The lowest level Marr sets up is the physical realization of the algorithm and representation. Although he claims that the three levels are only loosely coupled, I still think that a good computational theory both at the first and the second level should be *anatomically* plausible, taking into account the known anatomical properties of the visual system (tissue of

neurons, horizontal and vertical connections through which activation can spread within and between visual areas, etc.). However, I do not regard it necessary to take into account all phenomena revealed by *physiological* measurements (such as different kinds of receptive fields), or to rely only on those, when setting up a computational theory for *perceptual* phenomena. Modelling a set of perceptual phenomena in a way that does not merely rely on the already known physiological data might provide physiologists with new ideas, as Julesz has also claimed. If computational theories were restricted to rely on physiological results that have already been confirmed by such measurements, then such system-level neural interactions that are present in the visual system but there are no available physiological techniques yet to discover them, could be easily ignored.

To conclude, by discovering the regularities of various kinds of visual illusions, one can get closer to understand how the human visual system works, by establishing anatomically plausible computational models for these, thus complementing physiological techniques.

6.2 Theories of lightness-brightness perception

6.2.1 The roots

The domain of vision where illusions are most widely used as a tool of research is brightness¹ perception. Scientists have been attempting to find explanations for lightness-brightness illusions they discovered even since the 19th century. As early as in 1839, Michael Eugene Chevreul published a bunch of his systematic psychophysical experiments on brightness and colour illusions, such as the simultaneous contrast and the Chevreul illusion (see also Study II in this thesis), along with various after-effects in his work he made in order to improve the quality of tapestry dyes (Chevreul, 1839). In 1865, Ernst Mach published his psychophysical results he obtained by means of his rotating disks, which allowed him to produce various luminance profiles eliciting illusory dark and bright bands, known today as the Mach bands. These illusory bands are perceived when a luminance ramp progressing from

¹ In case of the illusions investigated here, homogeneous illumination is assumed. In this case, the concept of brightness and lightness collapse into each other (Gilchrist, 2006). Therefore, these terms will be used interchangeably throughout this thesis when discussing illusions.

black to white adjoins a black plateau at its black end (producing dark bands) and a white one at its white end (producing bright bands).

Prior to Mach, such illusions were generally accounted for by ‘unconscious inferences’ or ‘errors of judgement’ made by the observer (Ratliff, 1965). Mach, however, was dissatisfied with such explanations, for him, ‘they were merely various ways of expressing the still unexplained facts’ (Ratliff, 1965, p. 2). He therefore proposed a physiological explanation of the perceptual phenomena he discovered by means of psychophysical experiments, and gave a mathematical description of the supposed integrative actions in the nervous system, which is exactly the same approach as this thesis and our studies represent. According to Ratliff, he was the first anticipator of lateral inhibition, since ‘the basic neural process postulated in Mach’s mathematical formulation was a reciprocal inhibitory interaction among neighbouring elements of the retina’ (Ratliff, 1965, p. 2).

Another early scientist who also found the mentalistic explanations of such illusions vague, and also anticipated the concept of lateral inhibition, was Ewald Hering (1874/1964). He had a long debate with Helmholtz, who propagated a cognitive account of illusions elicited by even such simple images as the simultaneous contrast figure. Hering’s explanation was as follows: ‘the excitation corresponding to the target on the white background is strongly inhibited due to the much higher excitation of the surrounding retinal tissue that receives light from the white background. This strong inhibition does not occur for the target on the black background’ (Gilchrist, 2006, p.18). Hermann (1870), upon discovering the illusory spots at the intersections of a grid pattern created by the white background between the square-shaped, dark Chladni figures² in a physics book by Tyndall, provided a similar explanation (Spillmann, 1994, see also Study I in this thesis).

Although these early results converged towards contrast enhancement, a phenomenon of opposite direction was already known before the end of the 19th century. Von Bezold published an illusion in which a homogeneous surface appeared lighter when small white dots or lines were superimposed on it, and it appeared darker in case of dark spots or lines. This direction of phenomena, when the apparent contrast is reduced, will be termed as assimilation

² The typographer of the book organized the Chladni figures so that they formed a grid pattern. Since the figures were dark and the background (the white paper) was white, the illusory spots occurred, and were first described by Hermann. Of course there is no relation between the standing waves shown in Chladni’s figures and the Hermann grid illusion (see also Wade, 2004).

(Helson, 1963) throughout this thesis. This term will be used to refer only to the direction of the effect, and not as an explanatory principle, which is still not well-defined in the literature (Anderson, 2003). The phenomena of assimilation entirely contradict these explanations proposed by these early scientists. However, it would require further historical investigation whether they knew³ the then relatively new phenomenon that contradicted their theory, which is beyond the scope of this thesis.

6.2.2 Lateral inhibition – the classical textbook explanation

It is unclear whether the 19th century anticipators of lateral inhibition knew the work by von Bezold on assimilation effects. However, by the 1920s, electrophysiological studies of the nervous system were becoming more and more widespread (e.g. Adrian, 1926), and they also began to study the retina soon (Adrian and Mathews, 1927). According to Hartline's biography by Ratliff (1990), Hartline discovered an effect in the compound eye of the limulus already in the 1930s (but he first published it only in 1949), which was in line with the 19th century contrast illusions in humans. The discovery was probably accidental, as it turns out from his Nobel lecture he gave in 1967, where he describes the "lateral effect" (as it was then called according to Ratliff, 1965) as follows: 'I noticed that extraneous lights in the laboratory, rather than increasing the rate of discharge of impulses from a receptor, often caused a decrease in its activity. Neighbouring ommatidia, viewing the extraneous room lights more directly than the receptor on which I was working, could inhibit that receptor quite markedly'. (Hartline, 1967, p. 274).

The coincidence of his result with the 19th century contrast effects probably reassured him that this finding was not an artefact, since for him, it was immediately evident that he had found the neural implementation of lateral inhibition proposed by Mach and Hering: 'The role of this effect in enhancing visual contrast is obvious: brightly illuminated areas inhibit the activity from dimly lighted regions more than the latter inhibit the activity from the former.' (Hartline, 1949, p.253). On this basis, he and his followers considered it worth searching further on for this lateral inhibition effect in the retina of various species, ignoring the fact that assimilation phenomena were totally in contradiction with the principle of lateral

³ Gilchrist (2006) makes reference to the publication of the von Bezold effect in 1874, which is subsequent to the works published by Mach, Hermann and Hering, but according to Anderson's (2003) reference list, it was first published in 1862, which is 3 years before Mach published his first work on his contrast effects.

inhibition. Kuffler (1953) soon achieved to find a similar effect in the retina of the cat⁴. However, he and other physiologists, as cited above, were more careful with regards to explaining human visual illusions in terms of their physiological findings in various animal preparations.

Nonetheless, Baumgartner (1960) came up with an explanation for the Hermann grid illusion on the basis of these antagonistic receptive fields. In his explanation, he highlights a retinal receptive field that falls on a street section and one that falls on an intersection of the Hermann grid (see e.g. Fig. 3a in Study I). Thus, the inhibitory surround of the receptive field

⁴ It is not very well known, however, that Kuffler (1953) managed to show lateral inhibitory effects only under dark-adaptation: 'The characteristic response of the surround could always be made evident by using a dim background, or after a short period (several minutes) of complete dark adaptation. Decreasing the background illumination first expanded the area from which center-type responses could be elicited, then brought in „on-off” responses around its boundary and eventually disclosed discharges which were characteristic of the surround.' (Kuffler, 1953, p.51.) Under light-adaptation, he did not find any antagonistic surround in retinal receptive fields: 'As the background illumination is increased, the boundaries of the receptive fields “contract” and also the discharge pattern distributions change. The response type which is characteristic of the surround tends to disappear and the pattern of the center will predominate. In fact, some units even with careful exploration, using small 0.1-0.2 mm. light spots under photopic conditions, gave only pure “on” or “off” responses within the limits of the receptive field.' (Kuffler, 1953, p. 50-51.) In his symposium excerpt (Kuffler, 1952), which is based on the same series of experiments, he also claims that lateral inhibition disappeared under light-adapted condition: 'For instance, in a field with an „on” center, increased background light will first reduce the peripheral „off” fringe, i. e. the field will shrink. In the „on-off” zone, the lower frequencies of the compound discharge will drop out and eventually, with a bright background, the receptive field may appear to be composed of a small „on” area only.' (Kuffler, 1952, p.288). Receptive field organization under dark adaptation, however, is not really relevant with regards to our scope, since brightness illusions are usually observed under light-adapted state. Kuffler's own colleagues (Barlow et al, 1957) however, a couple of years later refer to Kuffler (1953) mistakenly as though he showed lateral inhibition under light-adaptation: 'It is already known (Kuffler, 1953) that such antagonism exists in the light-adapted cat's retina' (Barlow et al, 1957, p. 341). More than a decade later, Enroth-Cugell and Robson (1966) also cite Kuffler in accordance with their preconception: 'Kuffler (1952) found that the receptive fields of light-adapted cat retinal ganglion cells are approximately circular and have functionally distinct central and peripheral regions; he showed that stimulation of these two regions produces opposite and antagonistic effects upon the activity of the ganglion cells.' (Enroth-Cugell and Robson, 1966, p.518). Eventually, this mistaken version has become widely known, and Kuffler (1953) is still the study to be referred to when it comes to the physiological evidence of lateral inhibition supposed to lie behind numerous brightness illusions, ignoring the fact that he managed to show lateral inhibition only under dark-adaptation.

located at the intersection receives twice as much white as the one located in the street section. Therefore, according to Baumgartner's theory, the retinal ganglion cell, whose receptive field is at the intersection, will give a smaller response, since it receives twice as much inhibition as the other. This smaller response manifests itself as a dark spot at each intersection in the perceptual experience. The mathematical description of this ideal receptive field was given by Rodieck (1965), which is also known as the DoG (Difference of Gaussians) model (another mathematical realization is the ∇^2G operator described by Marr, 1982).

The explanation based on lateral inhibition in retinal ganglion cells has become so widely accepted, that as a piece of settled knowledge, it has become the textbook explanation of the Hermann grid illusion, and vice versa, the Hermann grid illusion has become the textbook demonstration of the manifestation of lateral inhibition in retinal ganglion cells. It has remained so even recently (Valberg, 2005; Blake és Sekuler, 2006; Snowden, Thompson and Troscianko, 2006; Goldstein, 2009). Moreover, the Chevreul illusion has been also included as an additional, clear-cut demonstration of the Baumgartner model in textbooks, which establish the way of thinking of generations of visual scientists. Besides, it is being taught to representatives of other professions, such as psychologists, dentists and doctors interpreting x-ray photographs (Delvin, 2006; De Lacey et al, 2008), as well as to graphic designers and visual artists (Ware, 2004).

However, textbooks demonstrating the supposed working mechanism of retinal receptive fields, do not even mention assimilation phenomena, although many of these have become known in the past couple of decades, in addition to von Bezold's work, such as the White effect (White, 1979), the checkerboard contrast (DeValois and DeValois, 1988), the deWeert illusion (deWeert, 1991), the Todorovic illusion (Todorovic, 1997) or the dungeon illusion (Bressan, 2001; 2006). None of these can be accounted for by lateral inhibition, since the perceptual effect is exactly the opposite of that in contrast illusions. Another type of illusion which contradicts the lateral inhibition account is the Craick-O'Brian-Cornsweet (COC) illusion, in which merely the specific luminance profile of the boundary edge causes the homogeneous grey areas of the image to be seen as different in lightness. Moreover, Gilchrist's (1977) results suggest that depth perception might modify the perceived lightness of surfaces, which is also not accounted for by lateral inhibition.

None of these effects that contradict lateral inhibition are discussed in textbooks, therefore, most students new to vision research might still believe that the lateral inhibition-

based explanation is correct, and when assimilation or other effects are encountered, those are vaguely attributed to different, yet unknown mechanisms. However, as discussed in the first chapter, explaining one or other set of brightness illusions in different ways would be weird, since in that case, the visual system should switch between different working modes depending on the perceptual input, which is not very much plausible.

Therefore, it seems that the only way to overthrow the widely accepted explanatory principle is to refute it by means of its two main textbook strongholds. In Study I, we have modified the Hermann grid by adding a slight curvature to it so that the illusory spots disappeared, while we did not change the conditions of the Baumgartner model. Therefore, it would wrongly predict spots even in our slightly distorted variants. In Study II, we replaced the usually used white background of the Chevreul staircase with a luminance ramp background, which made the illusion change completely (enhance or disappear, depending on the progression of the background ramp, compared to that of the staircase). The lateral inhibition-based explanatory theory would predict no perceptual change inside the staircase, since local luminance relations were left unaltered.

6.2.3 Recent lateral inhibition-based models

The concept of lateral inhibition survives even in current computational models. The basis of all these models is a variation of the DoG filter, which is the mathematical description of the ON-centre, OFF-surround antagonistic receptive field (Rodieck, 1965). Such models have been published by Watt and Morgan (1985), Kingdom and Moulden (1992), McArthur and Moulden (1999), Pessoa, Mignolla and Neumann (1994), Blakeslee and McCourt (1999; 2004), Dakin and Bex (2003), Otazu, Vanrell and Parraga (2008), and Shapiro and Lu (2011). The fundamental principle of these models is that they convolve each point of the input image with a weight function, which is a variant of the DoG filter. Thus, each point of the input image is replaced by the weighted sum of its environment, which constitutes the output image. This filtering process is conducted with various filter sizes in case of multiscale models, and the outputs of different filter sizes are averaged together to provide the final output, in which certain normalization processes might also be used.

6.2.3.1 Filtering and symbolic description

Earlier convolution models, such as the MIRAGE by Watt and Morgan (1985) and the MIDAAS by Kingdom and Moulden (1992) were implemented only in 1 dimension, which is

a serious limitation, since perception of certain image areas are influenced by their entire surround, not only by their left and right neighbours. Our variant of the Chevreul illusion introduced in Study II is an example for this limitation of 1-D models. The 1D MIDAAS was extended to 2D by McArthur and Moulden (1999). The common feature of the MIRAGE and the MIDAAS is that after the convolution, they apply certain rules to interpret the outputs of each filter, and the final prediction of the model is based on the features identified by using the rules. However, these models do not provide any exact algorithm for the interpretation process, which makes it difficult to test their predictions.

6.2.3.2 High-pass filtering

Other convolution models do not require interpretation rules. Their output is the filtered image itself (e.g. Shapiro, 2011), or the normalized average of filter outputs (e.g. Blakeslee and McCourt, 1999; Dakin and Bex, 2003). Shapiro and Lu (2011) use a high-pass filter (which attenuates low spatial frequencies and preserves only high spatial scales present in the image) in Adobe Photoshop. They claim that by eliminating low spatial frequencies this way, their model can predict numerous brightness illusions besides the brightness profile in natural images. They determine the size of the high-pass filter on the basis of the test-patch: the size of the filter is set (by hand) equal to it, whereby they eliminate spatial frequency content coarser than the test patch. As they put it, their model ‘explicitly acknowledges a role for spatial organization by stating that filter size depends on the size of the most relevant stimulus’ (p. 1458)..

However, Shapiro and Lu (2011) neither mention any algorithm, nor any principle about how the filter diameter is adjusted to the structure of the image, or about how they measure the size of the test disks automatically to adjust the filter sizes to that. Their only note on this issue is that the visual system somehow solves this problem: ‘The crucial factor for many brightness illusions may therefore reside in the physics of the stimuli, and human physiology may encode these physical properties by means of a neural process that is similar in principle to lateral inhibition’ (p. 1458). However, this issue would be the most important one - without this, the model is incomplete. This issue is the most difficult problem of such filter-based models to solve. It is unclear what they would do with an image in which test disks of different sizes were placed, or with one that had no well-defined test patches, such as the Craik-O’Brian-Cornsweet illusion (redrawn in Figure 1) or natural scene images. Multi-scale models were developed straight in order to resolve this issue (e.g. the ODOG model by McCourt and Blakeslee), however, no one has fully succeeded to date. Developers of

multiscale models aim to find a universally correct filter range, capturing most illusions, and they also aim to eliminate any free parameters from the model. The predictions of Shapiro and Lu's (2011) model depend on the actual setting of a free parameter, and they seem to adjust their filter size by hand to the given image, which is implausible with regards to the human visual system.

6.2.3.3 Multiple-scale filtering – natural image statistics

Dakin and Bex (2003) on the other hand, use a bank of DoG-like filters (Laplacian of Gaussian) including various spatial scales, after which they sum the outputs using different weights for each scale. The weights of each scale are actively computed by the model in an iterative manner, until the slope of the spatial scale distribution function of the final output image best fits the slope of the average distribution found in natural images. To support the adequacy of their filtering model as opposed to filling-in model types (that will also be discussed later in detail), they modify the Craik-O’Brian-Cornsweet (COC, redrawn in Figure 1) illusion in two ways. First, they scramble low spatial frequencies; second, they scramble high spatial frequencies in the COC image. In the first case, the illusion ceases, while it persists in the latter case. On this basis, they conclude that the low frequency structure is responsible for the illusion.

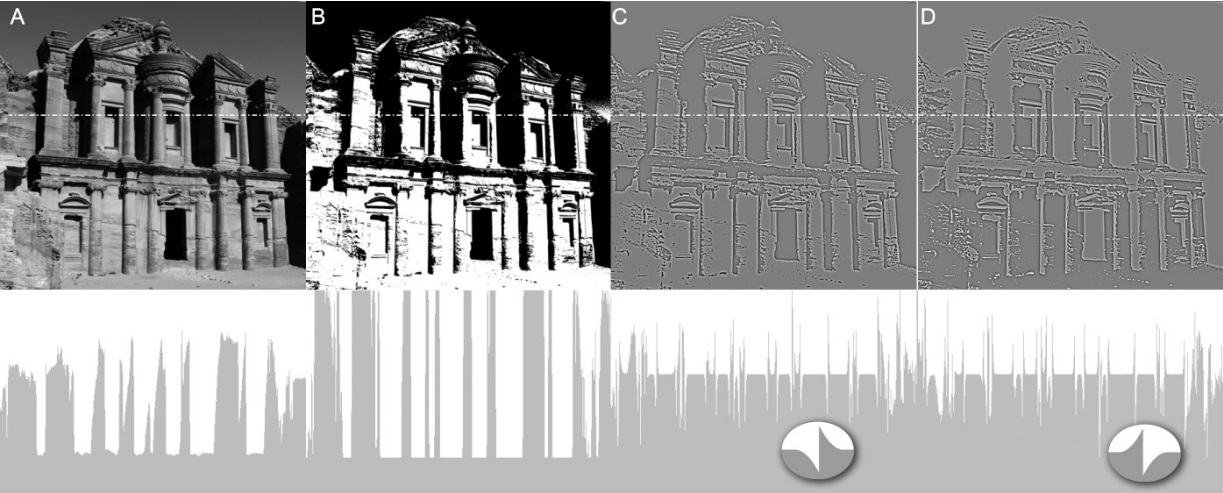


Figure 1 The Craik-O’Brian-Cornsweet (COC) illusion. Redrawn after Cornsweet (1970) by the author. The illusion is displayed in panel C and D, where all grey areas are physically identical, except for the edges. However, the shadowy parts of the building seem darker in C than the rest, whereas the effect is the opposite in D. This demonstrates that the effect depends on the luminance profile of the edges rather than on prior knowledge about shadows. The luminance profiles of the images are displayed below the images, and the enlarged edge-profile is displayed in the ellipses (courtesy of János Geier). The image is generated so that the contrast of the original greyscale image (A) is maximized (B), after which a high-pass filter is applied. D is generated by high-pass filtering the inverse of B.

However, one may ask what is regarded as low spatial frequency here. In Dakin and Bex's (2003) Figure 1e (not shown here due to copyright reasons), they plot the frequency distribution of their COC image. The cut-point between low and high spatial frequencies is also indicated in that figure, which is near the upper end of the scale, at 30 cycles per image. The reason for selecting this value as cut-point is never indicated in their paper, therefore it seems totally arbitrary. Moreover, to provide further support for the key role of low spatial frequencies in brightness illusions, they remove the low spatial frequencies from the White effect, whereby it also ceases. However, here they choose the cut-point at 4 c/image, giving no reasons even for this choice. Nor do they account for why they consider frequencies as low below 30 c/image in one case (COC), and below 4 c/image in the other (White effect). One may ask how they would choose the cut-point if the COC illusion and the White effect were printed on the same sheet of paper adjacent to each other, to cease both illusions. It is also questionable why they scramble frequencies in case of the COC, and why they remove them in case of the White effect instead of using a common method to demonstrate a common explanatory principle.

If it is taken into account that the cut-point of high and low is 4 c/image in case of the White effect, but they cut at 30 c/image in case of the COC, which is near the upper end of their x-axis, then it seems that they make the COC illusion disappear by scrambling a large range of spatial frequencies (at least much larger than in the case of the White effect), including low, middle and high frequencies too, while claiming that they phase-randomize only low spatial frequencies. What they preserve from the original image is only the extremely high frequencies. Therefore, it is not surprising that the illusion disappears, since the luminance profile of the edges of original COC image (which is the essence of the illusion!) is totally destroyed. On the other hand, when they scramble the frequencies beyond 30 c/image, it influences only some extremely high spatial frequencies, and the essence of the image is preserved. It is quite straightforward that the illusion remains. Thus, these phenomena do not seem to show anything about the role of spatial frequencies in the COC illusion.

To support the appropriateness of their model, they also show computer simulation outputs for the COC illusion and their frequency-scrambled variants. Below the simulation outputs, they also provide a luminance cross section diagram of their result. They claim that the model correctly predicts the presence of the illusion in the original COC image and in its high-frequency scrambled variant, and its absence in the other. However, it can be seen in the

cross-section diagrams that the model in fact predicts large brightness differences at arbitrary locations of the low frequency-scrambled image (Fig.1.j in Dakin and Bex, 2003), while the perceptual experience is that the noise in the image is homogeneous (see their Fig. 1g). On the other hand, the predicted size of the illusion itself in the COC and the high frequency-scrambled images (see their Fig. 1h and i) is smaller than the predicted brightness inhomogeneities for the perceptually homogeneous low frequency-scrambled image. Therefore, neither the presented phenomena, nor the simulation results are convincing with regards to this model.

6.2.3.4 Multiple-scale filtering – the oriented DoG model

According to Kingdom (2011), the best-known filtering model is still the ODOG (oriented DoG) model, developed by McCourt and Blakeslee (Blakeslee and McCourt, 1999; Blakeslee and McCourt, 2004) which Dakin and Bex (2003) acknowledge to have inspired their above-analyzed model. The main point of the ODOG model is that it takes the weighted sum of ODOG filters of various sizes within each of the six orientations it uses. Next, it filters the input image with all the six resulting oriented filters respectively, after which the filtered image of each orientation is normalized before averaging them together to construct the final output.

The most common demonstration they use to prove the goodness of their model is the White effect (redrawn in Figure 4A). Although the ODOG model is a lateral inhibition-based model, it is surprising that the White effect, which is a reverse contrast/assimilation effect, is successfully predicted by the ODOG model. The reason for this success is the contrast normalization for each orientation: ‘we find that the orientation selectivity of the filters and the non-linear stage of the ODOG model, in which the outputs of the six orientation channels are equated through contrast normalization, are also critical for explaining some brightness effects, such as White’s effect’ (Blakeslee and McCourt, 2004, p. 2486). In the output of the vertical filter, the response is strongest for the grey targets, and it is in accordance with the perceived illusion, while the response for the black and white stripes is weak. On the other hand, the horizontal filters give strong response for the long vertical stripes and weak for the targets. The normalization process enhances the presence of the vertical filters’ response to targets compared to the horizontal filters’ response to the high-contrast stripes in the final output (this is very illustratively represented in Figure 2 (f) and (g) in Blakeslee and McCourt, 2004). This contrast normalization process causes the White effect to occur in the final output.

However, it might be asked how this normalization process would handle a scene in which numerous White images were printed adjacent to each other in the same input image, each rotated by various angles compared to each other, so that their stripes would represent all the six orientations equally that the ODOG model uses. Such a potential input image is shown in Figure 2. In this case, the illusion is simultaneously visible for humans in all the six images. However, since the normalization process in the ODOG model is made for the entire input image, no difference would occur between the strength of the responses of differently oriented filters. (Figure 2 represents all the six orientations used by the ODOG model equally, and no other orientation is present in the image). Therefore, the effect of the normalization process would disappear in the simulation results, and the model would fail to predict the perception of the White effect.

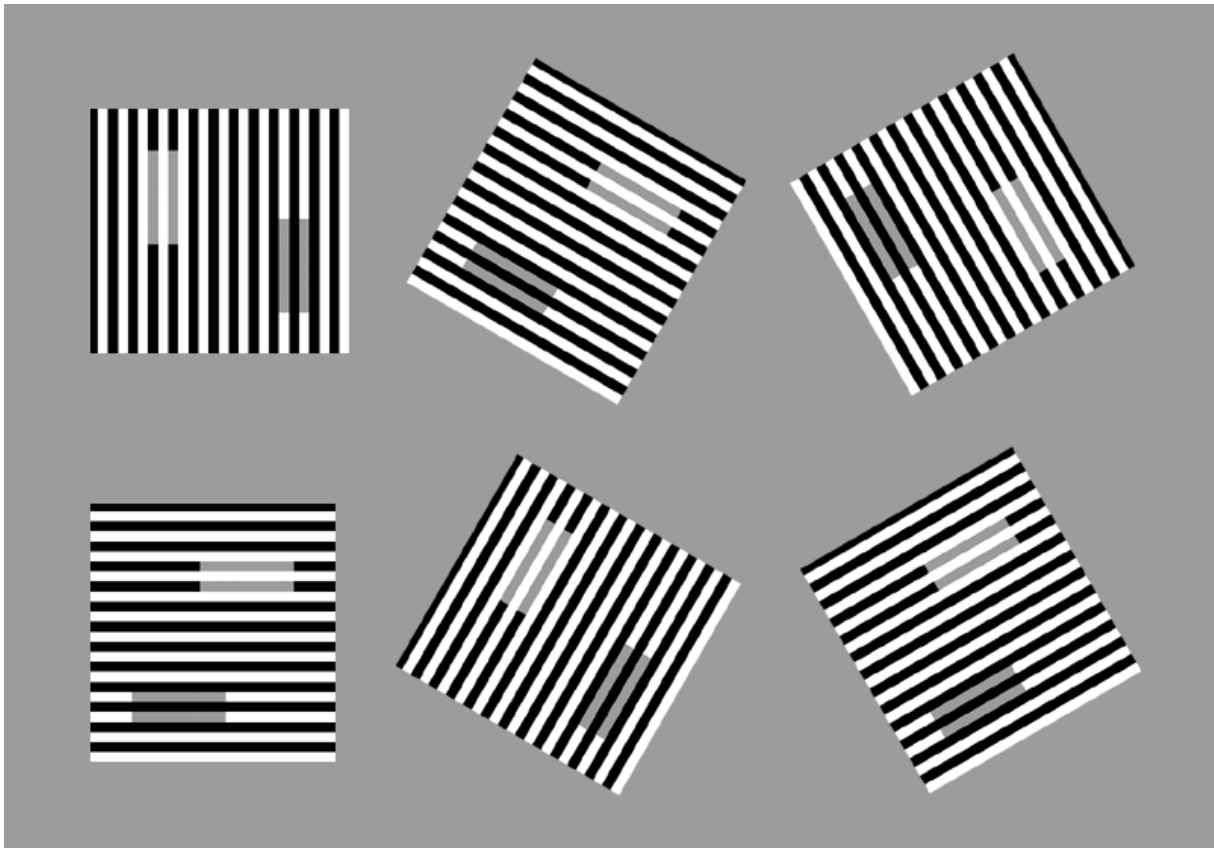


Figure 2. A potential input image for the ODOG model to challenge it. The White effect (redrawn after White, 1979) is rotated in the six orientations that the ODOG model uses, and included in the same input image. The grey targets embedded in a white stripe seem darker than the ones embedded in black stripes. This effect can be perceived simultaneously in all orientations in this image. The single original White effect is predicted by the ODOG model because its normalization process for orientations across the entire image enlarges the response for the targets, which is due to the dominance of only one orientation in the original single White image (e.g. vertical stripes). However, this image here contains all orientations that the ODOG uses equally (and only those), therefore, the

normalization process will not re-weight the orientations. Therefore, the ODOG model will fail to predict the presence of the White effect.

Another such example is the circular variant of the White effect by Howe (2005), redrawn in Figure 4B. Here the responses of differently oriented filters would be equal, since the image is circularly symmetric, therefore the effect of the normalization would disappear also in this case. The illusion, however, is still visible. The claim that this circularly symmetric variant of the White illusion challenges the ODOG model is not mentioned in Howe's paper; he created that image in order to refute the role of T-junctions (see section "Mid-level theories: intrinsic image models"). However, I consider this illusion a great challenge even for the ODOG model.

Not only reverse contrast or assimilation illusions cause problems to the ODOG model, but also variants of classical contrast illusions, such as our Chevreul variants presented in Study II. As we have pointed out in Study II, if a range of relatively small filter sizes are used only, then it cannot take into account the effect of the background ramp in the inner parts of the Chevreul staircase. If the full range of filter sizes are applied (among which the largest is 36 deg including the surround), then the outer ramp would dominate the predicted percept when the inner ramp is very thin, which is not the case according to our results (see Study II for further details). This weakness was also confirmed by Mark McCourt (personal communication, ECVP2011).

In McCourt and Blakeslee's papers, no attempt is found to simulate the Hermann grid illusion. However, even if the ODOG model were able to predict the presence of spots in the original Hermann grid, it is also unclear how it would capture the range of the Hermann grid phenomena presented in Study I, since the edge orientation at the intersections in four of our variants (out of five) did not change relative to the original Hermann grid (see Study I for the variants). Still, the illusion completely disappeared. However, the strength of the ODOG model as compared to simple DoG filtering is claimed to be its orientation sensitivity, so it might be expected that its predictions will be influenced by the curvature we added. However, although the orientations near the intersections remained unchanged in all of our variants (except for the sinusoid grid), the spots disappeared. If only smaller orientation-selective filters are used, then no change will be detected by them near the intersections compared to the original grid, so the predictions will be the same for the curved grids as for the original grid. If larger filter are also included, whose centre exceeds the area of the intersections, then the change in their stimulation caused by the curvature will influence their response even

outside the intersections. However, the perceptual change (i.e. the disappearance of the spots) is restricted to the inner area of the intersections.

To conclude, even current lateral inhibition-based models are unable to capture the overall pattern of brightness illusions by using universal, unchanged set of parameters for all illusions, which would be their general aim. In the next sections, we will discuss the success of other model types.

6.2.4 Mid-level theories: Intrinsic image models

Central to intrinsic image models is the idea that the visual system decomposes images to different layers, such as semi-transparent stripes or shadows superimposed on a background. According to Kingdom (2011), the antecedent of modern internal image models was a study by Gilchrist, Delman and Jacobsen (1984), but the roots can be traced back to Helmholtz. Gilchrist et al (1983) showed that the simultaneous contrast illusion became much stronger if the black and white background appeared to be induced by different illuminations, while local contrasts remained the same. Soon Adelson's (1993) mid-level approach emerged which argued that lightness was determined by perceived transparency or inhomogeneous illumination. Adelson (1993) showed numerous remarkable demonstrations of such effects, among which his "wall of blocks" illusion is one of those that induced a fruitful scientific debate, which beautifully demonstrates how small modifications on a perceptual phenomenon can evoke or refute theories about what is inside the black box of vision.

In Adelson's image (redrawn in Figure 3A), the rows of grey diamonds (indicated with 1 and 2 in all panels) are physically identical, still, the ones in row 1 seem much brighter than the ones in row 2. According to his explanation, row 1 is seen as dark diamonds behind a transparent light filter, whereas row 2 is seen as diamonds behind a transparent dark filter. It can be noted, however, that row 1 is surrounded by more dark than row 2, which would be compatible with a lateral inhibition-based explanation. He rejects any explanation based on local contrast, by showing another variant as a control (redrawn in Figure 3B): the local luminance relations remain the same; only the boundary of the stripes is changed from straight to a zig-zagged one, whereby the illusion largely decreases or disappears.

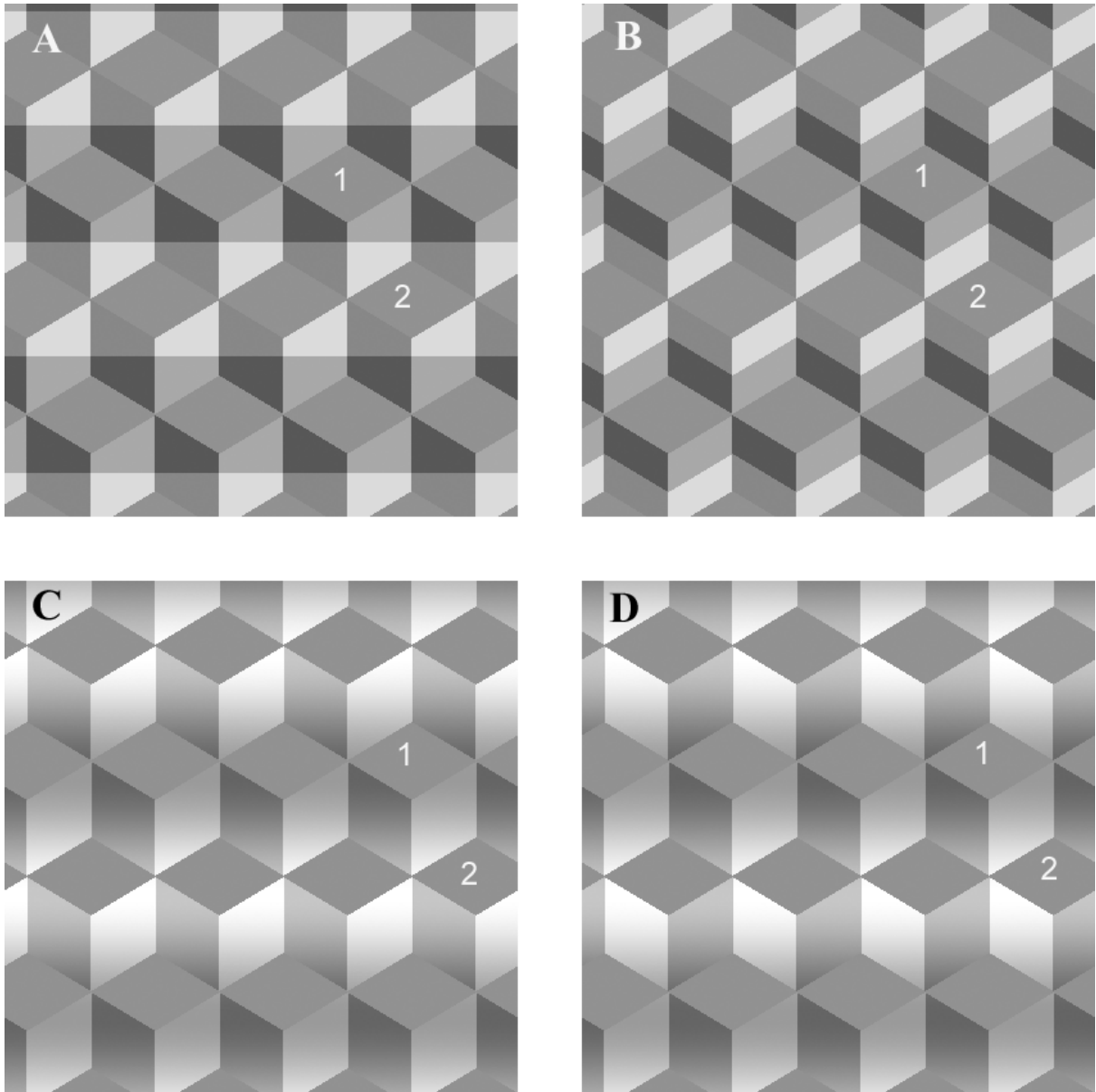


Figure 3. The course of the wall-of-blocks illusion debate. The rows of diamonds are physically identical in all panels. A: Adelson’s (1993) version: the stripes are claimed to be perceived as dark and light transparent filters, due to the X junctions. B: Adelson’s control image, where the straight edges of the stripes in A are zigzagged while leaving contrast relation untouched, therefore lateral inhibition is not sufficient here. No transparency is perceived due to the Y junctions. The illusion is largely decreased. C: Logvinenko’s (1999) version, adding a sinusoid luminance modulation instead of stripes. The image includes no junctions and transparency, but the illusion is still strong, suggesting that lightness-shadow invariance plays an essential role. D: Bressan’s (2001) variant: the dark and light sides of the blocks are exchanged in every second row, making the image shadow-incompatible. The illusion still remains, though. (All panels are redrawn by the author after the referred studies).

The mechanism that Adelson supposes to help the visual system interpret image parts as transparency is based on the junction structure of the image. He claims that due to the X-shaped junctions, comprising the horizontal edge of the stripe and the vertical edges of the

blocks, the visual system classifies the edge of the grey stripe as an ‘atmospheric boundary’, leading to the perception of transparency. Therefore, targets having the same physical luminance, but seeming to lie behind filters of different reflectance, their perceived lightness is altered accordingly. On the other hand, Y junctions signal a change in the 3D surface orientation, but no transparency, therefore, no illusion is seen in the zigzagged version.

Logvinenko (1999) however, challenged this line of thought by his variant redrawn in Figure 3C. Instead of stripes, he added a sinusoid luminance modulation to the image, leaving the diamonds untouched. In his version, neither X, nor Y junctions are present, but the illusion is at least as strong as in Adelson’s version. He therefore claims that grey-level junctions and perceived transparency are not necessary for lightness induction. Instead, he suggests that a shadow-compatible pictorial representation of inhomogeneous illumination lies behind the illusion, and claims that it is necessary to assume that the visual system takes into account the lightness-shadow invariance to explain this illusion.

Bressan (2001) however, came up with a simple but clever twist: she exchanged the dark and light sides of the blocks in every second row, thus making the image shadow incompatible (redrawn in Figure 3D). The perceived lighting of the wall of blocks now impossible, but the illusion does not decrease at all. This demonstrates that not even the shadow-interpretation is necessary to account for the illusion. Since neither transparency, nor the perception of non-uniform illumination is necessary for the illusion to occur, it seems that intrinsic image models are unable to capture this set of phenomena. Bressan (2001) offers an explanation in terms of Gilchrist’s anchoring theory, which she develops further to devise the double anchoring theory (Bressan, 2006). Both versions of the anchoring theory will be analysed in the next chapter.

According to Kingdom’s (2011) classification, the approach represented by Adelson and Logvinenko is the weak form of intrinsic image models, since they take into account only obvious regions of non-uniform illumination or transparency. However, strong forms of intrinsic image models apply the same line of explanation for images where no such regions are present. The most known example is the scission theory by Anderson (1997) by means of which he attempts to account for the White effect (redrawn in Figure 4A). The explanation provided by Anderson’s scission theory is as follows:

The Munker-White illusion is the consequence of a perceptual scission that splits the lower contrast region along the top of the T into multiple sources.
(...) When the grey bars are embedded in a black stripe, the hypothesized

scission mechanism will treat the grey region as a product of a continuous black stripe and a light colored filter that overlies this black stripe. But when the grey bars are embedded in a white stripe, a scission mechanism will treat the grey region as a product of a continuous white stripe and a dark colored filter that overlies this white stripe. The claim here is that this decomposition causes the grey bars in the white stripes to appear darker because some of the lightness in the grey bars is attributed to a continuation of the white stripes, rather than the grey bars themselves. In a similar vein, the grey bars in the black stripes appear lighter because some of the darkness in the grey bars is attributed to the continuation of the black stripes, rather than the grey bars themselves. (Anderson, 1997, p.427).

A central component of the scission explanation is the junction structure of the image, as well as in Adelson's (1993) theory. Here, it is the T-junction at the ends of the targets (a T-shaped junction of luminance edges rotated by 90 degrees) that acts as a cue for the scission mechanism. However, the crucial role of T-junctions can be challenged by altering the junction structure of White's image. For instance, if the targets are lengthened so that they are as long as any other stripe in the image, as I did in Figure 4B, then no T-junctions are present in the image at the targets. Nonetheless, the effect can still be perceived. An even more effective argument against the role of junctions is a stimulus image by Hong and Shevell (2004). A similar variant was argued to refute any T-junction-based explanation of the White effect by Howe (2005), redrawn in Figure 4C. This image does not contain any junctions, not even L junctions, as the one in Figure 4B. The circular version of the White illusion is still as strong as the original one, even though no junctions are present at all. Therefore, it seems that the scission theory along with any other internal image model that is based on the junction structure do not hold in the case of the White effect.

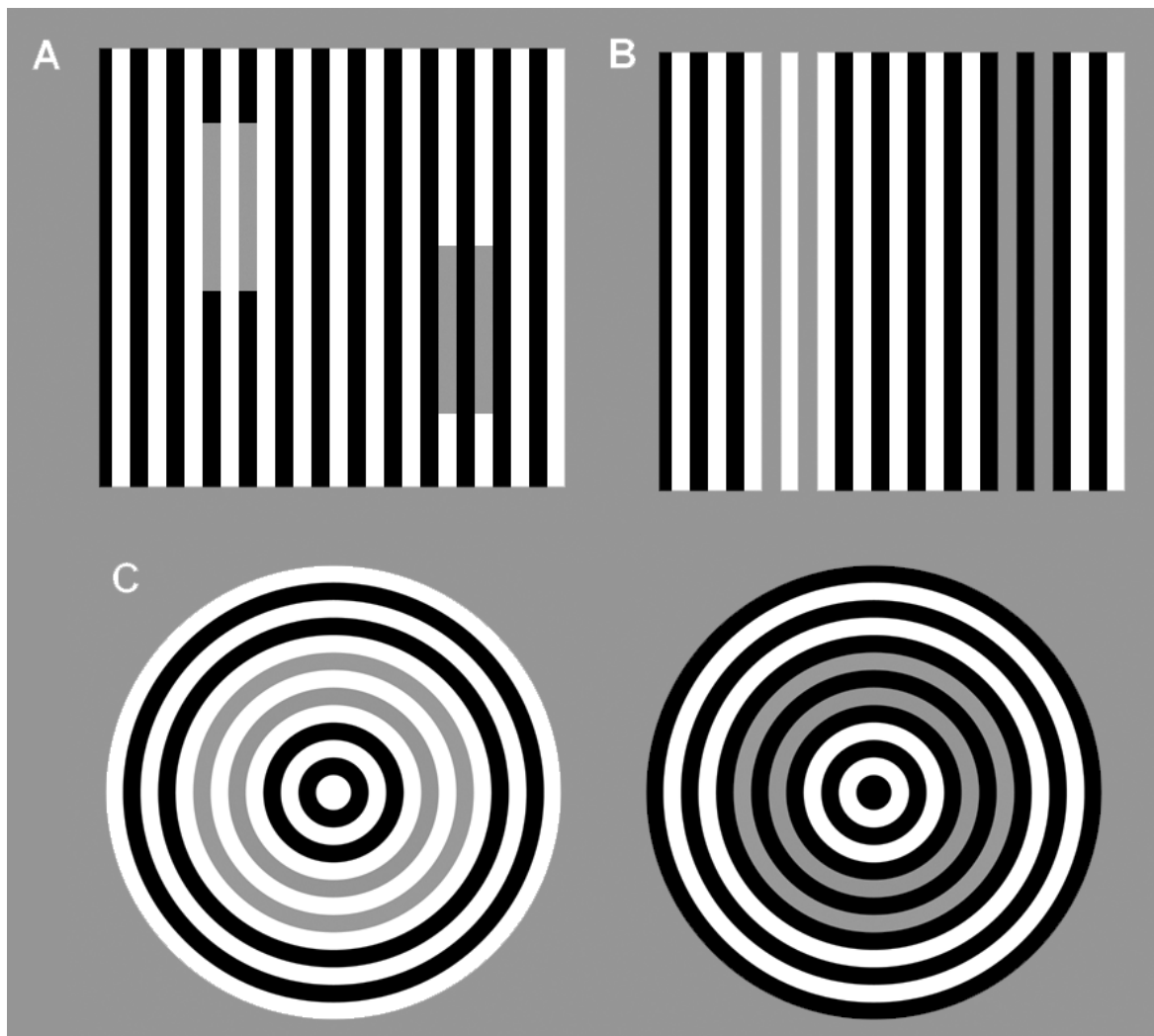


Figure 4. The White effect and its variants. In A, the original White effect is shown (redrawn after White, 1979). T-junctions are present at the ends of the grey targets comprising the luminance edges in the image. The stem of the T is the horizontal boundary edge of each grey target. The top of the T is the vertical edge segment adjoining the stem, separating the continuous black (or white) stripe from stripe interrupted by a grey target. Our variant in B includes no T-junctions, however, the illusion is preserved (unpublished). C shows that the illusion does not cease even when there are no junctions at all (redrawn after Hong and Shevell, 2004; Howe, 2005).

In the defence of the scission theory, however, one could argue that the scission mechanism could work based on a cue other than junctions to decompose the image into layers. For instance, due to the regularity in the pattern, the grey circles could be perceived as being superimposed on a black or a white circle (which could be inferred from the regularity of the pattern) and thus Anderson's above-cited explanation would still be plausible: the lightness of the grey circles could be attributed to the white ones on which they lie, and the darkness of the ones in D could be attributed to the black circles on which they are superimposed.

Contrary to this line of explanation is our set of phenomena we presented at ECVF 2009 (Hudák and Geier, 2009). We composed White's image of small randomly organised black dots replacing black stripes, and small randomly organised white dots replacing white stripes on a grey background. (Figure 5).

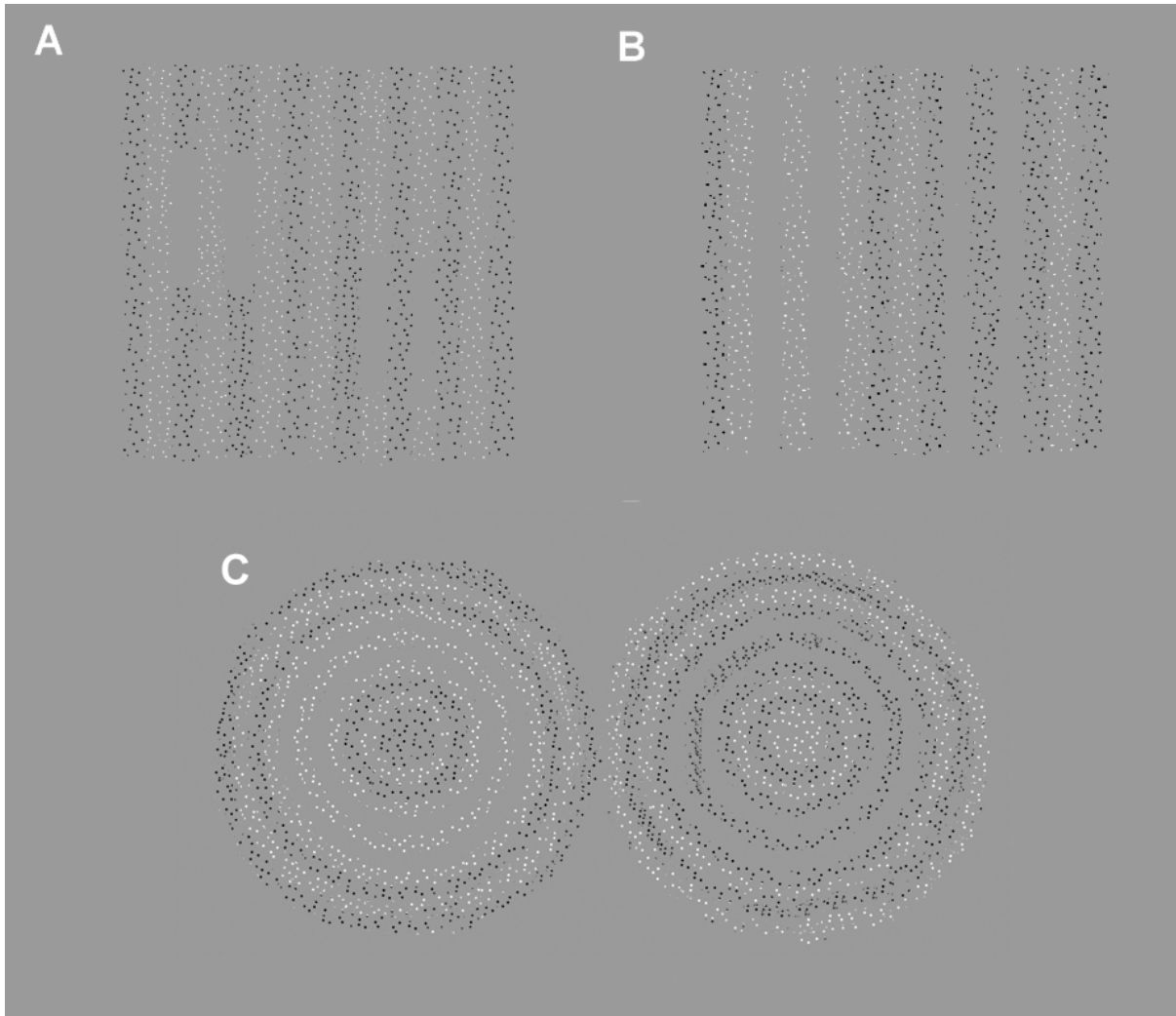


Figure 5. Dotted White effect and the dotted circular White effect. We composed White's illusion of white dots, black dots, and a homogenous grey background (A and B). The targets are therefore the gaps between the dots. The figure this way contains no junctions and no physical edges. White's effect, however, is still visible in this case: those gaps surrounded by white dots seem lighter than those surrounded by black dots. We also composed the circular White illusion of white dots, black dots, and a homogenous grey background. The illusion still works: the grey gap surrounded by white dots seems lighter than that surrounded by black dots.

The areas of the grey targets in the original White's illusion are left empty, so that they have the same luminance as the grey background of the whole pattern. Physically, the whole pattern is a homogenous grey except for the dots. White's effect, however, is still visible in

this case: those gaps surrounded by white dots seem lighter than those surrounded by black dots. Nonetheless, the figure contains no junctions. Here the only plausible cue for a scission mechanism would be to group white dots and black dots together, which appear to be superimposed on a grey background. However, at the locations of the targets, the only layer is the background itself; therefore, their different perceived lightness cannot be attributed to any layer decomposition mechanism.

In conclusion, neither the strong form (Anderson, 1997) nor the weak form (Adelson, 1993; 2001) of internal image models can fully account for the widened range of phenomena on which they are based. Therefore, it seems that a different type of theory should be sought. In the next chapter, another set of mid-level theories are reviewed, namely, the anchoring theory.

6.2.5 Mid-level theories: Anchoring

6.2.5.1 *The original anchoring theory*

Gilchrist et al (1999) and Gilchrist (2006) raise the issue that most models in lightness perception deal only with relative lightness values and ignore how certain luminance values are mapped into absolute shades of grey. Central to Gilchrist's anchoring theory is the problem how different luminance values are anchored to different shades of grey that are perceived.

He supposes three steps for this lightness computation made by the visual system. First, the visual scene is segmented into frameworks. Second, within each framework, two stronger (highest luminance rule and area rule) and one weaker (scale normalization) rules are applied for local anchoring to take place. Third, at the level of global anchoring, local values are weighted in accordance with the articulation and the area of the local framework, to receive their final absolute lightness values.

To demonstrate the anchoring theory at work, let us consider the explanation for the simultaneous contrast illusion. It comprises two frameworks. One framework is the grey target with its white surround, while the other framework is the other grey target with its black surround. First, according to the local anchoring, the target surrounded by black is assigned white, since this grey target has the highest luminance in its framework. The other target surrounded by white is not assigned white, since the luminance of its surround is higher. Second, due to the global anchoring, the target surrounded by black does not receive the value white, since the surround of the other target is also taken into account at the global

anchoring stage. Thus, since the target surrounded by black was assigned white in its local framework, and grey in its global framework, it will be assigned light grey. In contrast, the target surrounded by white is assigned grey both in its local and global framework, therefore its final value is mid-grey.

To segment the image to frameworks, as the first step of the anchoring theory, Gilchrist uses Gestalt grouping principles, such as grouping by similarity, common fate, good continuation and even T and X junctions. To support the role of T junctions in segmenting the image to frameworks, he uses the White effect. However, as it has been shown in the previous chapter (Figure 4 and 5) based on the work by Hong and Shevell (2004), Howe (2005) and Hudák and Geier (2009), the White effect does not depend on junction structure.

In further support of the role of belongingness, he also uses the checkerboard contrast illusion (DeValois and DeValois, 1988), redrawn in Figure 6A. The grey square surrounded by white ones seems lighter than that surrounded by black squares, which contradicts lateral inhibition. Gilchrist (2006) argues that essential to the illusion is that the grey square that seems lighter is grouped to the diagonal group of black squares, whereas the other grey square belongs to the diagonal group of white squares, on the basis of good continuation. Thus, the highest luminance rule (which will be discussed in more detail below), according to which the highest luminance in a local framework will be anchored to white, operates within the group of diagonal squares. The grey square belonging to the black group will therefore be assigned white within its local framework. The other grey square in the white group will not be assigned white, since it is not the highest luminance square in its group. Subsequently, due to the global weighting, the square in the black group will be assigned light grey, because in its local framework it was white, but in the global framework, the square is assigned grey (since the luminance of the white squares is even higher, therefore white will be assigned to them). The grey square in the white group, on the other hand, will not lighten, since it is not assigned white in its local framework, only grey.

It is also argued by Gilchrist that other ways of grouping are also present, such as the horizontal and vertical rows to which the grey squares belong due to good continuation; however, grouping by rows and columns predicts no illusion. On the basis of proximity, the grey squares could also be grouped with the adjacent white or black squares, but this grouping would predict a contrast effect rather than reverse contrast. According to Gilchrist, this is the reason why the reverse contrast effect is weak. However, he claims that the cause of the main effect is that the grey square is grouped to the diagonal group of white or black squares.

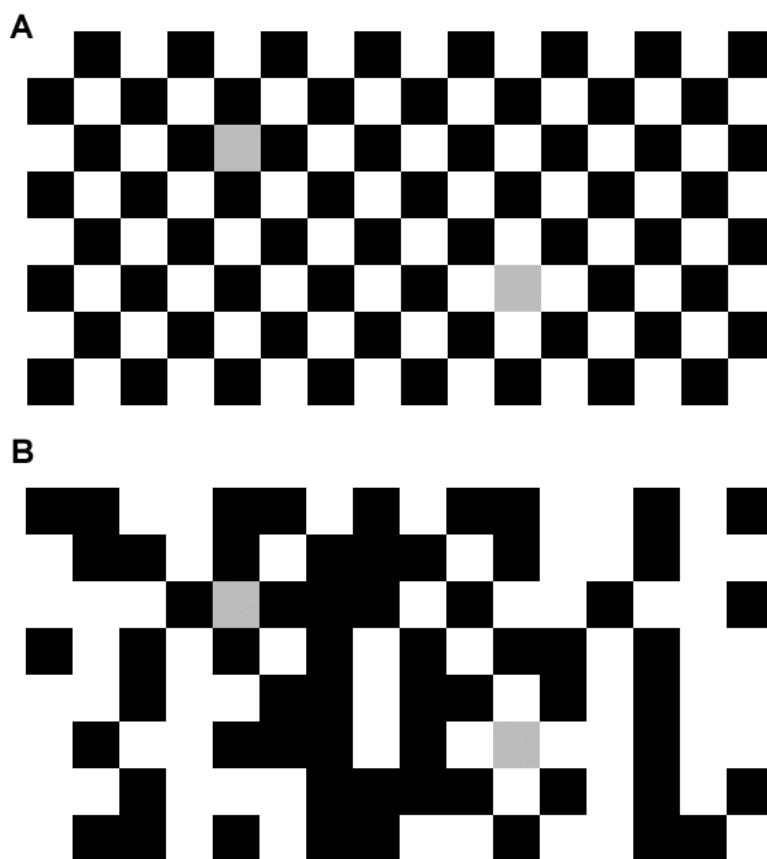


Figure 6. The checker-board contrast illusion (redrawn after DeValois and DeValois, 1988) and my randomized variant (in prep). In the original checkerboard contrast illusion (A), a reverse contrast effect occurs: the grey target surrounded by white squares seems brighter than that surrounded by black squares. Although the effect is attributed to the grouping of targets to the diagonal set of black or white squares and anchoring accordingly (Gilchrist et al, 1999; Gilchrist, 2006), the effect that the target surrounded by white is lighter seems to remain in my randomized variant (B), where no grouping to diagonal white or black set of squares is possible.

In Figure 6B however, I have modified the regular checkerboard background: the location of the black and white squares are randomized, maintaining the distribution of black and white in the image, and the articulation of the image also remains. The squares directly adjacent to the grey squares are kept constant, but the diagonal groups are scattered. Nonetheless, the effect that the target surrounded by white squares is lighter than the other seems to remain (in prep.). The illusion also persists when the background squares are flickered randomly, irrespective of the flickering rate (An animated demo is available at http://www.geier.hu/HM_Thesis/ , website courtesy of János Geier). In both versions, the effect seems stronger when the image size is reduced. Although this result is yet to be

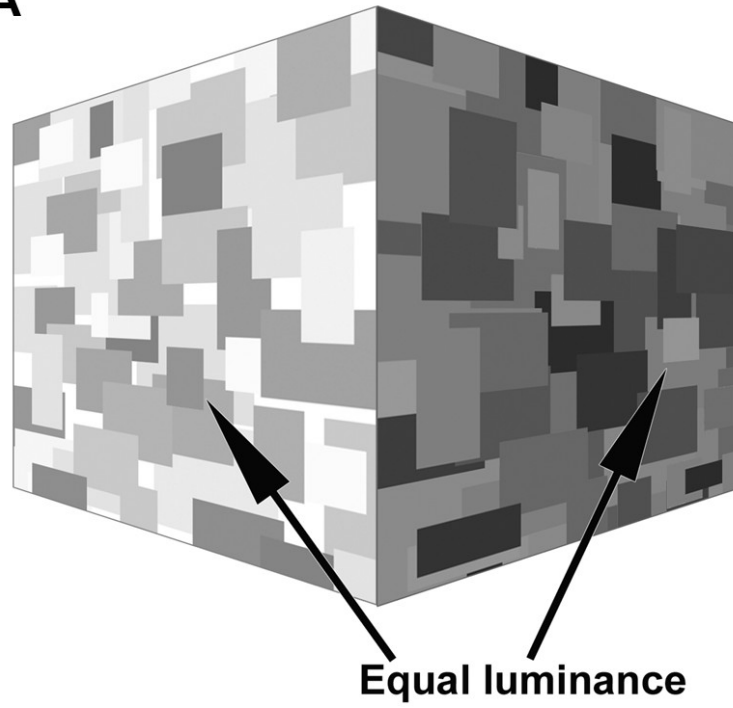
confirmed by more detailed psychophysical experiments with naive subjects in a next study, since at present only piloting data are available, it seems that belongingness and group segmentation by good continuation does not play a crucial role in the checkerboard contrast illusion. Nor does segmenting by T-junctions determine the presence of the White effect. Based on the above demo with the randomized checkerboard, it seems that the question of how the visual system segments the scene to frameworks in order to apply the anchoring rules within each framework might need to be further clarified, if these piloting results are confirmed by my next experiments, in which I plan to use nullifying technique.

According to the anchoring theory, after segmenting the image to frameworks, three anchoring rules are applied, among which the most essential one is the highest luminance rule. As it was mentioned above, the highest luminance rule implies that the highest luminance within a framework is automatically assigned white. Gilchrist demonstrates this rule at work by a Mondrian cube, redrawn in Figure 7A. His argument goes as follows:

‘Consider the two targets marked as equal in luminance. The target on the shadowed right side appears approximately white, *because it is the highest luminance in its framework*. It would be seen as pure white if the image on the right were painted onto the inside of a dome so that it filled the whole visual field. However, in the context of the adjacent lighted Mondrian, that target appears light gray rather than white. This illustrates the co-determination. Both parts of the compromise are phenomena available here. If there were local anchoring but no global anchoring, the right-hand target would appear white. If there were no local anchoring, it would appear the same as the left-hand target. Clearly the percept lies between these values.’ (Gilchrist, 2006, p. 300-301, italics by HM).

However, in Figure 7B, I have inserted three rectangles in the shadowed framework whose luminance is higher than that of the original target. Therefore, the original target should not be assigned white within its local framework. Still, the effect does not change: the target in the shadowed framework seems still lighter than the one in the illuminated framework. Therefore, the effect which is intended to demonstrate the highest luminance rule at work is not due to the highest luminance rule.

A



B

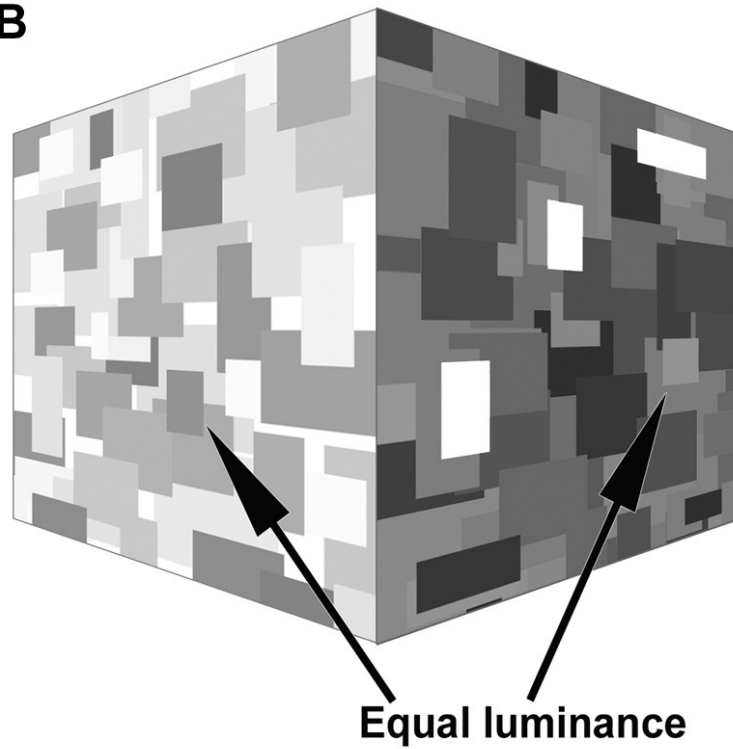


Figure 7. The highest luminance rule at work. In 7A (redrawn after Gilchrist, 2006), the right target seems lighter than the left target, although they are of equal luminance. The anchoring theory (Gilchrist et al, 1999; Gilchrist, 2006) explains this

phenomenon with the highest luminance rule, i.e. the right target is lighter because it has the highest luminance within its framework. In Fig. 7B, I have inserted three additional rectangles, whose luminances are higher than that of the target. Nonetheless, the illusion remains. Thus it cannot be explained by the highest luminance rule.

Another problem with the highest luminance rule is acknowledged by Gilchrist (2006), namely, the problem of self-luminosity. If one looks at a white ceiling, on which a light-bulb is turned on, then one will perceive the ceiling still white, although much more luminance is emitted by the bulb. As he puts it, ‘The very appearance of self-luminosity directly contradicts the highest luminance rule, according to which white is a ceiling above which no surface can appear.’ (p. 228). He argues that the lightness scale is finite, which is embedded in and slides along an infinite luminance scale. This means that the upper boundary of the lightness scale is the luminosity threshold, which can occur at any luminance level. However, it is still not clarified, how the highest luminance rule should be applied, when a self-luminous object is present in a framework that also contains white. Therefore, the area rule is also needed to account for the effect, which is the second major rule of the anchoring theory.

The area rule implies that the lightness of a surface depends on its relative area, while the relative luminance is constant. Gilchrist (2006) demonstrates its plausibility by a display redrawn in Figure 8A. Here, the larger dark grey disk on the right appears lighter than the small dark grey disk on the left, although they are physically equal. He argues that this difference in the perceived lightness is due to the difference in the area of the disks.

However, it is to be noted that the large disk on the right is surrounded by black (and thus it is an increment relative to its background), whereas the small disk on the left is surrounded by light grey (thus being a decrement). Therefore, this display might also be considered as a variant of the simultaneous contrast display. To test this claim, I have replaced the black background with a white one in Figure 8B. Although I have not yet confirmed it by psychophysical experiments at present, it can be seen in the demo that the perceived difference in the lightness of the two dark grey disks is largely decreased or ceased, which implies that the relative area has less effect here than the luminance ratios relative to the immediate surround.

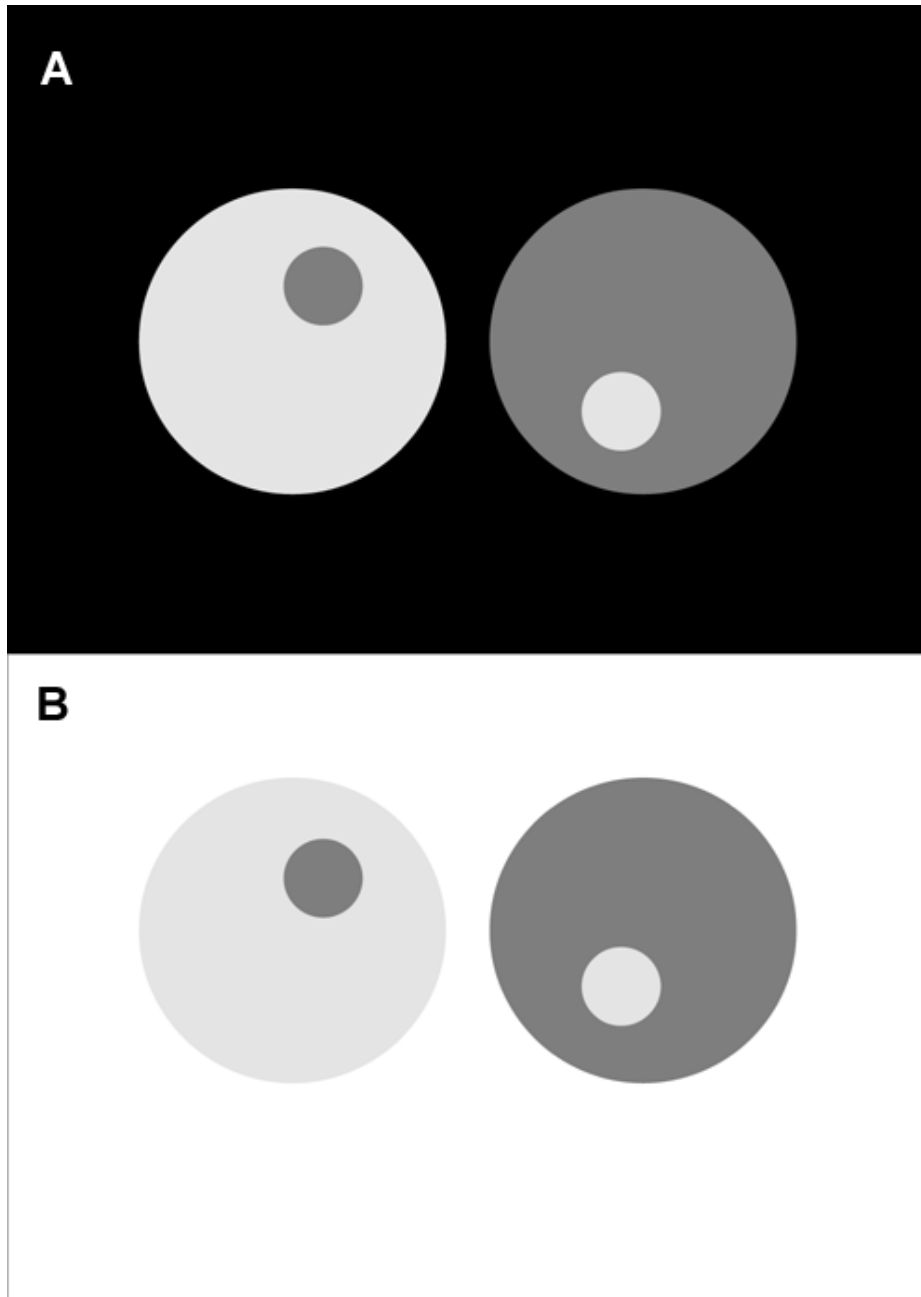


Figure 8. The area rule at work. In Figure 8A, the left small dark grey target seems darker than the right large dark grey target, which is attributed to the area rule by the anchoring theory. According to this rule, the larger area is perceived lighter if luminances are equal. However, the large grey disk on the right is an increment relative to its immediate background whereas the small grey disk on the left is a decrement. In 8B, I have changed the background to white, making both dark grey disks decrements relative to their immediate backgrounds, which made the illusion disappear. Thus, the area rule cannot account for this illusion.

The third, weaker rule upon which the anchoring theory builds is the scale normalization rule. Gilchrist (2006) defines it as ‘a hypothetical process by which the perceived range of greys in a framework shifts toward the standard white/black range (30:1),

relative to the physical range in the stimulus' (p. 379). When the luminance range in a framework is less than the white-black range, some expansion, i.e. a perceived contrast enhancement occurs, which is demonstrated by the contrast-contrast illusion by Chubb et al (1989). Since it is claimed to be a weaker rule by Gilchrist (2006), and applies only when the luminance range is other than the usual black-white range, leaving most known brightness illusions unmodified, no counter-arguments will be raised against this rule here.

However, based on the above demos that show the problems concerning the two main rules upon which the anchoring theory is built, and also the uncertainties concerning some factors of image segmentation to frameworks as discussed above (which are to be confirmed by experiments with naive subjects in my subsequent studies), it seems that the original anchoring theory (as described by Gilchrist et al 1999 and Gilchrist, 2006) needs to be further clarified. An attempt to develop the anchoring theory further was made by Paola Bressan, which will be discussed in the next chapter.

6.2.5.2 Double anchoring theory

Bressan's (2006) double anchoring theory is a very complicated theory, therefore describing it in full detail would exceed the scope of this thesis. The main points seem to be, however, that it uses two rules within each framework to assign provisional lightness values, then takes the weighted averages of these territorial lightness values of each framework as the final perceived lightness values. The first rule that operates within the frameworks is the highest luminance rule, as well as in Gilchrist's theory. The second is the surround-as-white rule. The double anchoring theory defines both the highest luminance of a framework and the surround luminance of a target region as white. Bressan defines the concept of surround as any region that is grouped together with the target, which is not necessarily retinally adjacent to that region. The grouping of regions takes place on the basis of Gestalt principles, such as proximity (retinal adjacency) or similarity (of shape or luminance polarity). The weight of each framework at the final lightness assignment depends on the relative strength of the grouping forces that work in co-existing frameworks.

The cardinal demonstration of the double anchoring theory at work is the dungeon illusion (Bressan, 2001; 2006), redrawn in Figure 9A and B. In Figure 9A, the physically identical grey disks on the left seem lighter than those on the right, although a contrast theory would predict the opposite.

Bressan's (2006) explanation is as follows: the target grey disks on each side are grouped to two separate frameworks: one framework is the rest of the disks, the other one is

the background. The target disks are grouped to the surrounding disks on the basis of (i) their identical luminance polarity compared to their common background and (ii) their shape similarity. On the other hand, the only factor that groups the target disk with the background is retinal proximity, which Bressan considers to be the weakest among grouping factors, since it implies only simultaneous presence in the visual field. Therefore, the lightness of the target disks are influenced more strongly by the surrounding disks than by the background, because there are two factors that links them together and both are stronger than the one that groups the target disks with the background. Applying the highest luminance rule within the framework of the surrounding disks, the targets on the left will be assigned white, whereas the ones on the right will be assigned grey. Due to the surround-as-white rule, the targets on the left will be super-white, while the ones on the right will be grey again. Therefore, the model correctly predicts that the disks on the left will be perceived lighter than those on the right.

However, it should be noted here that the role of shape similarity is not proved in Bressan's paper, since no image is included in which the target and the surrounding shapes vary randomly. If this variation does not modify the perceptual experience, then it is questionable whether the illusion is due to the stronger grouping to the surrounding disks indeed. This possibility is not investigated by Bressan.

In Figure 9B, Bressan's double-decrement variant is redrawn, in which the targets on the right are seen lighter. She argues that this phenomenon further supports her theory. According to her line of thought, if the target disks were grouped more strongly to the contextual disks both on the left and the right in Figure 9B (as it was in the case of Figure 9A), then this grouping would predict the opposite effect, i.e. the target disks on the right should be seen as darker than those on the left (since, in that case, the physical surround of the left-targets would be grey, while that of the right-targets would be white). However, the phenomenon is the opposite. She claims that this is because the framework of the contextual disks on the right is significantly weakened, since the luminance polarity of the target disks and that of the surrounding disks is not identical anymore compared to their common surround. Therefore, a strong grouping principle is abolished here. Thus, the disks on the right are grouped more strongly with the background, while the targets on the left are still grouped more strongly with the surrounding disks. On this basis, she claims that reverse contrast is abolished, and ordinary contrast occurs instead.

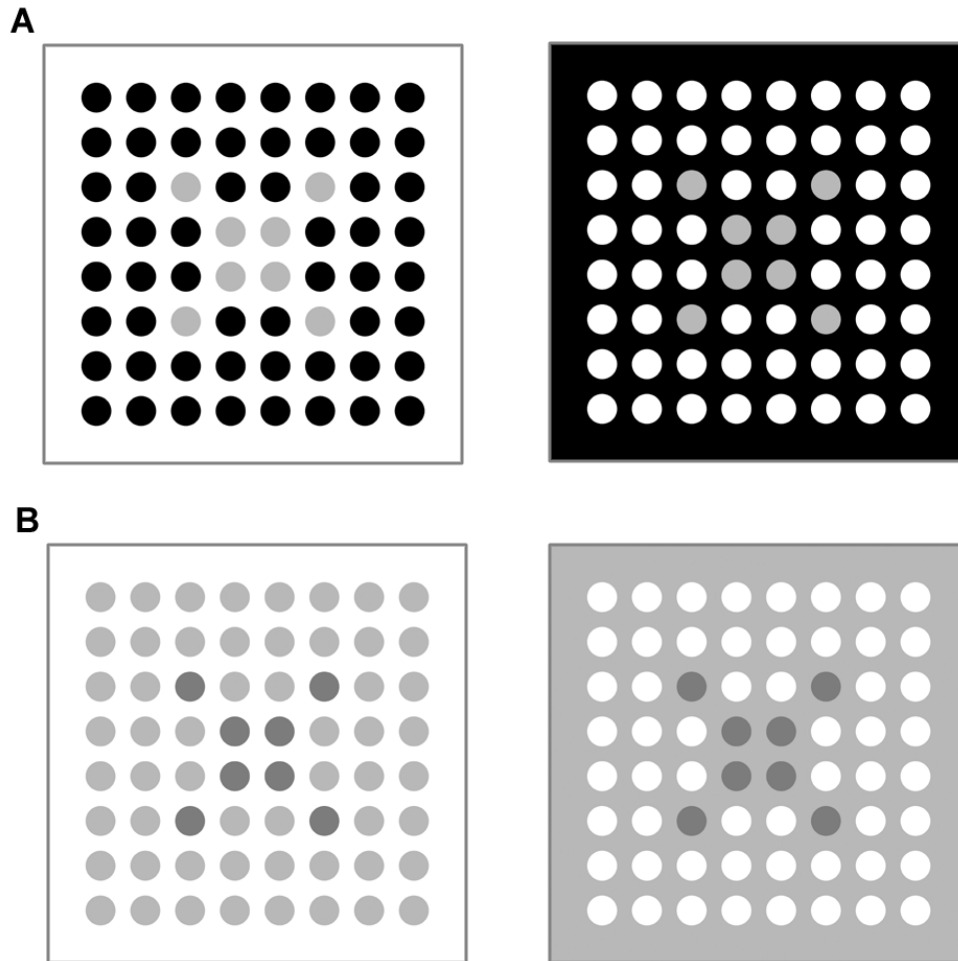


Figure 9. The dungeon illusion. The target disks in the middle of each panel are of equal luminance. In 9A, the original Dungeon illusion is redrawn after Bressan. Here a reverse contrast/assimilation effect is observed: the targets surrounded by white on the left seem lighter than those surrounded by black on the right. Bressan attributes this to the claim that targets are grouped to the surrounding disks rather than to the background due to their similar shape and their identical luminance relation relative to the background. Thus the highest luminance rule is applied within the framework of disks, which correctly predicts the effect. In 9B, ordinary contrast is perceived, i.e. disks surrounded by white seem darker. According to Bressan's explanation, in the right image, the luminance relations of target and surrounding disks relative to the background are not identical, thus there the targets are grouped to the background. According to Bressan, this accounts for the opposite effect. However, serious doubts can be raised against this claim (see text for details).

However, if this line of argument is analysed in more detail, then it seems to hold some imperfections. Bressan claims that on the left, the target disks are grouped to the contextual disks due to their identical luminance polarity relative to their common surround and their similar shape. On the right, however, the target disks are grouped to the background, since the identical luminance polarity is abolished. Thus, we will obtain a framework on the

left side in which the targets are physically dark-grey, and their surround (the contextual disks) are light grey, whereas on the right-hand framework, the targets are also dark grey and the surround is also light-grey (which is now the background due to the different grouping as suggested by Bressan). Thus, both on the right and on the left, the dark grey targets are grouped strongly to a light-grey surround, and loosely grouped to a white surround. Therefore, the relative luminances in the frameworks on the two sides are identical. It is now unclear why one should see any difference between the targets on the left and on the right, on the basis of Bressan's argument. However, the phenomenon is that there is a difference, which is thus unexplained by the double anchoring theory. The perceived phenomenon does not follow from the presented line of thought.

It might also be noted that even if the grouping factor of luminance polarity is abolished on the right side, it is not clear why the grouping with the background should be stronger than the grouping with the contextual disks, since the grouping factor in the first case is only retinal proximity, which Bressan has claimed to be the weakest among grouping factors. Grouping by shape similarity, which must be then stronger than proximity, however, would encourage grouping with the surrounding disks even on the right side. According to Bressan's previously mentioned claim, however, grouping with the surrounding disks on the right as well as on the left would predict an opposite effect to that actually perceived.

Consequently, it seems that the double anchoring theory cannot account for the phenomenon which was designed in order to support it. Neither does it resolve the problems discussed previously with regards to the highest luminance rule, upon which this theory also builds. However, the double-anchoring explanation of the dungeon illusion might be amended from other principles from the theory itself, described by Bressan elsewhere with regards to other brightness problems than the dungeon illusion, but without any explicit clarification, it is not clear how the double anchoring theory would handle the referred problem. Since the theory is complicated, it is difficult to draw clear predictions from it as a whole.

6.2.6 A low-level alternative: activation spreading alias filling-in

In our search for a theory that accounts for most known lightness-brightness illusions, we now return to an old idea which builds upon low-level mechanisms, namely, on the spreading of activation in the neural tissue. Although it is a low-level approach, it is essentially different from those that are based on lateral inhibition and filtering. Central to lateral inhibition-based models is the pointwise filtering of the image with a DoG-like weight

function that is the abstraction of lateral inhibition in receptive fields. As discussed above, such filtering may include various spatial scales (see section ‘Recent lateral inhibition-based models’), and the final predicted brightness profile is the sum (or weighted sum) of the filtered images. In a neural spreading or filling-in model, filtering serves only as a first step, as an input for the neural spreading level, where the spreading neural activity might either be inhibitory or excitatory. The other main difference is that the output of a filling-in model is not the direct result of filtering, rather the equilibrium of the diffusion of neural activity that starts from the locations of the tissue corresponding to the edges found in the image.

One of the most known filling-in model was elaborated by Grossberg and Todorovic (1988) in 2-D. An earlier version of this model contained only 1-D simulations (Cohen and Grossberg, 1984). They apply 6 levels of processing. The first level is to code the physical luminance distribution of the image, i.e. to submit the input image for the simulation. At the second stage, a DoG filtering is obtained. Here they refer to both OFF and ON centred antagonistic retinal ganglion cells, however, what they really use is only the outputs of the ON-centred ones, and as it turns out from the appendix, the only size is a 3x3 pixels filter, which is a Laplacian kernel (János Geier, personal communication). The output of the Laplacian filtering is afterwards rectified, and sent as an input for level 3 and 6. At level 3, an orientation-selective filtering takes place using 12 orientations, whereby the authors claim to simulate cortical simple cells. Level 4 preserves only the orientations from the output of Level 3, and disregards its contrast polarities, whereby the authors intend to simulate complex cells found in V1. Level 5 works as a thresholding mechanism: those Level 4 signals that exceed a threshold, will serve as boundary signals in level 5.

To understand the role of level 5, we must first have a look at level 6, which is the essence of the model, and whose output is the predicted perceived brightness profile. Level 6 simulates the activation spreading in the neural tissue. The input of this level is the output of Level 2, which is the inhibitory and excitatory poles generated by the 3x3-pixel ON centre-OFF surround receptive field. These excitatory and inhibitory signals diffuse along in the tissue comprising abstract neurons closely connected to each other. The signal from each cell therefore can easily spread to its immediate neighbours, and it spreads in an iterative manner in the computer simulation. The spreading of the signal is obstructed by edge signals generated in Level 5. The final predicted percept is the equilibrium level of the diffusion process.

Grossberg and Todorovic (1988) simulate some images in which no illusion is seen, such as a ying-yang square or a Mondrian. Using the 2D version of the diffusion model, they restore the original images properly. They also attempt to simulate some illusions as well. First, they present some 1-D simulation results. The simultaneous brightness contrast is rightly predicted by the 1-D simulation. They also claim to simulate brightness constancy by using an input stimulus, comprising a shallow luminance ramp containing two grey targets at its light and dark ends. They claim that this luminance ramp represents inhomogeneous illumination. However, it is questionable whether this stimulus is perceptually equivalent with inhomogeneous illumination indeed. They run the simulation for this image only in 1-D, which makes the ramp totally flat. However, if one looks at any of the ramped images in our Study II for instance, it can be seen that luminance ramps do not usually flatten perceptually. This mistaken prediction, which is not acknowledged by the authors, is probably caused by the fact that the 1-D simulation does not take into account the upper and lower boundary edges neither of the luminance ramp, nor that of the grey targets.

Thus, 1-D simulations are not really worth being taken into consideration, since both in natural images and in images eliciting illusions, the entire edge-structure of the image can influence the perceptual experience. In our Chevreul variants presented in Study II, for instance, a 1-D simulation cannot even take into account the effect of the luminance ramp. The authors themselves also acknowledge the problem of 1-D simulations by presenting two versions of the Craik-O'Brian-Cornsweet illusion. One variant has only the COC profile in the vertical midline of the image, but no upper and lower boundaries are present; there are no enclosed areas. In this case, the illusion disappears. In the other variant, the two halves of the image are enclosed by boundaries, and the illusion is visible. By means of the 2-D simulations of their activation-spreading model, they successfully predict the presence of the illusion in one image, and the absence in the other. Therefore, their 2-D model seem to be promising.

A frequent criticism against the Grossberg-model is that it is unable to predict the lightness-difference in a staircase pattern: 'Perhaps an even greater challenge to filling-in models is a luminance staircase distribution. The "steps" of the staircase presumably block diffusion, and it is not evident how a filling-in model can predict that different steps appear with different brightnesses (since "border contrast" is the same everywhere)' (Pessoa et al, 1995, p. 2216). This argument is also quoted by Gilchrist (2006) against the Grossberg-model. However, it is not clear why the Grossberg-model would fail to simulate a luminance staircase distribution (now irrespective of the Chevreul illusion it elicits), since in Grossberg

and Todorovic's (1988) paper, successful 2-D simulations of Mondrians are found, besides the Koffka-Benussi ring, which also contains at least three equal luminance steps and boundaries. Pessoa et al (1995) might have ignored the 2-D nature of the Grossberg model, which takes into account the horizontal boundaries as well as the vertical ones. Their criticism would hold probably only for the 1-D simulation of the staircase (Pessoa et al (1995) themselves use only 1-D stimuli and simulations).

Where the Grossberg model fails indeed is the Hermann-grid illusion, which is also acknowledged in the paper. Simulations are successful only if the streets of the Hermann-grid are so extremely narrow (2 pixels) that the diffusion cannot get into the street-sections. In order to simulate the original Hermann grid illusion, they suggest that they should apply emergent contours, which they claim to be out of the scope of their paper. No attempt is found in their paper to simulate the White effect, which is one of the basic phenomena that is expected to be predicted by a unified model of brightness perception. Moreover, neither the Mach bands, nor the Chevreul illusion is attempted to be simulated, which is an essential shortcoming, if the aim is to account for the overall pattern of brightness errors.

What is most apparent with regards to the Grossberg-model is its complicated nature. The model is presented in the appendix by means of a huge set of differential equations, including the calculation of membrane potentials of the hypothesised cells and other physiological features that are not indeed used. In addition, the textual description of the model aims to include all levels of known physiological phenomena, which seem to have been included in the model only to fulfil the expectation that a computational model should be aligned with physiological results. Hereby the levels described by Marr (1982) are mixed, which makes the model overcomplicated. It is probable that the over-complicated nature caused this type of model to be less appreciated and understood in detail among visual scientists.

An attempt to further develop the Grossberg-model in order to be able to predict a larger range of phenomena was made by Pessoa, Mignolla and Neumann (1995). However, two objections must be raised against this model. First, as it was mentioned above, they use only 1-D simulations, which is evidently unable to predict phenomena influenced by the 2-D structure of the image (e.g. COC, ramped Chevreul, as mentioned above). Second, instead of simplifying the model, they included additional components, including multiscale filtering as well. However, I regard it unnecessary to include all components known from physiological studies in a computational model, if it is able to simulate a wide range of brightness

phenomena successfully without including them. It is sufficient if such a model is anatomically plausible. If it is capable of modelling the overall pattern of brightness phenomena well, and it is anatomically plausible, then the model should be considered to be plausible physiologically as well: it might provide physiologists with new ideas concerning what mechanisms should be searched for.

Such simplified diffusion-based models have been developed by Tom Cornsweet (unpublished paper, personal communication) and János Geier (Geier, 2009, Geier, in prep.). Cornsweet's diffusion model contains 3 stages. The first stage is the input image itself. Second, it convolves the input image with a series of centre-surround antagonistic filters, whose total weight is always zero, and whose centre is always 1 pixel large. The size of the surround varies so that the total weight of each filter remains zero. The outputs of these different filter sizes are added up pixel by pixel to form the input for the final stage: the diffusion process, which works in an iterative manner, and interaction takes place between immediate neighbours within each iteration. The inhibitory and excitatory activation thus spreads along the entire image until the diffusion process reaches equilibrium (no further change takes place). The output of this filling-in stage corresponds to the predicted percept. Cornsweet's model thus does not contain edge detection and segmentation. The output of the equilibrium level is the exact copy of the input image, including a little blur.

In order to simulate illusions, Cornsweet argues that the filling-in process does not ever reach equilibrium, because eye movements interrupt the process earlier. If the simulation is stopped at a midway stage towards equilibrium, then it predicts the tendencies of illusions such as the simultaneous contrast, the Chevreul illusion, the White effect and the checkerboard contrast. However, the time at which the diffusion is stopped is arbitrary in the model (in some cases, it is after 300 iterations, in others, it is after 700). Moreover, stopping the simulation at such early stages wrongly predicts scalloping in perceptually homogeneous areas (e.g. a white or black area is only white or black near the edges, but it remains mid-grey towards the inner parts, since the diffusion has not reached there by the time the simulation is stopped). Thus, it can be said that the tendencies of the basic illusions are predicted relatively well, the output image, however, does not correspond with the perceptual experience.

János Geier has also devised a diffusion-based filling-in model (Geier, 2009, paper in prep). The basis of his model is the mathematical theorem that if an input image is filtered with a Laplacian filter, and if this filtered image serves as a constant input for a homogeneous linear diffusion process, then the output image will be identical with the input image at

equilibrium. In the model, the input image is the physical luminance distribution and the output image is the predicted brightness profile.

On the basis of this mathematical theorem, this model comprises 3 subsequent stages. At the first stage, the original greyscale image is taken as an input. This input image corresponds to the physical luminance distribution on the retina.

At the second stage, the input image is filtered by the Laplacian filter (which is a 3x3 pixel ON-centre-OFF-surround filter). Hereby the edge-structure of the image is extracted – or more precisely, the second-derivative structure of the image is mapped. This is how the retina represents the input according to the model. This representation is also an image, which might be considered as a sketch of the input image, in which the large homogeneous areas are yet empty. This image therefore comprises only the second derivatives of the original input image, i.e. the absolute luminance is not represented yet. This way, the visual system compresses the information into this sketch to forward it to the third stage, where the percept itself is generated.

At the third stage, neural signals spread from the edge-structure extracted by the second stage. This edge-structure or second-derivative structure serves as the source of signals that spread all over the image, generating the final brightness profile when reaching equilibrium at the end of the process. The spreading of signals is comparable to the diffusion of heat. The positive values in the image containing the second-derivative structure serve as the heat sources supplying the diffusion process, whereas the negative values are the “sinks” of the diffusion, where the heat leaks away. The common term for these sources and sinks is poles. From the positive poles, in neural terms, excitatory signals are spreading in the thick tissue of neurons, similarly to the spreading of warmth in a copper sheet that is heated at a certain location. Negative poles swallow the signals, analogously to the cooling of certain points of the copper sheet. If the sheet is heated at one point and cooled at another continuously and constantly, then after a while, no change of heat will occur at any point of the sheet. This is when the heat diffusion process reaches equilibrium. In the brightness model, there is also a point when no further change occurs in the balance of neural signals. That is the equilibrium of the model, which it reaches in an iterative manner in its computer simulation. This means that the process restores the original image merely from its second derivative-structure.

If the spreading of neural signals in the visual system followed the standard, theoretical diffusion equation of heat, then no deviation would occur in the perceptual

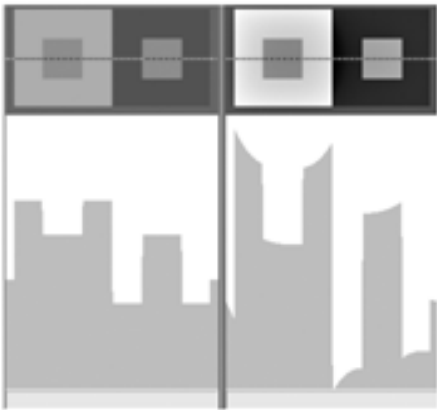
experience from the physical images. Thus, the predicted brightness profile would exactly be the same as the original physical luminance profile.

Therefore, the model postulates that the visual system deviates from the theoretical diffusion equation by not transferring all signals linearly. If this third, restoring stage were fully precise, then no illusions would occur; the original image would be restored without any error. However, according to the model, some imprecision occurs at this stage. Such non-linearities, for instance, could be the weakening or loss of signals when they are crossing other signal sources. On this basis, edges can obstruct activation coming from farther edges (see our double-ramped version of the Chevreul illusion in Study II). Another possible non-linearity is that the conductance between two neighbouring points decreases if the activity spreading increases between them. The image produced by the somewhat distorted theoretical diffusion of neural signals reaching equilibrium is the predicted brightness profile, which is supposed to match with what human observers see in case of the same input image.

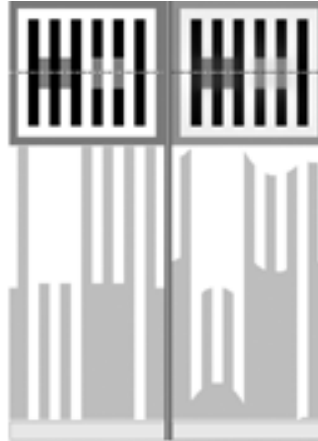
Therefore, if the standard diffusion equation is somewhat “ruined”, then it is capable of predicting a wide range of illusions fully in accordance with human perception, when applied at the final, filling-in stage. As opposed to Cornsweet and Pessoa, Geier does not apply multi-scale filtering prior to the diffusion process, nor does he apply preliminary edge detection, as opposed to Grossberg and Pessoa (i.e. the second derivatives extracted by the Laplacian filtering are not categorized to be edges or gradients; the raw output of the Laplacian filtering is used as source of the diffusion). The simulation always reaches equilibrium as opposed to Cornsweet’s method, and the illusions originate from the deviations from the standard diffusion equation at the third, filling-in stage. Thus, no arbitrary or free parameter is present in the model. Stopping the simulation earlier is not necessary to account for the illusions; the non-linearities used are fully sufficient to account for a wide range of phenomena.

By means of the same non-linearity parameter setting, the model successfully predicts the three basic illusions: the simultaneous brightness contrast, the White effect and the COC illusions (see Figure 10), which means that no separate mechanisms should be assumed to lie behind these seemingly rather different phenomena. The same parameters also predict both the original and our ramped Chevreul illusion, the Mach bands, the Vasarely illusion, the Todorovic illusion, the Logvinenko illusion, the checkerboard contrast illusion, the grating induction, as well as a range of illusions by Adelson, such as the checker shadow, snake, plaid, etc. illusions.

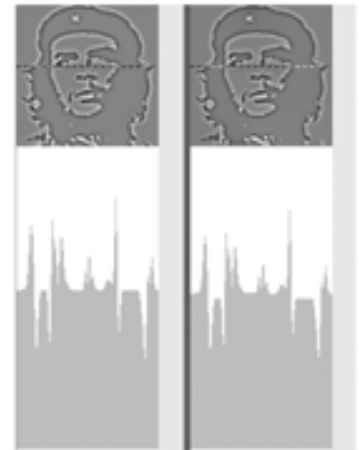
When applying the algorithm with the same parameters to real-scene pictures, the differences between the input image and the final output are undetectable (see Figure 10 for simulation output examples). Thus, approximately 90% of recently known brightness illusions can be predicted by the current version of the model without changing any parameter, and some others are also accounted for by slightly changing the parameters (e.g. our dotted White effect).



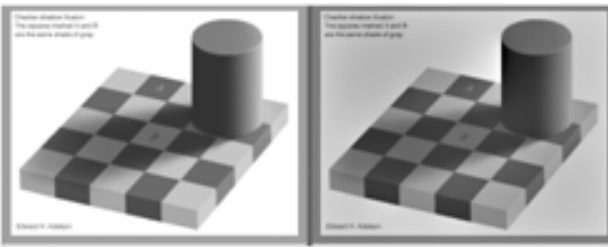
Simultaneous contrast



White effect



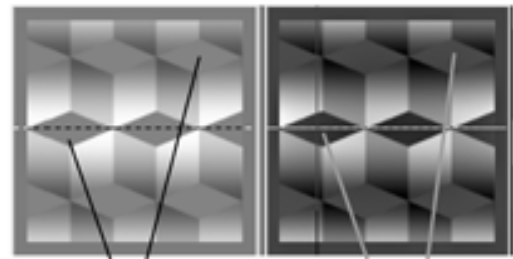
COC illusion



A=107 B=107

A=87 B=111

Adelson's Checker Shadow illusion

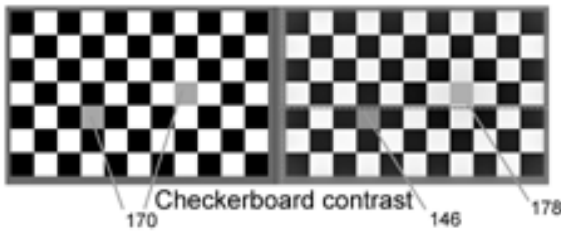


132

39

67

Logvinenko illusion

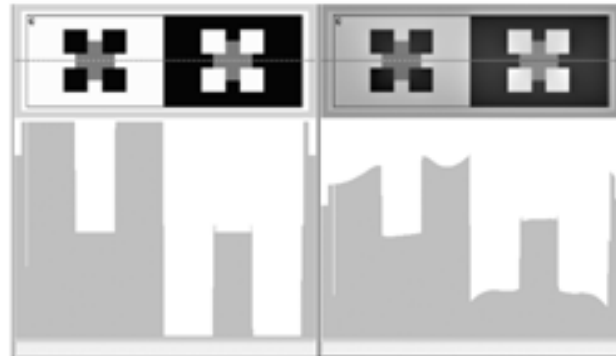


170

146

178

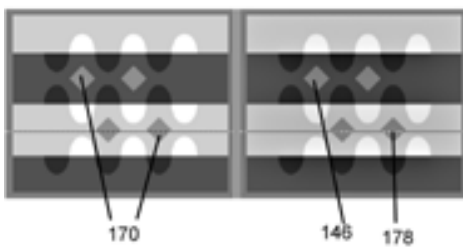
Checkerboard contrast



Todorovic's illusion



Ramped Chevrel illusion



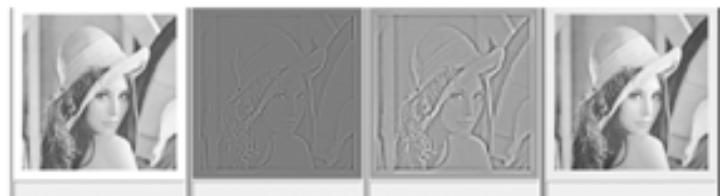
170

146

178

Adelson's snake illusion

Natural image



Input

Laplacian-filtered image

Midway towards equilibrium

Equilibrium

Figure 10. The input and output images of Geier (2009) model (images supplied by the author). In each image pairs, the left image is the original input image of the model, on which the simulation of the neural activation spreading was run. The right image is the output corresponding to the predicted brightness distribution. The grey plots below images represent a cross-section of the luminance profile of the particular image. Brightness values are given on a scale between 0-255, as represented by the computer. It can be seen that the model predicts all illusions presented here in accordance with human perception.

A challenge is a variant of Adelson's argyle illusion (Adelson, 1993, Fig. 4C). The model predicts well the presence of illusion of the original argyle, and its absence in the variant 4B. However, no illusion is predicted for 4C, where the illusion returns for human observers.

Another challenge for the current version is the Hermann grid illusion, since at equilibrium, the diffusion reaches the intersections as well as the street sections equally, thus no spots are predicted. (If the diffusion process is stopped earlier, as Cornsweet does, then the presence of the spots is predicted well, but in that case, the same criticism would hold as for Cornsweet's model).

However, an earlier version of Geier's model can account for the presence of the spots in the original Hermann grid and for their absence in our curved ones. This version of the model maps the first derivatives at the second stage, which is in fact a 2-D vector at each point, whose components are the partial derivatives of the luminance distribution in x and y directions. This version of the model also uses another formula at the third stage. Thus, the activation spreads in a somewhat different manner: from each edge segment, excitation spreads towards the light side of the edge, whereas inhibition spreads towards its dark side. This spreading is strongest in the direction perpendicular to the edges, and a weaker spreading takes place in other directions deviating from perpendicular in a Gaussian distribution. The spreading is weaker farther from the edges. This activation spreading model accounts for the entire range of the Hermann grid phenomena presented in Study I.

In case of the original, straight-edged Hermann grid, the excitation spreads to the white street sections perpendicularly to the black-white edges. Therefore, the street sections brighten. However, no excitation spreads into the intersections, since the direction of the spreading is perpendicular to the edge segments. In case of the curved grids, however, the spreading of excitatory signals reach the intersections as well, since due to the curvature, many edge segments are oriented so that a perpendicular spreading originating from them will

head straight into the intersections. Therefore, no difference will occur in the brightening of street sections and the intersections.

This is in contrast with the original Hermann grid, in which the intersections do not receive excitatory signals, thus they do not brighten as the street sections, which causes the brightness difference between the intersections and the street sections. Therefore, dark spots are seen at the intersections of the original Hermann grid, but no difference is perceived between the intersections and the street sections of the curved grids.

Besides the Hermann grid phenomena, other classical illusions, such as the Chevreul illusion or the simultaneous contrast are also predicted well by the computer simulation of this earlier version of the model.

Thus, now the challenge is to attune the two versions of the model so that it should be able to capture both the set of the Hermann grid phenomena and the rest of the brightness illusions. It should be born in mind, however, that the Hermann grid illusion might be an exception among brightness illusions: it is the only illusion that disappears under foveal vision, and in case of rotation by 45 degrees (Spillmann and Levine, 1971), which are both exceptional among brightness illusions. Thus, it is conceivable that its explanation requires a mechanism other than the rest simulated well by the current version of Geier's diffusion model.

As for Gilchrist's (1977) results that 3D perception has an influence on lightness, the filling-in approach has not yet been tested, since it has been developed on the basis of 2-D illusions. In the filling-in framework, as it has already been argued, the edge structure (or more precisely, the non-zero second derivative profile) is of crucial importance, since the input of the model is merely the edge structure of the image. However, the edge structure changed in both experiments by Gilchrist (1977) in which he demonstrated the role of depth in lightness perception. If the retinal pattern changes, even if only slightly, as it does, one cannot be sure that it is not that physical change that caused the perceptual effect.

In the parallel plane experiment, the depth effect is elicited by interposition. In the two conditions, the boundary edge of the target differs at its corner, suggesting occlusion in one condition and no occlusion in the other. In the stereopsis experiment, on the other hand, the edge structure of the two retinal images is slightly different (due to occlusion of some edge-parts in one image but not in the other, for instance). Therefore, the model is likely to predict different brightness values in the two conditions of the parallel plane experiment. In the stereo experiment, due to the slightly different edge-structure in the two eyes, it is possible that the model will also predict slightly different brightness values. Therefore, when the two retinal

images are coupled into a single 3D percept, the two slightly different brightness distributions might be combined so that it differs from the monocular brightness profile.

Although this is a hypothetical explanation for the influence of 3D on brightness, and it has not yet been tested, it seems that the filling-in approach might be capable of treating such phenomena as well. However, even if the model predicts differences under these conditions, we do not yet know the direction and the magnitude of the predicted difference, if any, so it also might happen that these phenomena will challenge the model.

Based on the foregoing, however, it seems that the most successful approach to date is the filling-in approach. Other filling-in models are also present in the literature (Arrington, 1996; Paradiso and Nakayama, 1991), however, I do not describe them here in detail, since they are much more complicated than those reviewed so far. Geier's (2009) model shows that it is unnecessary to overcomplicate a filling-in model in order to account for most known brightness phenomena.

Still, Kingdom (2011), argues that “‘Filling-in” should at best therefore be considered as a metaphor for the representation of uniform regions by relatively low spatial frequencies’ (Kingdom, 2011, p. 668). He bases this claim against the filling-in approach on two pieces of evidence. First, he argues that Dakin and Bex (2003) have shown that the COC illusion depended on the presence of residual low-frequency information. However, in section “Recent lateral inhibition-based models” above, I have already raised serious doubts against their conclusions.

The second piece of results that Kingdom (2011) considers to refute the filling-in approach is a paper by Blakeslee and McCourt (2008). Their experiment is based on the assumption that brightness induction should delay compared to the appearance of the physical luminance pattern. In their experiment, Blakeslee and McCourt use their grating induction illusion, which comprises a vertically oriented sinusoid grating, and a physically homogeneous grey band in its horizontal midline (test field). In the test-field, an illusory sinusoid grating (induced grating) is seen, whose spatial phase is the opposite to that of the inducer grating. The experiment is based on this phenomenon besides another: if a counterphasing sinusoid grating is added to another, whose spatial and temporal phase differ by one-quarter cycle, then a moving wave is perceived (leftward or rightward, depending on the sign of the phase difference). Blakeslee and McCourt combine these two phenomena to measure the temporal lag of brightness induction in their quadrature motion technique: they physically counterphase a sinusoid grating in the test-field in spatial quadrature to the

inducing grating (and to the induced grating), but varying in temporal phase. They assume that if a filling-in mechanism lies behind brightness induction, then the counterphasing illusory grating induced by the counterphasing inducer grating should have a time lag compared to the physically present counterphasing grating in the test field. Thus, if the filling-in theory holds, then the sum of the induced (illusory) grating and the physical grating in the test field should produce the percept of leftward or rightward motion.

However, this assumption is false with regards to filling-in theories, since the perception of both illusory brightness and physical luminance-based brightness is produced by the same mechanism in terms of the filling-in theory. In order to perceive the (physically present) inducer grating itself, it should be assumed that the filling-in process is already done. Thus, no delay in the perception of illusory brightness should be expected as compared to the perception of physically present luminance-based brightness, since both kinds of percept are produced by the same filling-in mechanism.

This claim is the basis of modelling illusory phenomena: it is assumed that the visual brain has a working mode, which processes the physical luminance distribution somehow. However, its way of processing makes some errors under certain conditions: these are visual illusions themselves. An overriding principle here is that no separate mechanisms should ever be assumed for perceiving illusions (here: the induced grating) and “real” objects (here: the inducer gratings). As I have already argued in the “Introduction” section, illusions derive from the normal working mode of the visual system.

As I pointed out above, in all filling-in models, the percept of the entire image corresponds to the output of the final stage, the filling-in process itself. The entire image is reproduced from the filtered image of the original image (containing only the edges, or more precisely, the non-zero second derivatives of the original image). Based on this, the filling-in process is necessary to produce the percept of both the physically present and the illusory gratings, which is done by the same filling-in mechanism at the same time. Thus the perception of a physical grating should not be expected to precede the perception of the illusory grating.

Blakeslee and McCourt (2008) did not manage to show any delay in the perception of the illusory grating as compared to the perception of the physical grating. However, in the light of the foregoing, this result is not at all surprising, nor does it undermine anything with regards to the plausibility of the filling-in approach contrary to their conclusions. The grating induction, incidentally, is rightly predicted by Geier’s (2009) diffusion-based model.

Finally, I present an additional set of illusions that favours the filling-in approach (Hudák and Geier, 2011). In Figure 11, the ramped Chevreul illusion is redrawn from our Study II. The two staircases are physically identical, except for their progression, which is the opposite. Due to the luminance ramp background the upper steps seem strongly crimped (the Chevreul illusion is enhanced) whereas the steps in the lower staircase seem homogeneous (the Chevreul illusion is ceased). In B, I have enclosed the middle parts of the steps in a rectangle outline. The very strong illusory crimpedness totally ceased in the area enclosed by the outline, while the area of the steps outside the outline stayed totally crimped. This phenomenon shows that the edges of the white outlines obstruct the activation spreading coming from the boundary edge of the staircase and the ramp from getting into the enclosed area, and the brightness of the area within the rectangles is determined by the luminance edge of the enclosed area and the outline. For a filtering model this phenomenon would entail a great challenge, since width of the outline is negligible to the area of larger-scale filters, whereas small filters could not produce a homogeneous, scalloping-free profile for the entire area of the enclosed rectangle.

Closure is of essential role in this phenomenon. I have inserted thin lines in the vertical midline of the steps (Hudák and Geier, 2011) as Morrone (1994) did in case of the original Chevreul illusion. The two halves of each step became homogeneous, but in the upper staircase we obtained a much stronger effect than Morrone (1994), and no effect in the lower one. This indicates that the upper and lower boundary edges of the staircase play as important role in this effect, as the edges separating the steps themselves. However, if the thin line does not reach the edges of the staircase, the strong scalloping returns in the upper staircase. It seems that the activation spreading can freely run in this case, by-passing the thin line in the middle.

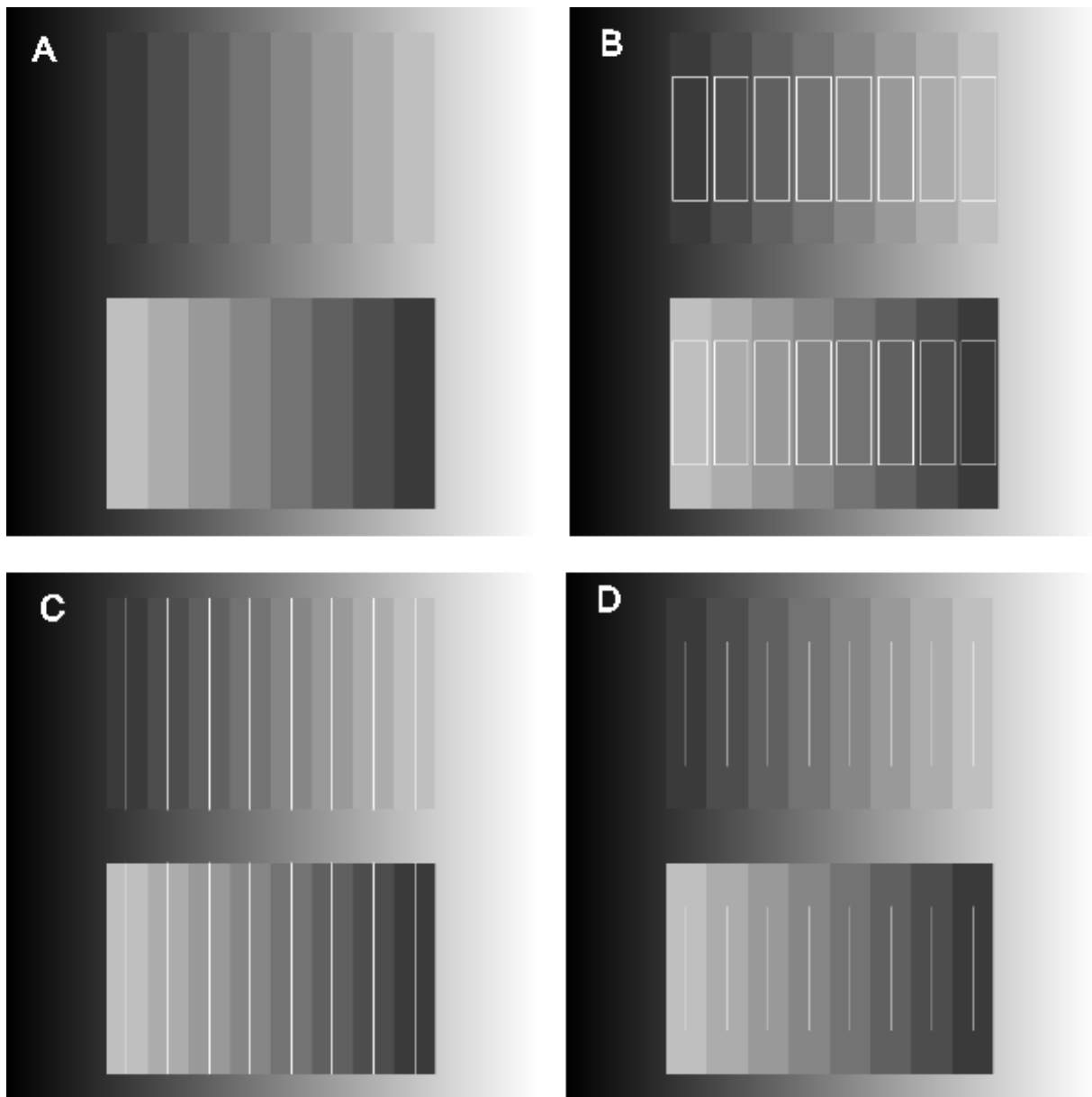


Figure 11. The ramped Chevreul illusion with segmenting thin lines (from Hudák and Geier, 2011). The staircases are physically identical in all panels, except for the opposite progression of the upper and lower staircases in each panel. In 11A (redrawn from Study II), the Chevreul illusion is very strong when the progression of the staircase is identical to that of the ramp, while the illusion is absent, when it is the opposite. In 11B, I have included rectangles from thin lines. The effect of the ramp does not affect the area within the rectangles, only the area outside it, which shows a segmenting role. In 11C, I inserted thin lines (after Morrone, 1994) that reach the upper and lower boundaries of the staircases. Here the two halves of each step became homogeneous, and no effect occurs in the lower one. However, when the thin lines do not reach the edges, thus no closure is present, the segmenting effect ceases, showing that the filling-in mechanism is not obstructed anymore.

6.2.7 Filling-in brightness modelling vs. anchoring: not mutually excluding concepts

So far, the concepts of lightness and brightness have been used interchangeably throughout this thesis, since homogeneous illumination is assumed in case of the illusions presented above, in which case they collapse into each other. However, I will now describe how I interpret these concepts, and argue that a filling-in approach and anchoring are not mutually excluding approaches. Rather, both are necessary at an appropriate stage.

It is not a new consideration that brightness perception is only a first stage, and further cognitive processes are necessary to convert relative brightness values into absolute lightness intensities. Gilchrist (2006) argues against such a conception. He considers such line of thought, which he quotes from Kingdom (2003), unfalsifiable: ‘Kingdom (2003) has argued that the many recent demonstrations challenging the lateral inhibition account of simultaneous contrast merely represent higher-level cognitive processes that modify the basic lightness errors produced by lateral inhibition. ... Given that the lightness values presumably produced by lateral inhibition may be subsequently overridden by higher-level processes, one can never really be sure what the lateral inhibition stage produced. Results that are consistent with the direction of lateral inhibition are attributed to lateral inhibition, while results that are inconsistent are attributed to overriding cognitive operations.’ (Gilchrist, 2006, p. 338). In this respect, I totally agree with Gilchrist’s argument: if the output of the lateral inhibition stage (or, in our approach, the output of the filling-in stage) were to be overridden by mid-or higher-level mechanisms, then modelling low-level brightness perception would be simply superfluous and of no use.

In another sense, however, I consider it still plausible that brightness perception precedes lightness judgements. In our approach, perception of brightness is an automatic low-level process, which is best described by filling-in models. The task of this level is to code relative intensities in the scene: this is what I define as brightness: the perceived relative luminance distribution in the whole scene. (This is in accordance with Gilchrist (2006), who defines brightness as perceived luminance and lightness as perceived reflectance). Due to the non-linearities in the filling-in process, relative intensities coded into brightness values already deviate slightly from the physical relative luminance distribution. Hence, brightness illusions are produced already at this early stage, and are not modified by higher processes. This level of processing might be compared to a black-box: mid-or high-level processes receive its output, however, they do not override the relative brightness profile. Rather, the

task of such levels is to interpret the received relative brightness profile without modifying it, by attributing absolute lightness categories (such as white, grey, black, etc) to the brightnesses encoded by the filling-in level. Thus I would suggest that the term *brightness* should always refer to a relative entity, which can be encoded as a scale variable, whereas the term *lightness* should be treated as a nominal variable, indicating an absolute entity.

One piece of evidence that the relative brightness profile is not overridden by higher cognitive mechanisms comes from brightness illusions, such as the Hermann grid illusion, the White effect, the simultaneous brightness contrast, COC, etc: although we know that these are merely illusions, we cannot stop seeing them if we look at the eliciting images, despite any intention to do so, and regardless to any previous knowledge. This implies that these illusions are produced indeed at a very low level, to which awareness or other cognitive mechanisms do not have any access; such mechanisms can only “read” these profiles out, but cannot modify them. Brightness illusions discussed in this thesis are considered to be the result of the processing mechanism of this early, filling-in stage.

Thus, I argue that the low-level brightness percept (i.e. the perception of relative luminance distribution) is present even at the final cognitive stages; it is only *interpreted* by such processes, but not *modified*. As an example, let us conceive a white paper, whose one half is strongly illuminated, while its other half is in shadow. I consider this example as a pure manifestation of the simultaneous presence of brightness and lightness in the perceptual experience. Obviously, under natural conditions, anyone can see that the illuminated half of the paper is brighter, and the one in the shadow seems darker. This is what I would term brightness perception, and this is what the filling-in stage models. (Of course, at this level, the darker part is not yet categorised as a shadow, this level only codes that that part of the image has lower luminance values). If this pure brightness profile were not perceived, then we would not be able to perceive shadows: the perception of the difference of brightness between the two halves of the paper (low-level) is a necessary condition to interpret it as being a shadow (mid-or high-level).

However, even though everyone can see that the illuminated half of the paper is brighter than that in the shadow (brightness), no one thinks that the paper is painted in two different shades of grey: the entire paper is perceived as white (lightness constancy), since the visual system interprets the output of the brightness stage as such, without modifying the perceived relative brightness pattern. The luminance difference between the two halves of the paper is still perceived (in our view, produced by filling-in), but the lightness judgement is

also correct; constancy works (probably due to anchoring the two brightness values to white, interpreting the darker part as shadow).

Zavagno and Daneyko (2010) also claim that many psychophysical experiments that were planned to measure absolute lightness values measure in fact only relative brightness perception. Such experiments usually use a matching paradigm, in which the target areas of images have to be matched with Munsell charts. However, Zavagno and Daneyko showed that the matches varied depending on the luminance environment of the Munsell charts themselves, not merely on the perception of the stimulus. The brightness of the Munsell charts serving as standards was thus also influenced by their background. Therefore, these results show that matching targets with Munsell charts measures the direction and the magnitude of the illusion reliably (thus, in my interpretation, these can be considered as good brightness studies), however, such a paradigm cannot on its own measure the absolute lightness values that subjects perceive.. Nonetheless, this argument would be valid only if different studies used different backgrounds for the Munsell chips. The study does not mention different illuminations in different laboratories. Still, it seems that determining the brightness of a target by a Munsell scale is quantitative data.

However, lightness, in my view is qualitative: it involves the categorization of brightness values as white, grey or black, and such a level of perception can only be measured in a qualitative way, for instance, by asking the subject to name the particular shade of grey. The matching paradigm can reveal only what a particular subject sees brighter than the other, but not what he or she sees as white. It is problematic to conclude, for instance, that if a subject matches a target with a 9.0 Munsell chart, then he perceives it as white, without actually asking him what colour he sees. It might be that a 9.0 Munsell chart is perceived as white under certain conditions and light grey under others. However, whether the subject categorizes it as white or light grey, it will not change his judgement that the target is most similar to Munsell 9.0, thus lightness will not override brightness.

Thus, the perception of brightness and lightness are not mutually excluding processes, but are produced by different stages of visual processing, and are simultaneously manifested in the perceptual experience. In order to produce the relative brightness percept, the filling-in stage is necessary. In order to make lightness judgements, anchoring rules are necessary, that anchor brightness values in the entire scene to lightness values (e.g. white), but the application of the anchoring rules does not have any influence on the relative brightness distribution of the scene, which is already determined by the filling-in stage. Thus, brightness

illusions (even those that are not congruent with the lateral inhibition account) are produced at the filling-in stage. Thus, relative brightness values are delivered by this stage for the next one, without the need to override them. What the next stage needs to do is “only” to judge which brightness value in the given relative brightness profile should be attributed white, grey, black, etc; which image areas are in shadows, which image areas represent self-luminous objects, without modifying the relative brightness profile, received as "read only material" from the previous, filling-in stage. Besides anchoring rules, this interpretation process might involve pattern recognition processes as well: the perception of self-luminosity, for instance, might involve sensitivity to such fine patterns in the brightness profile that are comparable to object-or face-recognition processes. As for anchoring rules, Gilchrist and his co-workers have collected plenty of evidence for the highest-luminance-is-white rule, and other arguments exist for the average-luminance-as-grey rule. (see Gilchrist 2006 for a review). Whichever rule is applied by the visual system to attribute absolute lightness values, in our view, the judgement of absolute lightness should not have an influence on the already produced relative brightness profile. Thus, the task of low-level brightness models is to determine the relative brightness distribution in the whole scene, whereas the task of mid-and higher level mechanisms is to categorize these brightness values as colours, or in other words, to anchor them to specific colours. Hence, I would conclude that low-level brightness models are expected to account for the overall pattern of errors in the perception of relative intensities in the scene, whereas anchoring rules are expected to account for constancies, i.e. to interpret the reflectance, illumination, shadows and transparency from the perceived luminance (i.e. brightness) profile produced by the filling-in stage.

6.3 Chromatic illusions – the potential application of a good brightness model to chromatic stimuli⁵

Even if one manages to devise a good brightness model that predicts the overall pattern of brightness errors correctly, the question emerges how one can account for illusory phenomena occurring in the chromatic domain. We attempted to extend Geier’s activation-spreading model for chromatic illusions (Hudák and Geier, 2007), however, this extension could be applied to any brightness model that can simulate the occurrence of illusions well.

⁵ Parts of this chapter have been published at ECV2007; Hudák and Geier (2007). Perception Supplement, 36, p. 173

The additional principle is that the chromatic input images are split into red, green and blue channels. These three channels are widely accepted in the literature being equated by the three cones (Zeki, 1995). In our model, each channel is processed separately. Finally the output images of the three channels are rejoined into one final chromatic output image.

To test the plausibility of the extended version of the model, we used the chromatic Hermann grid illusion in our psychophysical experiments to compare the predictions of the model with the perception of human observers. Hermann-grids are split into R, G, and B channels, resulting in three separate images. The simulation of the model is run on each of them. Finally, the three outputs are rejoined into one, resulting in spots of definite colour at the intersections. If (for example) a red and white Hermann grid is split into R, G and B channels, there will be no grid in the R channel (see Figure 12). It is because both white and red equally contains red light, since white is the additive mixture of red, green and blue. On the other hand, the squares will be black on B and G channels, since the red squares contain no red light, so the light intensity of the squares will be minimal in these two channels. When the simulation is run on these three images, the intersections will relatively darken on the B and G channels, but nothing will happen on the R channel, as there are no edges from which the activation spreading could start. Therefore, the light intensity in the intersections will be the highest in the Red channel, resulting in reddish spots.

If, on the other hand, a red and black Hermann grid is split into R, G and B channels, there will be a grid only on the R channel. It is because black streets contain no red, green or blue, so streets will be black in all channels. On the contrary, the red squares contain maximal intensity of red light, so they will be bright in the Red channel. However, on the green and blue channels no grids will be present, since the red squares, that contain no green, nor blue light, will be as dark as the streets themselves. Thus, as there are no edges on G and B channels, the the activity spreading will only influence the red channels: the intersections will brighten relative to the streets. Therefore, the red channels will be the brightest among the three channels on the rejoined output.

This principle can be applied to any colour combinations. There will be spots of definite colour at the intersections of the simulation outputs of any arbitrarily coloured Hermann-grids. At arbitrary "house"/"street" constellation, we can predict the perceived colours of the spots by the same concept.

In order to compare the simulation results with perception, I devised an experimental paradigm in which subjects ($n=31$) adjusted the colour of real spots placed in a Sinusoid grid, until they were the same colour as the illusory ones. On the lefthandside of the black computer screen, subjects were shown a chromatic Hermann grid with illusory spots (various colour-combinations were used, including compementer and isoluminant colour-pairs). On the righthandside, a Sinusoid grid of the same colour-pair was shown, in which physical spots were drawn by the program (illusory spots are not visible in the Sinusoid grid, see Study II.) The colour of these real spots had to be adjusted by the subjects until the colour and intensity of the real spots matched the colour of the illusory spots in the Hermann grid. By using the Sinusoid grid as the environment of the real spots, we aimed at providing an environment similar to that of the illusory spots, in order to avoid influence of different environment on colour perception. The subjects were allowed to use any colour from the Windows colour-palette, and they also could adjust the intensity/transparency of the chosen colour. The program stored the RGB codes of the colours set by the subject, so that we were able to compare them statistically with the simulation of the model.

We obtained the result that the correlation between the R, G and B values of subjects and of the simulation is above 0.9 in all the three channels. Consequently, the model gives a correct prediction for the perceived colour of the illusory spots in chromatic Hermann-grids.

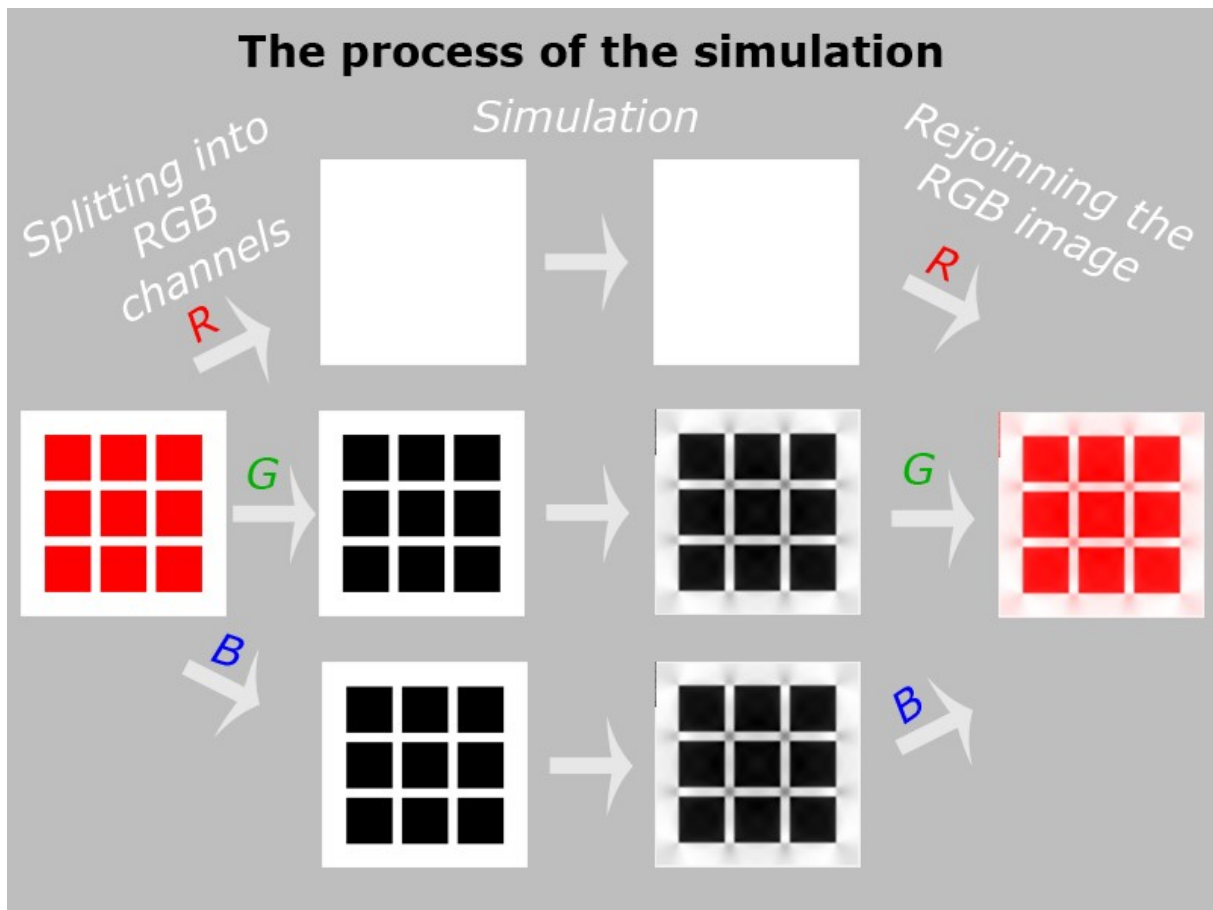


Figure 12. The process of the simulation of chromatic stimuli. First, the image is split into R, G and B channels. Then the simulation is run on each channel separately. Finally, the outputs of the three channels are recombined, which gives the final prediction of the model.

This extension of a brightness model to the chromatic domain is suitable to predict the Lotto-Corney illusion, and under certain colour-combinations, the colour-contrast illusion and the chromatic version of the Munker-White illusion.

However, this principle also meets some limitations. Chromatic versions of brightness illusions whose achromatic variant comprises more than two shades of grey, but whose chromatic version contains only 0 or 255 values in each channel, entail a challenge to the three-channel model. Such is a Munker-White illusion, comprising, for instance, yellow and red stripes and blue targets. In this case, in the red channel, black targets in a homogeneous white background will be seen, since the value of red is 255 both in yellow and red, but it is 0 in blue. In the green channel, on the other hand, the image will comprise black and white stripes, which are interrupted at the positions of the targets, since the value of green in yellow is 255, but it is 0 both in blue and red (thus the targets will be black as well as the black

stripes, thus the targets will merge with the black stripes). Third, in the blue channel, white targets will be obtained in a homogeneous black background, since there only the blue value is 255, the rest is 0. Consequently, the image eliciting the Munker-White illusion will not be present in any of the channels, thus no model can simulate the White effect in any of the three channels. The same logic holds for any colour combinations comprising only two brightness values in all the three channels. Another challenge for our three-channel model is the chromatic version of the COC-illusion, the Watercolour effect by Pinna (Pinna, 1987; Pinna et al, 2003). This illusion is predicted totally the opposite way to human perception.

To resolve these limitations, we suggest that the concept of three channels should be amended with a fourth one, which codes the achromatic brightness distribution of the image, and the final output should be the sum of these four output images instead of the three. However, this extension of the model is subject to future research.

6.4 Dynamic illusions

So far, only static percepts have been dealt with elicited by static images. However the temporal characteristics of the visual system can also be investigated by means of illusions. Such illusion might reveal information about the temporal dynamics of the filling-in process both in the achromatic and the chromatic domain. However, the dynamics of the visual system does not have so many comprehensive models as brightness perception does. Thus, phenomena presented here might only serve as a basis for a deeper understanding of dynamic phenomena, and much further research is necessary to devise such complex models described in case of lightness-brightness perception. Still, these phenomena will be discussed largely with regards to the concept of filling-in.

6.4.1 Dynamic illusions elicited by static images: where filling-in gets confused

6.4.1.1 The Scintillating grid illusion⁶

One of the most striking static images that shows abrupt changes although the image is entirely still is the Scintillating grid illusion. The recently known version of the Scintillating grid was created by Lingelbach et al (Schrauf, Lingelbach, & Wist, 1997). They set the lines of the original Hermann grid to grey, and they placed white disks to its intersections. As a

⁶ Part of this chapter will be published in the Oxford Compendium of Visual Illusions, edited by Todorovic and Shapiro (Geier and Hudák, in press).

result, a strong scintillation was perceived in these images. The first Scintillating grid was introduced by Bergen (1985), who low-pass filtered the Hermann grid, which resulted in the perception of flashing at the intersections instead of static illusory spots. At this point, it could be suspected that the removal of high spatial frequencies was a necessary condition for scintillation to appear. However, Lingelbach et al elicited scintillation without low-pass filtering, i.e. without removing high spatial frequencies. Thus, they have proved that the phenomenon is not high-spatial frequency dependent, rather, the scintillation occurs when the intersections are brighter than the streets.

In addition, we found that the straightness of the streets is also a necessary condition for the scintillation to occur (Geier and Hudák, in press), as well as in the case of the Hermann grid illusion (see Study I). By applying the same distortions to the Scintillating grid, the scintillation also stops (Figure 13). It is noteworthy that for the illusion to disappear, it is sufficient to raise the amplitude of the sine wave to less than 10% of its wavelength (Geier; 2001; Geier, Séra and Bernáth, 2004; Geier and Hudák, in press).

We conducted the same psychophysical experiments with the Scintillating grid as with the Hermann grid presented in Study I. The results were similar in case of both illusions: the distortion tolerance was significantly higher in case of the Half-sided hump, and the other factors had no effect. Comparing the distortion tolerance of the Hermann grid and the Scintillating grid, we obtained approximately twice as large means in case of the latter.

To date, there is no generally accepted explanation for the Scintillating grid illusion. The fact that curvature eliminates the scintillating effect, too, makes it necessary to search for a common background for the Hermann grid and the Scintillating grid illusions, and to develop a general theory for these effects. Moreover, straightness plays an essential role in both phenomena, since both illusions are difficult to be eliminated if one side of the streets remains straight. Furthermore, no spots in the Hermann grid and no scintillation in the Scintillating grid are seen, when three streets meet at the intersections instead of four. Finally, no scintillation occurs at the end of the streets, similarly to the lack of Hermann spots there.

In conclusion, it seems that the sufficient and the necessary conditions of the Hermann grid illusion and that of the Scintillating grid illusion largely overlap. However, we have also found a difference between the necessary conditions (Hudák, Geier and Lingelbach, 2010). When only horizontal or vertical streets are present, the disks still scintillate. Therefore, it is sufficient to have exclusively horizontal or vertical lines in case of the scintillating grid, but obviously this is not the case for the Hermann grid.

We proposed a unified explanatory principle for the presence and absence of the Hermann grid illusion in Study I. The task to extend it to the Scintillating grid phenomena, or to provide a better unified theory for all these illusions and non-illusion, remains the task of future research. Eye movements are necessary for the scintillation to occur. Thus, we suggest that the scintillation might be the result of the different filling-in characteristics (either spatial or temporal) of the fovea and the periphery, which might emerge from the anatomical differences between these retinal areas (e.g. Curcio et al. 1990; Curcio & Allen 1990; Dacey and Petersen, 1992).

Due to saccadic eye movements, the image parts projected to the fovea and to the periphery interchange abruptly. As the Hermann spots disappear under foveal vision, and the location of the disappearing spot changes with the movement of the eye, the same phenomenon occurs in the scintillating grid, in a much more pronounced fashion. A possible explanation is that reaching the equilibrium is prevented in the periphery but not in the fovea by saccades due to the supposedly different temporal characteristics of the filling-in process in the fovea and the periphery, leading to the disturbance of the filling-in process. It is reasonable to suppose that the filling-in process is faster in the fovea than in the periphery, due to the much more dense distribution of ganglion cells (Curcio et al. 1990; Curcio & Allen 1990), and the dendritic trees are smaller (Dacey and Petersen, 1992). An afterimage in support for this claim will also be discussed in the next chapter (Geier and Hudák, 2007). However, the reason why certain images cause such disturbance in the filling-in process, and not others, remains an open issue to future research.

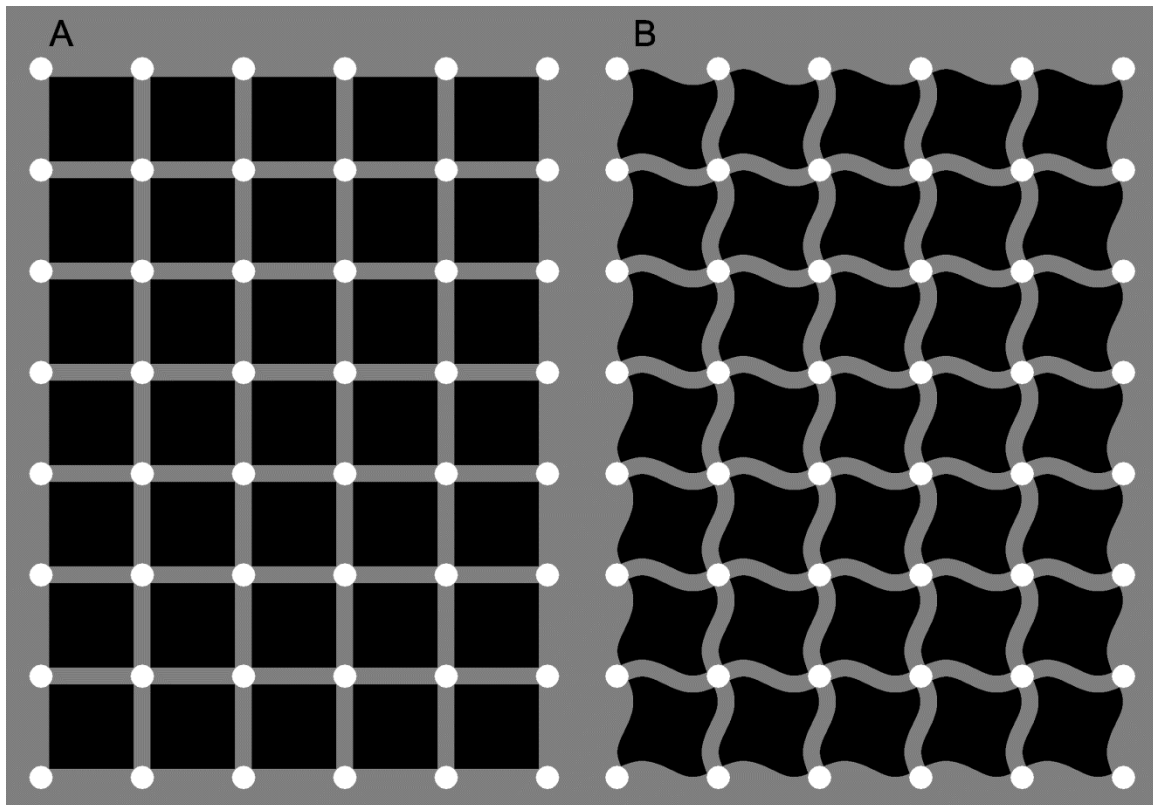


Figure 13. The Scintillating grid and our curved version. In 13A (redrawn after Schrauf et al, 1997), the spots seem to be scintillating while the eyes are moving. The spots that is fixated disappears. In 13B, we have curved the grid which made the scintillation disappear, similarly to the Hermann grid. This suggests that a common background should be sought behind the Hermann and the Scintillating grid illusions.

6.4.1.2 Kitaoka's induced movement illusions

Another set of images that never remains a static under eye-movements were designed by Akiyoshi Kitaoka. The most known one among the numerous variations is the rotating snakes illusion (Figure 14; Kitaoka and Ashida, 2003). In this image, the disks seem to be rotating slowly and continuously under peripheral vision. Hisakata and Murakami (2008) found that the rotation stops under foveal viewing with strong fixation. According to Murakami et al (2006), chromaticity is not a necessary condition for the rotation to occur, rather it is dependent on the luminance pattern of the image.

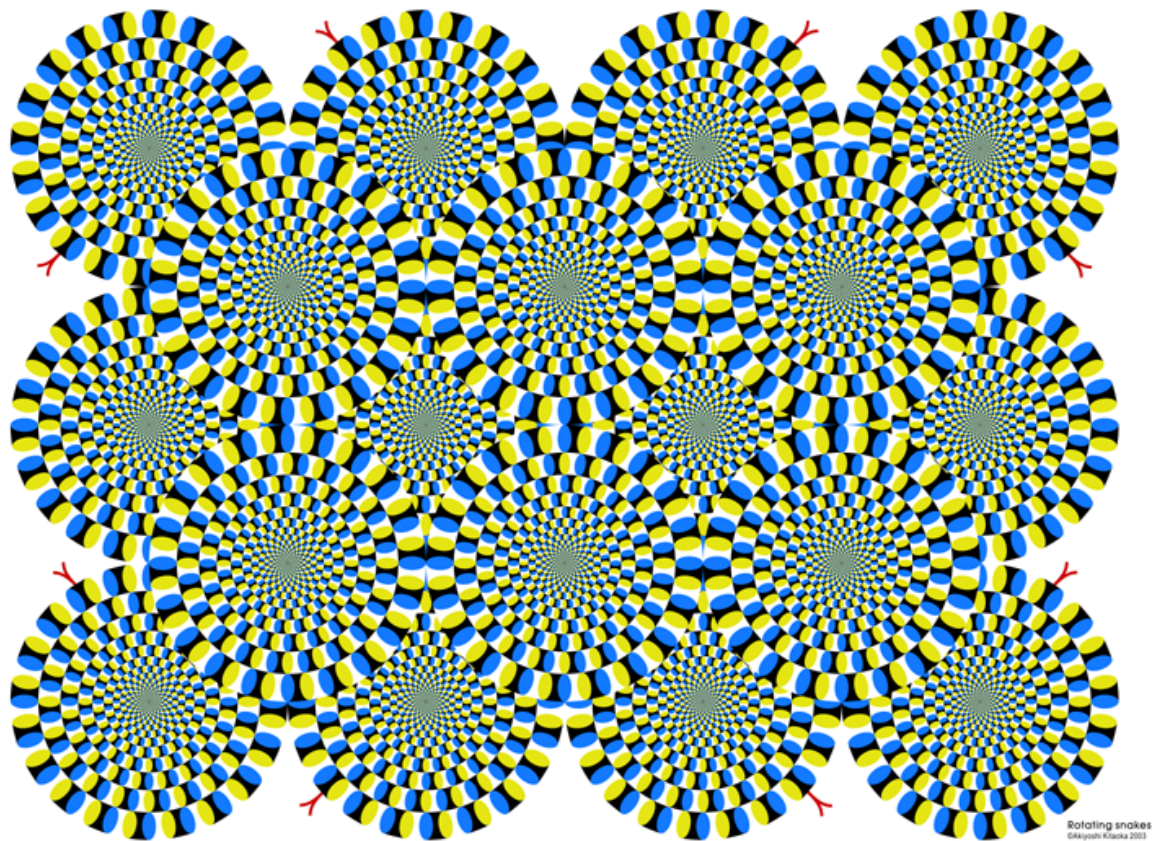


Figure 14. Kitaoka's Rotating Snakes illusion (supplied by Akiyoshi Kitaoka). Although the image is physically static, the snakes seem to rotate as the eyes move.

There is no generally accepted explanation for the rotating snakes illusion. According to Ashida et al (2012), however, the most common view is that those parts of the image having low contrast are transmitted to the cortex slower than those having high contrast (Faubert and Herbert, 1999). Thus motion signals are elicited, which Ashida et al (2012) showed to be present as early as in the V1. However, if it is taken into account that both the Hermann grid, the Scintillating grid, the Rotating snakes and other Kitaoka illusions disappear in the fovea under foveal fixation, and they all show changes under eye movements, a common background might be suspected here. The appearance and disappearance of the spots in the Hermann grid illusion can be modelled by a unified filling-in principle (Study I), and the prerequisites of the scintillation in the Scintillating grid largely overlap with that of the presence of the Hermann spots. Moreover, it is plausible that the temporal characteristics of this filling-in mechanism slightly differ in the fovea and in the periphery due to anatomical differences (Curcio et al. 1990; Curcio & Allen 1990; Dacey and Petersen, 1992), and the Rotating snakes illusion is also different under foveal and peripheral vision, as well as the Hermann grid and the Scintillating grid, and only these. Thus, it might be suggested that the

rotating snakes illusion is caused by the same disturbance of the filling-in process as the one that elicits the Scintillating grid illusion.

6.4.1.3 Stabilized retinal images

The most static image that is physically possible to create is the stabilized retinal image. However static physically, it is still subject to perceptual change. Under normal viewing conditions, the eyes make tremors all the time even under rigid fixation (according to Yarbus, 1967, this rate is 30-150 movements per second), therefore, the retinal image always moves a little relative to the retina. Retinal stabilization might be achieved by means of several methods (see Ditchburn, 1973), either by precisely positioned projector, mirrors and contact lenses (e.g. Cornsweet, 1974) or caps sucked to the eyeball (e.g. Yarbus, 1967), however, such experiments require extraordinary precision. Phenomena studied under conditions in which the retinal position of the stimulus was well stabilized, constitute a straightforward set of evidence for a crucial role of edges and a filling-in mechanism in the visual system.

When stabilized retinal images are presented to a subject, the image is seen first sharply and clearly for a duration of approximately 1-10 seconds (Yarbus, 1967; Ditchburn, 1973; Cornsweet, 1974). After this period, the image fades away and either a uniformly grey or a totally dark surface is reported. According to Ditchburn (1973), it also occurs that the visibility of the image fluctuates intermittently, either locally or globally. In this case, parts or the entire picture become hazy and the percept is comparable to a blurred and low-contrast version of the physical image. However, good stabilization, comfort of the subject and lack of disturbing noise are such conditions that support the total disappearance of the image, perceiving complete darkness instead of a grey surface or any intermittent fluctuation (p. 135). Intermittent fluctuation is attributed to neural noise (p. 195). Ditchburn also emphasises that the perception of stabilized images are entirely different from normal perception: ‘Appearances obtained with the stabilized image are not exactly like anything seen in normal vision. Since the words used to describe the appearances are necessarily drawn from normal visual experience they are not adequate to describe the essentially new features of a different visual experience.’ (Ditchburn, 1973, p. 134). For the reappearance of the stabilized image in a normal vision-like manner, time-varying signals are necessary, such change in the luminance and contrast, or the displacement of the image relative to the retina, as it has been confirmed by numerous experiments (reviewed by Yarbus, 1967; Ditchburn, 1973; Cornsweet, 1974).

Ditchburn (1973), based on experiments of his own and that of many others reviewed in his book, concludes that for normal vision to occur, movement or change of the retinal image is necessary. He emphasises the role of edges in normal vision, claiming that if the information provided by edges are removed by means of stabilization, the perceived image will totally be distorted (p. 383).

Cornsweet (1974) proves the role of edges in visual perception by means of the following simple line of thought. If one uses large fields with sharp boundaries as stimuli under stabilized vision, then it is clear that physical change will occur only at receptors near the edges, when the retinal image happens to move after the disappearance elicited by stabilization (Cornsweet, 1974). However, in this case, the entire image reappears, including the brightness and the hue of large homogeneous areas, not only the edges (Cornsweet, personal communication, 2013). Therefore, the areas of the image must be filled in by the signals coming from edges.

Yarbus (1967) also confirms this claim, based on several experiments reviewed in his book. He concludes that under normal vision, no physical change occurs during the perception of large uniform surfaces. In this case, an empty field should occur in the inner part of this surface. However, this is not the case: 'The empty field always takes the color of the surroundings and, in ordinary conditions, is never seen by the human subject. In other words, the visual system extrapolates the apparent color of the edges of the surface to its center.' (Yarbus, 1967, p. 100). He also claims that all contours disappear when the image is well stabilized within 1-3 seconds, and they reappear only when something disturbs the strict stabilization of the retinal image, such as movement or light intensity change, which he proved by several stabilized retinal image experiments (see Yarbus, 1967).

6.4.2 Afterimages elicited by short presentation: the temporal dynamics of filling-in vs. adaptation

A set of visual illusions which are usually considered as the microelectrode of the psychologist, are aftereffects. Visual aftereffects are also illusions in a sense that when the afterimage is perceived, physically no such stimulus is present. Such phenomena can be elicited by a shorter or longer exposure to a stimulus, subsequent to which the inverted form of that stimulus is perceived. This phenomenon is usually attributed to neural adaptation. However, according to a recent review on adaptation by Webster (2011), the definition of adaptation is still unclear. According to Webster (2011), the operational definition of

adaptation is that an aftereffect is elicited by a brief exposure to the stimulus. On the other hand, a functional definition is difficult to devise, since a great variety of dynamic and experience-dependent adjustments are exhibited by the visual system. Thus it is difficult to distinguish adaptation from other forms of plasticity. He reviews various phenomena which are all labelled by the umbrella-term "adaptation" ranging from very low (e.g. contrast) to high level (face recognition) aftereffects, including multiple time-scales from seconds to days. The neural mechanism of adaptation is thus not a well-defined one; rather, various mechanisms might lie behind the various after-effects. He lists three different possible functions of adaptation, that can be found in recent literature among others. One possible function is to match the dynamic range of the visual system to the intensity levels in the stimulus. A second function attributed to adaptation is to signal errors that deviate from the implicitly represented expected mean of the stimulus. A third hypothetical function of adaptation is to maintain constancies by discounting variations in the signal.

In our view, another adaptational function might serve to enhance the speed and thus the efficiency of the filling-in process. To investigate this issue, we introduced a low-level aftereffect, the Dynamic patch illusion (Geier & Hudák, 2007; for demos see <http://geier.hu/ECVP2007/BRI-OVERSHOT/index.htm>, where this part of the text has already been published as an online support for our poster presented at ECVP 2007). The aftereffect occurred even at a very short exposition ($<1s$), was also perceived at very low contrast ($<10\%$), and it was eliminated by eye movements (as opposed to classical aftereffects elicited by long fixation periods). The phenomenon was elicited as follows. If the contrast of a patch (Gauss patch, sharp edged disk, Gabor patch, etc.) in a homogeneous background was continuously reduced to zero and the observer was fixating a signed point, then the illusory inverse of the patch was perceived at (or even before) the end of the contrast reduction process, or, in case of a Gabor patch, an illusory displacement was perceived. The illusion occurred even on a totally white or black background, so that the inverse of a black patch on a white background appeared even brighter than the white background itself, though the dark patch was still present at that point. If three or more Gauss patches disappeared physically at the same time, most subjects reported a delayed sequence of illusory overshoots: the fixated leftmost patch overshoot first, then the middle one, and last the rightmost patch turned into inverse. In other words, the delay of the overshoot depended on retinal eccentricity, foveal vision being faster. Furthermore: the illusory inverse of the most eccentric

t patch is the biggest in diameter. This peripheral delay also supports that the characteristics of the filling-in mechanism in the fovea is different compared to the periphery.

In our experiment (n=20), subjects had to stop the computer controlled contrast-reduction the moment when they perceived the disappearance (the beginning of turning into inverse) of the patch. Our result is that the patch turns into illusory inverse much before its physical contrast reaches zero.

We have modelled the phenomenon by a retinotopical set of PID controllers: according to our hypothesis, the cause of the overshoot is the "maladjusted" D component. According to our theoretical model, the mode of operation of each retinotopical point can be considered as a PID controller, which predicts the perceived brightness of the given point over time. When the patch merges into the background, the local lightness-alternation stops, but the maladjusted D component has proceeded much forward with the prediction of the perceived brightness by that time, so that is why a much lighter patch is seen, even if the dark patch is still present. The explanation is the same in the case of a white patch darkening until its contrast is zero. In this case, it is the darkening of the patch what is over predicted by the D component. The illusory movement of the Gabor patch is modelled by the same concept: the dark phases of the Gabor patch overshoot into white, while the light phases overshoot into black. By the illusory replacement of each phase, the displacement of the whole Gabor-patch is perceived. Our model is a theoretical model, i.e. it does not refer to any concrete brain area or neural structure. The connection between our theoretical model and the knowledge about the visual system needs further investigation

Our model also provides a theoretical explanation for the Breathing Light illusion (Gori and Stubbs, 2006). In the simplest version of this illusion, the physical stimulus is a static Gauss patch. When one is moving towards it, the Gauss patch is being perceived bigger and brighter, whereas the opposite is perceived when receding from it. The illusory size and brightness is restored when one stops and fixates the stimulus statically. This causes the impression of breathing. Physically, moving towards or away from the stimulus is equivalent with the gradual change of the intensity of each retinal point, which is what happens in our Dynamic patch stimulus. Our explanation is that when observing the Breathing Light illusion, the theoretical retinal PID controllers predict this local brightness change forward, resulting in the illusory brightening at each point, thus to the illusory enlargement of the image when moving towards it.

In conclusion, it seems that the visual system attempts to predict the brightness at each point from the flow of intensity change at the given retinal point, so that it might help the filling-in process in computing brightness and colours faster.

However, the question might arise whether this predictive process is accomplished by each and every retinal point or only by those from where the filling-in process starts, i.e. edges or non-zero second derivatives. In case of both the Gabor patch and the Gauss patch, the second derivative equals zero in none of the points of the stimulus. We substituted the Gauss patch with the image of the simultaneous brightness contrast, whose contrast was also gradually reduced to zero⁷. However, in its afterimage, the illusion was also perceived, although no physical change occurred within the area of the targets; only the black and the white surrounds were transferred into grey. Still, the grey target which was surrounded by white in the afterimage looked darker than the other grey target, surrounded by black in the afterimage. The phenomenon that the brightness-overshoot occurred even where no physical change took place implies that this must originate from the edges of the image, thus it seems that it is the non-zero second derivative points that accomplish the feed-forward control.

Another phenomenon in support of this claim was published by Vergeer, Van Lier and Anstis (2009). They presented an eight-pointed star for 1 second whose arms were coloured alternately red and cyan. This was followed either by the thin black outline of the red-or the cyan-armed part of the star for 0.5 second on a white background, while no chromatic color was present physically. When the thin outline of the cyan armed star-part was presented, the entire area within the outline was perceptually filled in with red and vice versa. No afterimage of the arms outside the outline was perceived, showing that the filling-in mechanism takes place only within these edges; starting from them and being gated by them even in this short-term afterimage. The perceived colour of the afterimage was thus determined merely by the orientation of the outline contour in the test image. Anstis, Vergeer and Van Lier (2012) provide several additional related afterimage phenomena as evidence for a filling-in mechanism between contours.

Anstis (2013) also showed that the visual system can adapt even to contours besides contrast, which has a strong influence on the perceived brightness of the homogeneous surfaces enclosed by the contours to which one has already adapted. The outline of a grey star

⁷ This phenomenon was presented in our talk in the ECV2010 satellite conference in Leinroden, Germany, 2010.

was flickered between black and white at 3-8 Hz for 2 seconds, after which the grey star was presented statically without any outline. The edges of the star disappeared totally, rendering the entire shape invisible, melting into the background, so that the inner part of the star were also perceived being equally bright with the background. On the other hand, the star shape that had not had a flickering outline during the adaptational period, were clearly visible subsequently. These aftereffect phenomena also provide clear evidence for a filling-in mechanism starting from the edges, since if the edges of a shape are rendered invisible, then its inner part is not filled in with its colour, rather, it merges into the background, the whole shape becoming invisible for a couple of moments.

Adaptational phenomena reviewed so far all involved a short timescale, such as a few seconds. However, longer-term afterimages also exist that show the role of edges in filling-in enclosed surfaces. Such aftereffect is the McCollough effect (described e.g. by Barlow, 1990). During the adaptational period which lasts several minutes, a vertical red grating alternates with a horizontal green one, each is shown for a few seconds. The test stimulus is a black-white grating. In this grating, the vertical lines seem to be tinged with green and the horizontal lines in red, which are the complementary colours of the adaptational gratings respectively. Therefore, in this illusion the colour of the afterimage also depended merely on the orientation of the contour in the test image, similarly to the short-term aftereffect presented by Vergeer et al (2009). Thus, it seems that even in afterimages elicited by a longer adaptational period, edges still govern the perceived intensity and hue of the enclosed surfaces, providing evidence for a filling-in mechanism that works in the low-level visual system.

6.4.3 Adaptation and temporal integration

These phenomena listed so far in this thesis, including static and dynamic illusions as well, show how the visual system integrates brightness and colour information spatially. This type of information is governed by edges in the image, or more precisely, by non-zero second derivatives. These spatial changes in intensity are detected by the visual system, and the brightness or colour information is computed for homogeneous surfaces (where the second-derivative is zero) from these areas where there is a change. As discussed above, stabilized retinal images decisively showed that the visual system is sensitive only to changes directly, besides several other pieces of evidence provided by illusions described so far. Homogeneities are computed from inhomogeneities in space.

However, the question arises whether the visual system also integrates temporal changes without obvious spatial guidelines. We investigated this issue by eliciting afterimages

of unseen shapes (Study III.). To achieve this, we used randomly flickering small squares, to which subjects had to adapt for a minute. However, some squares that together constituted a letter, was implicitly biased towards green (or in the achromatic version, towards white). Thus subjects did not see any letter during the adaptational period, only squares flickering in random colours (or black/white in the achromatic version). However, when the homogeneous white test field was presented, they were able to name the letter, whose magenta-tilted afterimage was perceived, despite the fact that no letter was seen during the adaptational period.

Thus, similarly to the spatial integration that takes place by means of a diffusion-like filling-in mechanism, this phenomenon shows that the visual system is sensitive to temporal physical changes, which are integrated so that the constant bias is rightly computed over time from the seemingly totally random and quick changes.

6.4.4 A dynamic illusion for the two eyes: binocular rivalry and the role of adaptation in it⁸

So far, only such visual phenomena have been discussed, for which one eye is sufficient to work. However, our visual system relies on two eyes, therefore, binocular vision is also an important issue to be investigated. The two eyes can also be provoked so that the perceptual experience will deviate from what is physically present. Such a binocular illusion was created by Béla Julesz (Julesz, 1971/2006). Although two 2-D random dot images are presented for the two eyes respectively, a 3D image is perceived. The square floating in front of the background is not present physically; it is the visual system that builds up a 3-D model relying merely on binocular disparity, which is the only relevant piece of information that is directly included in the stimulus. As it has already been discussed in the introduction of this thesis, this phenomenon revealed an important characteristic of binocular vision: no shape recognition is necessary for stereopsis, contrary to what had been previously thought. This example clearly demonstrates how visual illusory phenomena reveal facts about the visual system.

Julesz's Random Dot Stereogram models real vision in the sense that the stimulus comprises two images that more or less overlap; the only difference between them is what would be caused by binocular disparity. However, it is also interesting to study how binocular vision works if the two images do not overlap at all. Surprisingly, the two different images are

⁸ Parts of this chapter have been published in Hudák, Jakab and Kovács (2013).

not merged into one by averaging them, or are not perceived simultaneously adjacent to each other, as could be expected if the visual system were such that it always shows what is physically present. Rather, instead of two static images, one continuously changing dynamic image is perceived. This two-eye illusion is termed binocular rivalry in the literature, since the two images seem to compete to be represented in the actual perceptual experience. The two images are perceived to be constantly alternating, during which the mosaic of the two images are also perceived for some time. Investigating the dynamics of this binocular illusion might reveal important facts on binocular vision.

For instance, it had been widely accepted that it is the two eyes that are competing under binocular rivalry, which was believed to take place at a low level in the visual system by the suppression of monocular neurons whose signals originate from the two eyes (e.g. Blake, 1989). However, Kovács, Papathomas, Yang and Fehér (1996) cast doubt on this hypothesis. In their experiment, they used isoluminant stimuli, comprising image pairs of green and red disks on a yellow background, in order to exclude all cues other than hue. If one disk on the right image was green, then the disk in the same position in the left image was red and vice versa. Thus they obtained a complementary patchwork of an image with green disks and an image with red disks on a yellow background. They found that the dominance time of the pure green or the pure red disk percepts elicited by the patchwork stimuli exceeded the expected dominance time of pure green or red percepts that should have occurred if merely the two eyes competed irrespective of the stimulus. Thus it is feasible to think that binocular rivalry also involves higher visual areas where grouping mechanisms are at work besides low level areas.

We investigated binocular rivalry in a wider context (see Study IV). Perceptual bistability is not only present in binocularly rivalrous images. Many characteristics of binocular rivalry are shared by ambiguous figure perception as well. These are higher level illusions where physically only one image is present, however, the visual system alternates between two interpretations. Such images are the Necker-cube or the duck-rabbit figure (FIG. 15).

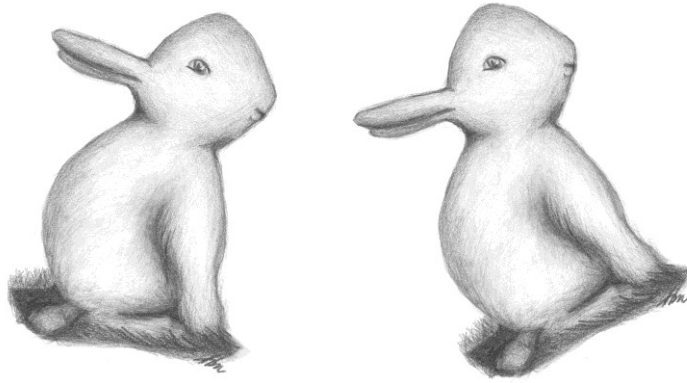


Figure 15. The duck-rabbit figure (redrawn after Ehrenstein, 1930). The same image can be perceived both as a rabbit and as a duck, but the two percepts cannot be observed at the same time; they periodically alternate. However, the orientation of the image might help one or the other percept to dominate. Here the left image is easier to see as a rabbit, while the right image is more likely to trigger the duck interpretation.

The common features are, for instance, the gamma distribution of the dominance times of each percept, the high inter-subject variability of the frequency of reversals, the significant influence of stimulus properties on reversal rates, and the fact that both can be influenced by the voluntary control of the subject (see Kornmeier and Bach 2005).

According to the findings reviewed by Leopold and Logothetis (1999), stimulus properties, such as brightness, contrast and spatial-frequency content can have a significant impact on the balance of dominance and suppression. In addition, high-level properties of the stimuli can also modify dominance periods in multi-stable perception. Such properties include recognisability or semantic content. For instance, if a recognizable figure is inverted upside down, then its perceptual dominance might significantly be altered in both figure/ground stimuli and binocular rivalry.

Voluntary control is another factor affecting multi-stable perception. Subjects' voluntary control had a stronger influence on the perception of ambiguous figures than that of binocularly presented rivalrous stimuli (van Ee, van Dam, and Brouwer 2005). Taddei-Ferretti et al (2008) also point out that the rivalry between the two possible percepts of an ambiguous figure is less automatic than the competition between two different images presented binocularly. An additional common feature of binocular rivalry and ambiguous figures that Taddei-Ferretti et al. (2008) mention is that both are influenced by eye-movements (Ellis and Stark 1978; Sabrin and Kertesz, 1980).

According to Pastukov and Braun (2011), neural adaptation is also an important factor in the numerous types of bistable perception, though it is difficult to discern its effect. They list numerous studies in which no negative correlation was shown between past and future dominance periods. periods (Borsellino, De Marco, Allazetta, Rinesi, & Bartolini, 1972; Fox & Herrmann, 1967; Lehky, 1995; Walker, 1975). In order to find a more effective indicator of adaptational effects in bistable perception, they introduced the concept of cumulative history, which they define as ' an integral of past perceptual states, weighted toward the most recent states' (p. 2). By means of this measure, they showed that past and future dominance periods exhibit significant linear correlations which they attribute to neural adaptation to the dominant percept. They suggest that when the adaptive states of competing percepts are balanced, perceptual fluctuations are governed by stochastic factors.

In Study IV, we investigated these adaptational factors under binocular rivalry encompassing a longer timescale. Our results show that the visual system integrates these illusory changes that occur under binocular rivalry, besides the integration of physical hue and intensity changes over time and space as discussed in the previous chapter. We also found developmental differences in the characteristics of this type of adaptation as shown by the novel measures introduced by Pastukhov and Braun (2011).

6.5 Developmental aspects of visual illusions⁹

When investigating perceptual development, an inherently interesting question is, what is children's perceived world like, and how does it differ from that of adults? The data reviewed in this chapter is intended to shed some light on this question.

Illusions are invaluable tools for studying perception, since by means of investigating the 'errors' made by the visual system meticulously, we can draw conclusions on its working mechanisms. By studying differences in perception of illusions in different age-groups, answers to crucial developmental questions can be unveiled. Unfortunately, however, few data is available in the literature concerning the perception of illusions in children.

One such study was conducted by Yang, Kanazawa and Yamaguchi (2009). Their findings suggests that infant colour perception can be deceived similarly to that of adults, which implies that the mechanism behind colour perception must be well-developed at such

⁹ This chapter has been published in Hudák, Jakab and Kovács (2013).

an early age. They used the neon colour spreading illusion to investigate this issue. The image in which neon colour spreading illusion is perceived, comprises of a black grid on a white background, where the intersections of the grid are coloured (usually red or blue, etc.). The background areas around the coloured crosses of the intersections are physically uniform white. However, a chromatic veiling disk spreading in a neon-like manner is perceived around the coloured crosses.

In their study, 3-4-month-old infants showed evidence (preferential looking) of experiencing neon colour spreading illusion in moving stimuli, but not in static ones. 5-6-month-olds on the other hand preferred neon colour spreading stimuli in both static and moving form. It is known that 4-month-old infants can perceive transparency in chromatic and moving patterns (Johnson and Aslin, 2000). It has also been demonstrated that the perception of transparency is necessary for the emergence of neon colour spreading (Meyer and Dougherty, 1987; Nakayama, Shimojo, and Ramachandran, 1990; Bressan, 1993). These data suggest that the perception of transparency and that of neon colour spreading develop together. Therefore, it seems that 5-6-month-old infants experience colours in ways comparable to that of older children and adults.

In addition to the neon colour spreading illusion, the Munker-White effect was also studied by Yang, Kanazawa and Yamaguchi in another study (Yang, Kanazawa and Yamaguchi, 2010). They showed that infants aged 4-8 months could perceive the illusion, that is, infants perceived pink targets more saturated if they were surrounded by more red than yellow. A looking preference paradigm was applied, based on the assumption that infants prefer high subjective saturation. In accordance with this expectation, infants showed significantly longer viewing times for the image in which the pink targets looked more saturated. However, the overall ratio of red in those images was inherently higher compared to yellow, whereas the images, whose pink targets looked less saturated, contained twice as much yellow as red. This entails that the images did not only differ in the perceived (illusory) saturation of the pink targets, but the overall physical saturation was higher in the images containing more red. Thus, in a second, control experiment, the authors applied the same colours but altered their spatial arrangement: the three colours of the original Munker-White configuration were shown as three large rectangles, dividing the image into three spatially uniform parts. In one of the two variants used, the red part covered half of the image, while it covered only its quarter in the other. Between these two figures, no significant difference in looking times was obtained; therefore, the authors concluded that the preference in the first

experiment was due to the higher illusory saturation of the pink targets, rather than the higher overall ratio of red in those images. It can be noted, however, that in the second experiment, which was used as a control condition, children may have fixated exclusively the large uniform red squares, irrespective of their sizes, not scanning the image as a whole. This could also account for not obtaining significant difference in looking times in the control experiment. It would be worth applying an eye-tracker in the control experiment of such studies, or to use a randomly mixed spatial arrangement of the colours while keeping their proportions constant. Nonetheless, to summarize the results reviewed so far, it seems that infants, as young as a few month of age, perceive colours in an adult-like manner.

Another study that suggests that the perception of colour and luminance is genetically preprogrammed, or at least that it occurs particularly early in life, was conducted by Chien, Palmer and Teller (2005). This study compared the luminance perception of infants with that of adults. The authors examined whether infants' luminance perception deviated from Wallach's ratio rule in the same manner as the luminance perception of adults does. According to Wallach's (1948) ratio rule, the perceived lightness of a disk is determined by the ratio of the luminance of the disk and that of its surround. This rule provides a good approximation of human luminance perception, however, an approximately 10% deviation occurs in the direction of a luminance match. In a forced-choice novelty preference technique in combination with a cross familiarization paradigm, Chien, Palmer, and Teller (2005) found that children's luminance perception was more similar to that of adults, involving a certain deviation from Wallach's ratio rule, than to what Wallach's ratio rule would predict. In other words, infants deviated from Wallach's ratio rule in the same way as adults did. This result also supports the early and quick development of luminance perception.

Though many crucial visual functions are shown to emerge during the first year of life, visual development is not finished until the end of childhood (Kovács 2000). There is an observable inhomogeneity in the development of different visual functions and the maturation of neuroanatomical circuits participating in visual information processing. In contrast with the data that suggest that colour vision develops early in life, integration of contours (Kovács, 2000) or of the visual context (Káldy and Kovács, 2003) is not fully developed even at the age of 4-5 years.

Káldy and Kovács (2003) examined the effect of visual context on size perception by means of the Ebbinghaus illusion (or Titchener circles). They compared the magnitude of the Ebbinghaus illusion in 4-year-old children and adults. Applying a 2AFC design, in which the

subjects had to judge which of the two presented disks was bigger, they found that children were significantly less deceived by the illusion than adults, and perceived the target disk surrounded by disks of different sizes in accordance with its veridical size. The perception of adults was more misled by the context. The authors suggest that the reduced contextual sensitivity in children is due to immature cortical connectivity.

Hanish, Konczak and Dohle (2001) also used the Ebbinghaus illusion to investigate the effect of spatial context in older age groups, between the ages of 5 and 12 years. The perceptual judgement task was to judge whether the two disks presented in the contexts of two different sizes were of the same or different size. They randomly exchanged the target disks to larger and smaller ones, repeating each 3 times, while keeping the size of the reference disk constant. They report that when pure perceptual judgements had to be made, children were deceived by the illusion to the same extent as adults, i.e. they produced the same size estimations, which might imply that maturation is gradual, and although 4 year-olds are not deceived by the context (Káldy and Kovács, 2003), neural connectivity is getting closer to the adult level by 5-12 years of age. On the other hand, in Hanish, Konczak and Dohle (2001)'s study, when subjects were presented again with the configuration using the same disk sizes they had previously judged as equal, adults were deceived significantly more (81%) than the two groups of children (55% for 5-7 year-olds and 63% for 8-12 year-olds).

Another illusion that involves the integration of spatial context in the perception of size is the Müller-Lyer illusion. It comprises two parallel lines, whose lengths are identical. One of them ends in an outward-pointing arrow, while the other ends in an inward-pointing arrow on both ends. However, the line ending in an outward-pointing arrow looks much shorter than the one ending in an inward-pointing arrow.

Rival and her co-workers (2003) investigated the Müller-Lyer illusion in children aged 7, 9 and 11 years. The task of the subjects was to select the bar from the 5 bars of different sizes, whose size matched that of the target bar, presented in the illusion context. Their perceptual task results imply that the illusion was present in children, though 11 year-olds were more deceived than 7-year-olds. All the three age groups underestimated the size of the line with outward-pointing arrows at its end, but the inward-pointing arrows made only the 11 year-olds overestimate line size. Unfortunately, this study did not include an adult control group either.

As for binocular vision, the earliest age at which the presence of stereopsis was shown, is 3 weeks (Mocan, Wright, and Salvador 2007). Aslin and Dumais (1980), however, list a

number of constraints that prevent infant binocular functions from being adultlike, such as acuity and contrast sensitivity, accommodation, and facial dimensions. Infants younger than 3 months of age might also have a difficulty in keeping stable bifoveal fixation (Aslin and Dumais 1980).

Whether there is a critical period in human development for binocular vision, and what is perceived by infants before the occurrence of binocular 3D perception are debated issues. The existence of a critical period in the development of binocular vision in the cat has long been known (Hubel and Wiesel 1965). As for humans, children who suffer deprivation of binocular input in the first 3 years of their lives, never develop normal binocular function, even when their eyes are aligned by surgery. Sensitivity to binocular deprivation can be found up to the age of 9 years (Aslin and Dumais 1980). However, there also exist data that support plasticity after the supposed critical period, implying that proper treatment can reassemble binocular functions (Blake and Wilson 2011). Data on the development of binocular rivalry and other forms of bistable perception, which shows spectacular changes during human lifespan, is reviewed in Study IV.

To conclude, the emerging view seems to be that concerning luminance-and colour perception, the perceptual world of children might be very similar to that of adults, even such early ages as a few months. Colour and luminance discrimination and perception seem to work in an adult-like manner in children. Regarding illusory colour experiences, young children and adults exhibit important similarities.

In contrast, at higher levels of perception, such as binocular vision or the interpretation of ambiguous figures, as well as the integration of spatial information present in the entire visual field, longer periods of maturation and learning are necessary in order to attain the perceptual abilities and therefore, the phenomenology experienced by normal-sighted healthy adults. This maturation continues up to at least pre-puberty, and plasticity for such perceptual skills can also be shown in adult subjects, in line with our findings presented in Study IV.

Based on the reviewed data, the conclusion can be drawn that the development of colour perception involves a genetically preprogrammed maturation to a considerable extent. In contrast, the perception of form and space as well as binocular vision and perception of ambiguity of forms rely heavily on perceptual learning through childhood

7 The aims and synopses of the thesis¹⁰

The basic aim is to investigate the regularities and dynamics of brightness/colour perception and binocular vision by means of psychophysical experiments utilizing the immense potentialities offered by various types of visual illusions.

First, we attempt to capture both assimilation and contrast phenomena elicited by brightness and colour illusions by a unified model. Measuring different physical parameters on which illusions depend may help us provide a unified model for all known brightness/colour illusions, and thus for the basic mechanisms of vision. The unified model is a key issue, since on the phenomenal level, seemingly opposite effects occur. However, it cannot be assumed that the nervous system, on recognising the image, would switch from “assimilation method” to “contrast method”. It is more plausible to suppose that the same processes are used when seeing assimilation, contrast, or real pictures.

This provides the basis for our refutation of lateral inhibition-based models: since those models predict the same percept both in the classical and our modified images, they should be rejected in accordance with the forgoing demand for a unified model.

The search for a unified model for both types of phenomena including assimilation and contrast is the most crucial aim in our research. Investigating and modifying the physical parameters of illusions and studying how these parameters influence the perceptual experience offer a promising way to capture what works inside the 'black box'. Quantitative experimental data on perceptual changes depending on the physical characteristics of illusions are well comparable with the predictions of different computational models, obtained by means of computer simulations. In this paradigm, we find that it is a filling-in type of computational model that provides the best predictions for brightness phenomena.

The foregoing phenomena work even monocularly and statically. However, to understand the system level, it is necessary to investigate the dynamics of vision, since natural stimuli involves temporal changes and relies on two eyes. Therefore, besides the spatial integration of luminance and hue, the temporal integration of changes is also important to investigate. Visual illusions serve as priceless tools for studying even these issues. Afterimages reveal information on how temporal integration takes place, whereas binocular

¹⁰ Parts of this chapter will be published in Geier and Hudák (in press).

illusions, among which the most studied one is binocular rivalry, might help us understand how inputs from the two eyes are processed by our visual system.

Thesis 1.

Modified classical lightness-brightness illusions show that generally accepted local explanatory principles based on lateral inhibition should be rejected.

Two illusions that had served as strongholds for the concept of lateral inhibition for decades are the Hermann grid illusion and the Chevreul illusion. The classical explanation is described in Chapter 6.2.2 and in Study I-II.

a.) In Study I, we curved the streets of the Hermann grid which made the spots disappear. If the cause of the spots were indeed the larger proportion of lateral inhibition at the intersections, then the same illusory spots should be perceived in the curved grid as in the straight grid, since the stimulation of the corresponding receptive fields projected to the straight and the curved grids is equal. However, no spots are seen in the curved grid. Therefore, the Baumgartner model, which is merely based on the different stimulation of receptive fields at the intersections and in the street sections, is not tenable. The fact that curvature significantly changes the Hermann grid illusion calls for the rejection of the classical explanation and for developing a new one.

b.) In Study II, we placed the Chevreul staircase in a luminance ramp background, which considerably affected the illusion: it significantly increased or decreased, depending on the progression of the ramp relative to the staircase. When the progression of the staircase was identical with that of the ramp, the illusion was enhanced, whereas when the staircase and the ramp progressed in opposite directions, the illusion ceased. (We placed the staircase into the ramp so that the staircase itself remained physically unchanged).

We also noted that the change in the illusory effect was equally strong through the entire height of each step. In other words, the change of the illusion is not limited to the immediate neighbourhood of the upper and lower edges of the steps, where they adjoin the ramp. This is so, even when any inner point of the staircase far from the ramp is fixated for several seconds.

The significance of the ramp effect is that it challenges the generally accepted explanation of the Chevreul illusion. In our modified Chevreul illusions, the replacement of the original white background with a luminance ramp background causes physical luminance change exclusively *outside* the area of the staircase, while no physical change has occurred

within the staircase. Classical lateral inhibition-based explanations build exclusively upon luminance relations of the steps *within* the staircase. Therefore, if classical lateral inhibition-based explanations were tenable for the Chevreul illusion, then the perception within the steps should not have been changed by the ramp. This explanation, at the best, can predict change merely near the upper and lower boundaries of the staircase, but not through the entire height of the steps. This is in contradiction with the phenomenon that the illusion has changed through the entire vertical height of the staircase merely due to the surrounding luminance ramp. Consequently, it can be concluded that the classical explanation based on lateral inhibition is not tenable for the ramp effect.

It still could be reasonable to think that multiscale models can predict the phenomena presented in our images. However, such models fail to predict our double-ramped variants, where a thin inner ramp is included in the original outer ramp, adjacent to the staircase. Although the area of the inner ramp is negligible compared to the outer one, it still dominates perception. The reason for the failure of multiscale models is that the large filters (e.g. in the ODOG model, the largest filter diameter is 36 deg including the surround) are influenced by the outer ramp to such an extent that the outer ramp will dominate the predicted perceptual experience, contradictory to human perception (for a more detailed analysis, see Study II.). In case of the application of small filters only, however, the inner parts of the staircase will not be influenced even by the inner ramp.

Consequently, it can be stated that DoG-based models fail to predict the ramp effect phenomena, since neither small, nor large filters are able to capture these changes, irrespective of whether they are circularly symmetric or elongated.

Thesis 2.

Towards a unified theory: brightness illusions show that it is a filling-in mechanism that integrates spatial changes in luminance, in which edges play a crucial role.

a.) In our search for a unified model, we attempted to find the crucial characteristics of the Hermann grid. To investigate the necessary conditions for the spots to disappear, we applied further distortion types in addition to the sine curves.

Our psychophysical experiments were based on a measure that we introduced as distortion tolerance (Study I.). We defined the term "distortion tolerance" as the amplitude of curvature at which the illusory spots disappear. Our aim was to reveal, by means of empirical data, on what parameter distortion tolerance depended.

Our experimental results demonstrate that higher amplitude of curvature is necessary to eliminate the illusion, when one side of the streets remains straight. On this basis, we concluded that the main cause of the Hermann grid illusion is the straightness of the black /white edges of the streets.

As a unified explanation of the presence of spots in the classical Hermann grid, and their absence in the curved grid, we propose that a diffusion-like activation-spreading (or filling-in) mechanism should be sought behind these phenomena, in which the straightness of the edges is crucial. In Study I, we provided a qualitative description of the model.

b.) If we aim to find a new, unified explanatory principle also for the Chevreul illusions with and without ramps, we have to notice that due to placing the ramp around the staircase, not only the area outside the staircase has been changed physically, but the boundary edges of the staircase, too. In Study II, to decide which of these plays a more important role in the change of the Chevreul illusion, we placed another, narrow ramp around the staircase, whose direction was opposite to that of the original, larger ramp.

The result of this modification is that although the area of the inner ramp is significantly smaller than that of the outer ramp, the inner one still governs the change in the Chevreul illusion. If the inner ramp is replaced by a homogeneous rectangle, then two the Chevreul staircases are perceived as identical (progressing in opposite directions), and the outer ramp will have no effect.

This result supports that the upper and lower boundary edges of the staircase control the perceptual experience, and not the area size of the ramp, since such a narrow ramp as half a degree can prevail against the effect of the much larger outer ramp. Therefore, we conclude that it is the boundary edges in the image that govern perceptual experience instead of the large background areas, and long-range interactions should be supposed between edges and the areas enclosed by them.

Thus, the implications of the Hermann grid illusion in Study I and that of the Chevreul illusion in Study II largely overlap both concerning the refutation of their traditional explanations and the role of edges and filling-in in a new, unified theory.

Thesis 3.

Dynamic illusions and after-images show that the temporal changes in luminance and hue are integrated in time by the visual system even without spatial cues, such as form.

Besides the investigation of spatial integration of luminance, we also investigated one aspect of temporal integration by means of a novel afterimage. Observers (n=130) were presented with a movie in which a field of randomly coloured or black/white flickering squares were watched for 45 s. A shape of a capital letter was hidden in the display, by means of an implicit bias towards green (or in the achromatic version, towards white). Observers could not perceive this letter. Thus, although only randomly flickering squares were seen, subjects readily reported the pink afterimage subsequently, naming the letter correctly. This demonstrates that the visual system integrates the changing colours over time and stores them. A certain type of adaptation occurs for the average of each retinal point, which results in a recognisable shape in the afterimage, although no coherent shape is present during the adaptational period.

Thesis 4.

An illusion for two eyes: binocular rivalry demonstrates that the visual system is capable of integrating merely perceptual changes even without physical ones, which shows differences during the course of development.

Not only physical changes are integrated in time by the visual system, but illusory changes as well. This is well demonstrated under binocular rivalry, where two static images are shown to the subject, however, dynamic illusory changes in the mixture of the two images are perceived.

We investigated this binocular illusion in psychophysical experiments, for which the paradigm was developed in international cooperation (Study IV.). Here subjects were requested to continuously point by a joystick to the image they are seeing at the moment, while their response was recorded by the computer. Hereby the dynamics and the neural adaptational effects behind the phenomenon can be investigated.

We studied binocular rivalry in 9 and 12 year-old and in grown-up populations. (Study IV). Our results are interpreted in Pastukhov and Braun's (2011) framework, assuming that the visual system integrates the dominance time of the given percept, which influences its future dominance times. Thus the model describes a certain type of neural adaptation behind bistable perceptual phenomena, which was confirmed by our results. We also found

significant developmental differences within this framework: children alternated and adapted more quickly and showed a stronger adaptation effect than adults. The developmental curve, however, is incomplete; further investigations on adolescents seem fruitful.

8 References

- Adelson, E. H. (1993). Perceptual organization and the judgment of brightness. *Science*, 262 (5142), 2042–2044.
- Adelson, E.H. (2000). Lightness Perception and Lightness Illusions. In: The New Cognitive Neurosciences, 2nd ed., M. Gazzaniga (ed.). Cambridge, MA: MIT Press, pp. 339-351, (2000).
- Adrian, E.D. (1926). The impulses produced by sensory nerve endings. Part 4. Impulses from Pain Receptors. *J Physiol.*, 61(2), 151–171.
- Adrian E.D. & Mathews, R. (1927). The action of light on the eye. Part I. The Discharge of Impulses in the Optic Nerve and its Relation to the Electric Changes in the Retina. *J Physiol.*, 64(3), 279–301.
- Anderson, B. L. (1997). A theory of illusory lightness and transparency in monocular and binocular images: the role of contour junctions. *Perception*, 26 (4), 419-53.
- Anderson, B. L. (2003). Perceptual organization and White's illusion. *Perception*, 32, 269 – 284.
- Anstis, S. (2013). Contour adaptation. *Journal of Vision*, 13 (2), 25.
- Anstis, S, Vergeer, M. & van Lier, R. (2012). Luminance contours can gate afterimage colors and "real" colors. *Journal of Vision*, 12(10), 2.
- Arrington, K. F. (1996). Directional filling-in. *Neural Computation*, 8, 300-318
- Ashida, H., Kuriki, I., Murakami, I., Hisakata, R. & Kitaoka, A. (2012). Direction-specific fMRI adaptation reveals the visual cortical network underlying the “Rotating Snakes” illusion. *Neuro Image*, 61, 1143–1152.
- Aslin, R. N., & Dumais, S. T. (1980). Binocular vision in infants: a review and a theoretical framework. In: Reese, H. W. & Lipsitt, L. P. (eds.) *Advances in Child Development and Behaviour*. New York, USA: Academic Press Inc. pp. 53-94.
- Barlow, H. B., Fitzhugh, R., & Kuffler, S. W. (1957). Change of organization in the receptive fields of the cat’s retina during dark adaptation. *J. Physiol.*, 137, 338-354.
- Barlow, H. B. (1990). A theory about the functional role and synaptic mechanism of visual aftereffects. In Blakemore, C. (Ed.). *Visual coding and efficiency*. Cambridge, UK: Cambridge University Press, pp. 363–375.

- Baumgartner, G. (1960). Indirekte Größenbestimmung der rezeptiven Felder der Retina beim Menschen mittels der Hermannschen Gittertauschung. *Pflugers Archiv für die gesamte Physiologie*, 272, 21-22.
- Bergen, J. R. (1985). Hermann's grid: new and improved (abstract). *Investigative Ophthalmology and Visual Science, Supplement 26*, 280.
- Blake R. (1989). A neural theory of binocular rivalry. *Psychol. Rev.*, 96, 145–167.
- Blake, R. & Sekuler, R. (2006). *Perception*. Boston: McGraw-Hill.
- Blake, R. & Wilson, H. (2011). Binocular Vision. *Vision Research*, 51, 754–770.
- Blakeslee, B. & McCourt, M.E. (1999). A multiscale spatial filtering account of the White effect, simultaneous brightness contrast and grating induction. *Vision Research*, 39, 4361-4377.
- Blakeslee, B. & McCourt, M.E (2004) A unified theory of brightness contrast and assimilation incorporating oriented multiscale spatial filtering and contrast normalization. *Vision Research*, 44, 2483–2503.
- Blakeslee, B. & McCourt, M.E (2008). Nearly instantaneous brightness induction. *Journal of Vision*, 8(2),15.1–15.8.
- Borsellino, A., De Marco, A., Allazetta, A., Rinesi, S., & Bartolini, B. (1972). Reversal time distribution in the perception of visual ambiguous stimuli. *Kybernetik*, 10(3):139-144.
- Bressan, P. (1993). Neon colour spreading with and without its figural prerequisites. *Perception*, 22, 353–361.
- Bressan, P. (2001). Explaining lightness illusions. *Perception*, 30, 1031–1046.
- Bressan, P. (2006). Inhomogeneous surrounds, conflicting frameworks, and the double-anchoring theory of lightness. *Psychonomic Bulletin & Review*, 13(1), 22-32.
- Brown, S. P., He, S. & Masland, R. H. (2000): Receptive field microstructure and dendritic geometry of retinal ganglion cells. *Neuron*, 27, 371-383.
- Chevreul, M. E. (1839). *De la loi du contraste simultané des couleurs et de l'assortiment des objets colorés*. - translated into English by Charles Martel as *The principles of harmony and contrast of colours* (1854)
- Chien, S. H., Palmer, J. & Teller, D. Y. (2005). Achromatic contrast effects in infants: adults and 4-month-old infants show similar deviations from Wallach's ratio rule. *Vision Research*, 45, 2854-2861.
- Cohen, M.A. & Grossberg S. (1984). Neural dynamics of brightness perception: features, boundaries, diffusion, and resonance. *Perception and Psychophysics*, 36, 428-456.
- Cornsweet, T. (1974) *Visual Perception*. New York: Academic Press.

- Curcio, C. A. & Allen, K. A. (1990). Topography of ganglion cells in human retina. *The Journal of Comparative Neurology*, 300, 5-25.
- Curcio, C. A., Sloan, K. R., Kalina, R. E., & Hendrickson, A. E. (1990). Human photoreceptor topography. *The Journal of Comparative Neurology*, 292, 497-523.
- Dacey, D. (2004). Origins of perception: ganglion cell diversity and the creation of parallel visual pathways. In: Gazzaniga M. S. (ed.) *The Cognitive Neurosciences*. Cambridge, MIT Press, pp. 281-301.
- Dacey D.M. & Petersen, M. R (1992). Dendritic field size and morphology of midget and parasol ganglion cells of the human retina. *Proc. Natl. Acad. Sci.*, 89, 9666-9670.
- Dakin, S. C. & Bex, P. J. (2003). Natural image statistics mediate brightness ‘filling in’. *Proc. R. Soc. Lond.*, 270, 2341–2348.
- De Lacey, G., Morley, S. & Berman, L. (2009). *The chest X-Ray: a survival guide*. Spain: Elsevier.
- Delvin, H. (2006). *Operative dentistry: A Practical Guide to Recent Innovations*. Berlin, Heidelberg: Springer-Verlag.
- De Valois, R. L., & De Valois, K. K. (1988). *Spatial Vision*. New York: Oxford University Press.
- DeVries, S.H. & Baylor, D.A. (1997). Mosaic arrangement of ganglion cell receptive fields in rabbit retina. *J. Neurophysiol.* 78, 2048-2060.
- DeWeert, C. (1991). Assimilation and contrast. In: Valberg, A. & Lee, B. (eds.). *From Pigments to Perception*. New York: Plenum Press. pp. 305–311.
- Ditchburn, R. W. (1973). *Eye movements and visual perception*. London: Oxford University Press.
- Ehrenstein, W. (1930). Untersuchungen über Figur-Grund-Fragen. *Zeitschrift für Psychologie*, 117, 339-412 (Fig. 3, p. 369).
- Ellis, S. R. & Stark, L. (1978). Eye movements during the viewing of Necker cubes. *Perception*, 7, 575–581.
- Enroth-Cugell, C. & Robson, J. G. (1966). The contrast sensitivity of retinal ganglion cells. *J. Physiol.*, 187, 517-552.
- Faubert, J. & Herbert, A.M. (1999). The peripheral drift illusion: a motion illusion in the visual periphery. *Perception* 28, 617–621.
- Fox, R. & Herrmann, J. (1967). Stochastic properties of binocular rivalry alternations. *Perception and Psychophysics*, 2(9), 432-446.

- Geier J. (2009). A diffusion based computational model and computer simulation for the lightness illusions. *Perception*, 38, *ECVP Abstract Supplement*, 95.
- Geier J., Séra L. & Hudák M. (2007). Whiter than white, blacker than black-overshot in lightness perception. *Perception*, 36, *ECVP Abstract Supplement*.
- Geier J., & Hudák, M. (in press). The curved grid non-illusions: eliminating Hermann's spots and Lingelbach's scintillation. In: Todorovic, D. and Shapiro, A. (eds.). *The Oxford Compendium of visual illusions*. London: Oxford University Press.
- Geier J., & Hudák, M. (in press). Changing the Chevreul Illusion by a Background Luminance Ramp. In: Todorovic, D. and Shapiro, A. (eds.). *The Oxford Compendium of visual illusions*. London: Oxford University Press.
- Gilchrist, A. L. (1977). Perceived lightness depends on perceived spatial arrangement. *Science*, 195, 185-187.
- Gilchrist A. (2006). *Seeing Black and White*. Oxford: Oxford University Press.
- Gilchrist, A., & Jacobsen, A. (1984). Perception of lightness and illumination in a world of one reflectance. *Perception*, 13, 5–19.
- Gilchrist, A., Kossyfidis, C., Bonato, F., Agostini, T., Cataliotti, J. & Li, X. (1999). An anchoring theory of lightness perception. *Psychological Review*, 106(4), 795–834.
- Goldstein, E. B. (2009). *Sensation and perception*. Belmont: Wadsworth Cengage Learning.
- Gori, S. & Stubbs D. A. (2006). A new set of illusions—the dynamic luminance-gradient illusion and the breathing light illusion. *Perception*, 35(11), 1573 – 1577.
- Gregory, R.L. (1968). Perceptual illusions and brain models. *Proc. Royal Society, B* 171, 179-296. http://www.richardgregory.org/papers/brainmodels/illusions-and-brain-models_all.htm
- Gregory, R.L. (1997). Visual Illusions Classified. *Trends in Cognitive Sciences*, 1(5), 190-194.
- Gregory, L. R. (2009). *Seeing through illusions*. London: Oxford University Press.
- Grossberg, S., & Todorovic, D. (1988). Neural dynamics of 1D and 2D brightness perception: A unified model of classical and recent phenomena. *Perception and Psychophysics*, 43, 241–277.
- Hanisch, C., Konczak, J., & Dohle, C. (2001). The effect of the Ebbinghaus illusion on grasping behaviour of children. *Experimental Brain Research*, 137, 237–245.
- Hartline, H. K. (1949). Inhibition of activity of visual receptors by illuminating nearby retinal areas in the Limulus eye. *Federation Proceedings*, 8(1), 69-69.

- Hartline, H. K. (1967). Visual receptors and retinal interaction. *Les Prix Nobel en 1967*. Nobel Foundation 1968, 1969, 242-259.
- Helson H. (1963). Studies of anomalous contrast and assimilation. *Journal of the Optical Society of America*, 53, 179-184.
- Hering E. (1874/1964). *Outlines of a theory of the light sense*. (translated by L M Hurvich, D Jameson). Cambridge, MA: Harvard University Press. [originally published in 1874]
- Hermann L (1870) Eine Erscheinung simultanen Contrastes. *Pflügers Archiv für die gesamte Physiologie*, 3, 13–15.
- Hisakata, R. & Murakami, I. (2008). The effects of eccentricity and retinal illuminance on the illusory motion seen in a stationary luminance gradient. *Vision Research*, 48, 1940–1948.
- Hong S. W. & Shevell S. K. (2004). Brightness induction: Unequal spatial integration with increments and decrements. *Visual Neuroscience*, 21, 353-357.
- Howe, P. D. L. (2005). White's effect: Removing the junctions but preserving the strength of the illusion. *Perception*, 34(5), 557 – 564.
- Hubel, D. H. & Wiesel, T. N. (1965). Binocular interaction in striate cortex of kittens reared with artificial squint. *Journal of Neurophysiology*, 28, 1041–1059.
- Hudák M. F. & Geier J. (2007). Modelling with flying colours: The application of the RadGrad model to chromatic Hermann grids. *Perception*, 36, *ECVP Abstract Supplement*.
- Hudák M. & Geier J. (2009). White effect without physical edges. *Perception*, 38, *ECVP Abstract Supplement*, 51.
- Hudak M. & Geier J. (2011). The segmenting effect of diagonal lines in the ramped Chevreul illusion. *Perception*, 40, *ECVP Abstract Supplement*, 202.
- Hudák M, Geier J. & Lingelbach B. (2010). Scintillation in the Spillmann–Levine grid. *Perception*, 39, *ECVP Abstract Supplement*, 166.
- Hudák M., Jakab Z. & Kovács I. (2013). Phenomenal qualities and the development of perceptual integration. In: Albertazzi, L (ed.). *Handbook of experimental phenomenology: visual perception of shape, space and appearance*. Chichester: John Wiley & Sons Ltd. pp. 145-163.
- Johnson, Scott, and Richard Aslin. 2000. “Infants’ Perception of Transparency.” *Developmental Psychology*, 36: 808-816. DOI: 10.1037//0012-1649.36.6.808
- Julesz B. (1971/2006). *Foundations of Cyclopean Perception*. University Of Chicago Press/MIT Press

- Káldy Z., & Kovács I. (2003). Visual Context Integration is not fully developed in 4-year-old children. *Perception*, 32, 657 – 666.
- Kingdom, F. A. A. (2003) Levels of Brightness Perception. In: Harris, L. & Jenkin, M. (eds.). *Levels of Perception*. Springer-Verlag
- Kingdom, F. A. A. (2011). Lightness, Brightness and Transparency: A quarter century of new ideas, captivating demonstrations and unrelenting controversy. *Vision Research*, 51, 652-673.
- Kingdom F. & Moulden G. (1992) A multi-channel approach to brightness coding. *Vision Research*, 32 (8), 1565–1582.
- Kitaoka A, & Ashida H. (2003). Phenomenal characteristics of the peripheral drift illusion. *Vision*, 15, 261–262.
- Kornmeier, J., & Bach, M. (2005). The Necker cube—an ambiguous figure disambiguated in early visual processing. *Vision Research*, 45, 955–960.
- Kovács I. (2000). Human development of perceptual organization. *Vision Research*, 40, 1301–1310.
- Kovács, I., Papathomas, T., Yang, M. & Fehér Á. (1996). When the brain changes its mind: interocular grouping during binocular rivalry. *Proceedings of the National Academy of Sciences*, 93, 15508–15511.
- Kuffler, S. W. (1952): Neurons in the retina: organisation, inhibition and excitation problems. *Cold Spring Harbor Symposia on Quantitative Biology*, 17, 281-292.
- Kuffler, S.W. (1953): Discharge patterns and functional organization of mammalian retina. *J. Neurophysiol.* 16, 57-68.
- Lehky, S. R. (1995). Binocular rivalry is not chaotic. *Proc Biol Sci*, 259(1354). 71-76.
- Leopold, D. A. & Logothetis, N. K. (1999). Multistable phenomena: changing views in perception. *Trends in Cognitive Sciences*, 3, 254–264.
- Logvinenko, A. (1999). Lightness induction revisited. *Perception* 28, 803–816.
- Mach, E. (1865). Über die Wirkung der räumlichen Verteilung des Lichtreizes auf die Netzhaut [On the effect of the spatial distribution of the light stimulus on the retina]. *Sitzungsberichte der mathematischnaturwissenschaftlichen Classe der kaiserlichen Akademie der Wissenschaften*, 52, 303–322.
- Marr D, (1982): *Vision*. San Francisco: CA., W H Freeman
- McArthur, J. A. & Moulden, B. (1999). A two-dimensional model of brightness perception based on spatial filtering consistent with retinal processing. *Vision Research*, 39(6), 1199-1219.

- Meyer, G. & Thomas D. (1987). Effects of flicker-induced depth on chromatic subjective contours. *Journal of Experimental Psychology: Human Perception and Performance*, *13*, 353-360.
- Mocan, M. C., Wright, K. W., & Salvador, M. G. (2007). Evidence of Binocular Fusion in a 3-week-old Infant with Transient Abducens Nerve Paresis. *Journal of American Association for Pediatric Ophthalmology and Strabismus*, *11*(2), 199-200.
- Morrone, M. C., Burr, D. C. & Ross, J. Illusory brightness step in the Chevreul illusion. *Vision Research*, *34*, 1567-1574.
- Murakami, I., Kitaoka, A. & Ashida, H. (2006). A positive correlation between fixation instability and the strength of illusory motion in a static display. *Vision Research*, *46*, 2421–2431.
- Nakayama, K., Shimojo, S. & Ramachandran, V. S. (1990). Transparency: relation to depth, subjective contours, luminance, and neon colour spreading. *Perception*, *19*, 497-513.
- Otazu X., Vanrell M. & Párraga A. (2008). Multiresolution wavelet framework models brightness induction effects. *Vision Research*, *48*, 733–751.
- Paradiso, M. A. & Nakayama, K. (1991). Brightness perception and filling-in. *Vision Research*, *31*, 1221-1236.
- Pastukhov, A. & Braun, J. (2011). Cumulative history quantifies the role of neural adaptation in multi-stable perception. *Journal of Vision*, *11*(10), 12.
- Pessoa, L., Mignolla E. & Neumann, H. (1995) A contrast- and luminance-driven multiscale network model of brightness perception. *Vision Research*, *35*(15): 2201–2223.
- Pinna, B. (1987). Un effetto di colorazione. In V. Majer, M. Maeran, and M. Santinello, *Il laboratorio e la città*. XXI Congresso degli Psicologi Italiani, 158.
- Pinna, B., Werner J.S., & Spillmann, L. (2003). The watercolor effect: A new principle of grouping and figure-ground organization. *Vision Research*, *43*, 43–52.
- Ratliff F (1965) *Mach Bands: Quantitative studies on neural networks on the retina*. San Francisco, Amsterdam, London: Holden-Day Inc.
- Ratliff, F. (1990). Haldan Keffer Hartline. In: Raven, P. H. and Sherman, E. J. (eds). *Bibliographical memoirs, Volume 59*. National Academy of Sciences of the United States of America. pp 197-214.
- Rival, C., Olivier, I., Ceyte, H. & Ferrel, C. (2003). Age-related differences in a delayed pointing of a Müller-Lyer illusion.” *Experimental Brain Research*, *153*, 378–381.
- Rockhill, R., L., Daly, F. J., MacNeil, M. A., Brown, S. P. & Masland, R. H. (2002). The diversity of retinal ganglion cells in a mammalian retina. *Journal of Neuroscience*, *22*(9), 3831–3843

- Rodieck, R. W. (1965). Quantitative analysis of cat retinal ganglion cell response to visual stimuli. *Vision Research*, 5, 583–601.
- Sabrin, H. W. & Kertesz, A. E. (1980). Microsaccadic Eye Movements and Binocular Rivalry. *Perception and Psychophysics*, 28, 150–154.
- Schrauf, M., Lingelbach B., & Wist, E. R. (1997). The scintillating grid illusion. *Vision Research*, 37, 1033-1038.
- Shapiro, A. G. & Lu, Z.L., (2011). Relative brightness in natural images can be accounted for by removing blurry content. *Psychological Science*, 22(11), 1452-1459.
- Spillmann L. (1994) The Hermann grid illusion: a tool for studying human perceptive field organization. *Perception* 23, 691-708.
- Snowden, R., Thompson, P. & Troscianko, T. (2006): *Basic Vision - an introduction to visual perception*. Oxford: Oxford University Press.
- Taddei-Ferretti, C, Radilova, J., Musio, C., Santilloa, S., Cibelli, E., Cotugno, A. & Radil, T. (2008). The effects of pattern shape, sublimina stimulation, and voluntary control on multistable visual perception. *Brain Research*, 1225, 163–170.
- Todorovic, D. (1997). Lightness and junctions. *Perception*, 26(4), 379–394.
- Valberg, A. (2005). *Light, vision, colour*. Chichester: John Wiley & Sons Ltd.
- van Ee, R, van Dam, L. C. J. & Brouwer, G. J. (2005). Voluntary control and the dynamics of perceptual bi-stability. *Vision Research*, 45, 41–55.
- Van Lier, R., Vergeer, M. & Anstis, S. (2009), Filling-in afterimage colors between the lines. *Current Biology*, 19 (8), R323-R324.
- Walker, P. (1975). Stochastic properties of binocular-rivalry alternations. *Perception and Psychophysics*, 18(6):467-473.
- Ware, C. (2004). *Information Visualization, Second Edition: Perception for Design*. Elsevier, London.
- Watt, R. J., Morgan, M. J. (1985): A theory of the primitive spatial code in human vision. *Vision Research*, 25(11), 1661–1674.
- Webster, M. A. (2011). Adaptation and visual coding. *Journal of Vision*, 11(5), 3, 1–23.
- White M. (1979): A new effect of pattern on perceived lightness. *Perception*, 8(4), 413 – 416.
- Yang, J., Kanazawa, S. & Yamaguchi, M. K. (2009). Perception of neon colour spreading on 3-6-month-old infants. *Infant Behavior & Development*, 32, 461-467.

Yang, J., Kanazawa, S. & Yamaguchi, M. K. (2010). Perception of Munker–White illusion in 4–8-month-old infants. *Infant Behavior & Development*, 33, 589–595.

Yarbus, A. L. (1967). *Eye Movements and Vision*. New York: Plenum Press
(Translated from Russian by Basil Haigh. Original Russian edition published in Moscow in 1965.)

Zavagno, D. & Daneyko, O. (2010). Measuring the meter: on the constancy of lightness scales seen against different backgrounds. *Behav. Res.*, 43, 215–223

Zeki, S. (1995). *A vision of the brain*. Bilbao, Spain: Printek SA.

Straightness as the main factor of the Hermann grid illusion

János Geier, László Bernáth[¶], Mariann Hudák[¶], László Séra[#]

Stereo Vision Ltd, Nádasdy Kálmán utca 34, H 1048 Budapest, Hungary; [¶]Institute of Psychology, Eötvös Loránd University, Izabella utca 46, H 1064 Budapest, Hungary; [#]Department of Psychology, Kodolányi János University College, Fürdő u. 1, H 8000 Székesfehérvár, Hungary; e-mail: janos@geier.hu

Received 5 April 2006, in revised form 4 July 2007; published online 1 May 2008

Abstract. The generally accepted explanation of the Hermann grid illusion is Baumgartner's hypothesis that the illusory effect is generated by the response of retinal ganglion cells with concentric ON–OFF or OFF–ON receptive fields. To challenge this explanation, we have introduced some simple distortions to the grid lines which make the illusion disappear totally, while all preconditions of Baumgartner's hypothesis remain unchanged. To analyse the behaviour of the new versions of the grid, we carried out psychophysical experiments, in which we measured the distortion tolerance: the level of distortion at which the illusion disappears at a given type of distortion for a given subject. Statistical analysis has shown that the distortion tolerance is independent of grid-line width within a wide range, and of the type of distortion, except when one side of each line remains straight. We conclude that the main cause of the Hermann grid illusion is the straightness of the edges of the grid lines, and we propose a theory which explains why the illusory spots occur in the original Hermann grid and why they disappear in curved grids.

1 Introduction

The Hermann grid illusion is a well known classical illusion in which illusory spots are visible at the intersections of the grid lines (see figure 2). It is very robust, since the occurrence of the illusory spots is tolerant to a wide range of geometrical parameter changes, such as line width, line spacing, direction, angle of the lines, etc (for a review see Spillmann 1994).

The generally accepted explanation, which may be considered as the official textbook account of the Hermann grid illusion, is Baumgartner's (1960) hypothesis, according to which the illusory spots are the product of centre/surround antagonism within the ON–OFF or OFF–ON receptive fields of the retinal ganglion cells. The generally used computer simulation of Baumgartner's explanatory principle is based on the 'Mexican-hat' weighting function. This computational model is also referred to as the difference-of-Gaussians (DOGs) model (Marr 1982, page 63).

Although Baumgartner's explanatory principle is a local one, some authors have criticised it, showing that in addition to local factors, global ones also play a role in the explanation of the illusion (Wolfe 1984; for a review see Ninio and Stevens 2000). To prove its robustness, the purpose of these authors was to modify the Hermann grid while the illusion persisted.

Our aim is the opposite: we have introduced some minor distortions to the grid lines that make the illusory spots disappear totally. We then demonstrate that the predictions based on Baumgartner's hypothesis contradict perception; this discrepancy forms the basis of our paper. On the grounds of our psychophysical experiment based on the concept of distortion tolerance we have introduced earlier (Geier et al 2005), we demonstrate that the straightness of the black–white edges is the main cause of the illusory spots. Finally, we present an alternative theory, which accounts for the appearance of spots in the Hermann grid as well as for their disappearance in the distorted grids.

2 Theoretical problems raised by Baumgartner's hypothesis

First, let us point out some deficiencies of Baumgartner's hypothesis. It raises at least one unresolved question and one discrepancy.

2.1 The unresolved question

According to empirical data, the illusion occurs for a wide range of grid-line widths, while concentric receptive fields of several different sizes can be discerned. Simple geometric considerations and computer simulation (see figure 1) demonstrate that the computational model of concentric receptive fields works only in the case of an 'optimally' set diameter of the Mexican-hat weighting function at any given grid-line width.

Figures 1b, 1c, and 1d were generated by a computer program. The input in all cases was the same bitmap image of the Hermann grid (figure 1a). The program generated

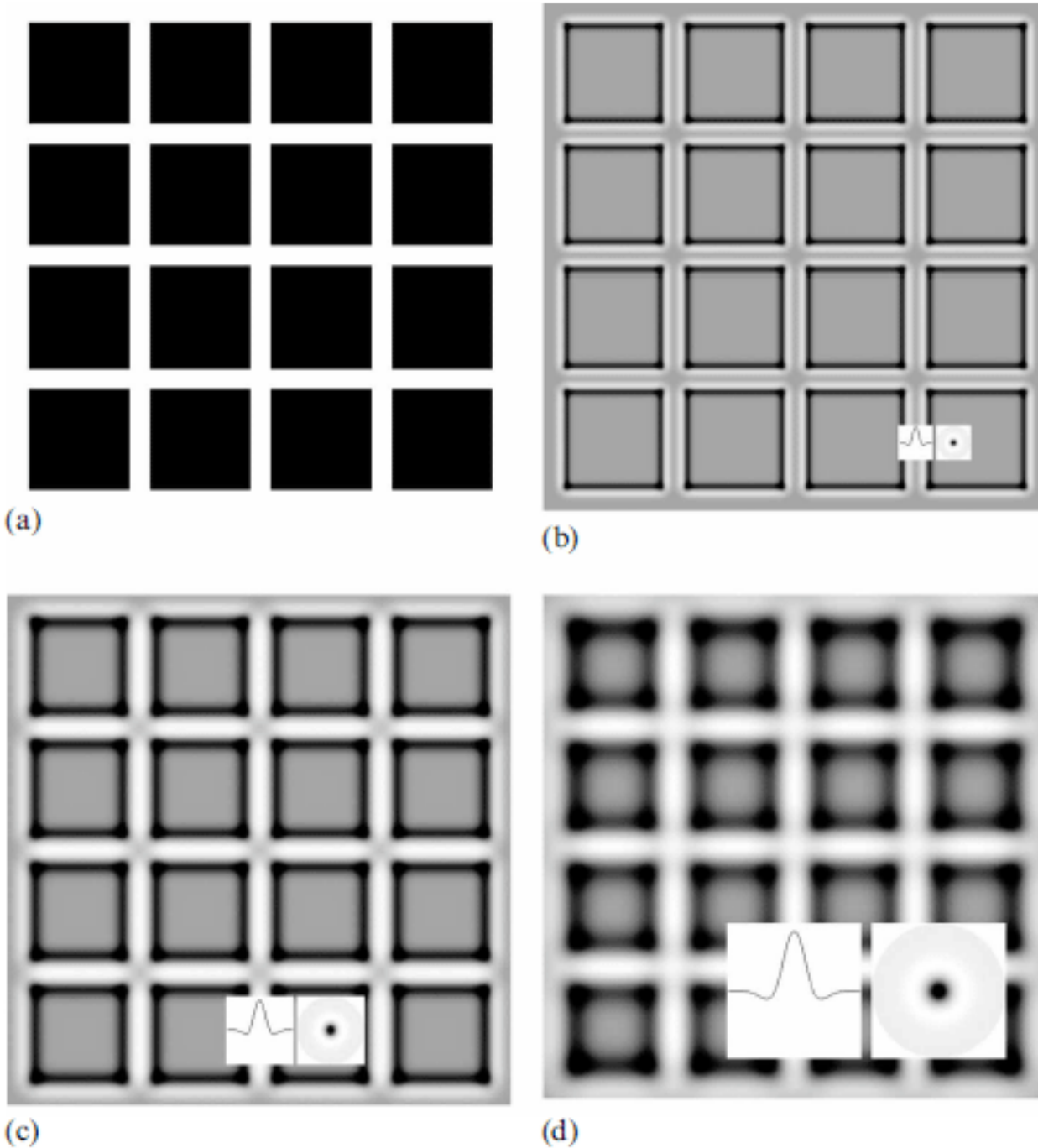


Figure 1. An undistorted Hermann grid (a) and its filtered outputs generated by computer simulation, using the Mexican-hat weighting function of different σ parameters: (b) $\sigma = 4$, (c) $\sigma = 8$, (d) $\sigma = 16$. It is clear that illusory spots occur only in the case of one optimally set diameter, figure (c), while in the case of a smaller diameter, no spots are produced. Moreover, spots ensconce themselves in the grid-line sections and the intersections turn light when a σ larger than the optimal one is used [see (d)] and the two diagrams in which the grey scale cross-sections of the centre lines of the images are illustrated. Several unwanted byeffects occur even in the case of the optimal diameter, such as small balls at the corners of the squares, or blurred grid line edges. In addition, the interior of the squares also turns lighter. We have placed the cross-section and the plan of the Mexican hat on the filtered images. In the plan diagram, the light-grey level stands for the inhibition, whereas the dark one represents the stimulation. Image sizes = 600 x 600 pixels; grid line width = 24 pixels; distance of the lines = 144 pixels.

filtered versions of figure 1a by replacing each of its points with the weighted means of their environments, where the weighting function was a Mexican hat with σ deviation. The deviations in figures 1b, 1c, and 1d were $\sigma = 4$, $\sigma = 8$, and $\sigma = 16$, respectively.

Obviously, it is only figure 1c which produces an effect somewhat similar to human perception. In figure 1b, the spots cannot be circumscribed and the centres of the grid lines become dark. The spots are away from the intersections in figure 1d, and the entries to the grid lines appear darker than the intersections. Hence, the following question arises: for a given grid-line width, why are only those receptive fields active whose diameter is 'optimally set', while all the others are not? Or, in computational terms: what would be the algorithm for determining the optimal diameter of the Mexican-hat weighting function for a given grid-line width?

Baumgartner's hypothesis provides no answer to these questions. Theoretically, it would be possible to devise an algorithm to select the optimal receptive field diameter, but such models are not available in the literature.

2.2 The discrepancy

When gazing at a classical Hermann grid, one observes homogeneous black squares, sharp edges, and a homogeneous white border surrounding the Hermann grid. Illusion (ie the difference between reality and perception) occurs only at the intersections. Nonetheless, what one can see in figure 1 is that the sharp edges and corners of the squares are blurred, and small balls have been generated at the corners by the computer simulation of Baumgartner's account. While the computer simulation predicts illusory spots at the intersections almost correctly, there are several other predictions that disagree with human perception.

Furthermore, as shown in figure 1, if the σ parameter of the Mexican hat is optimal for generating illusory spots ($\sigma = 8$), the corners of the black squares become rounded, and vice versa: if σ is smaller than the optimal value, the rounding is negligible, but no illusory spots are predicted by the simulation.

Schiller and Carvey (2005) propose an alternative account of the Hermann grid illusion. In fact, their hypothesis is a modification of Baumgartner's hypothesis, in which the illusory effect is largely attributed to the relative activity of neurons driven by the ON-OFF systems. They assign principal role to the orientation-selective simple cells (SI) in the primary visual cortex (V1), whose receptive fields are elongated along their axis of orientation. Their main suggestion is that "illusory smudges are the result of the relative degree of activity of the ON and OFF SI cells at the intersections, as compared with activity at non-intersecting locations" (Schiller and Carvey 2005, page 1389).

This hypothesis raises two objections. First, it is obvious that there is only one specific size and orientation of the SI receptive field, which is optimal for eliciting the illusory effect. But what about SI cells whose receptive fields are at the same location but have different axes of orientation? Here the authors provide no explanation. If these neurons are inactive, the mechanism activating solely those cells that are optimal for eliciting the illusion should be specified in their argument. On the other hand, if these cells are assumed to be active, the process in which the responses of cells sharing the same location are combined to produce the output response of the particular location should be described in detail. These two questions are, in fact, identical to those we have raised during the analysis of Baumgartner's account. However, the authors leave both questions unanswered in their paper.

Second, in their figure 11 (page 1387), Schiller and Carvey place the axes of the elongated receptive fields precisely on the edges of the grid lines; therefore the inner areas of the intersections are left empty, and none of the elongated receptive fields is indicated as being located there. Thus, no spot is predicted to appear in the middle of

the intersections on the basis of the working principle of S1 cells; it is only at the entrance of the grid lines where illusory darkening is expected to occur in accordance with this idea. Consequently, the foregoing line of reasoning does not provide sufficient explanation for the most essential aspect of the Hermann grid illusion, namely that illusory spots are manifestly darkest at the centre and tend to lighten towards the periphery, as has also been reported by our subjects. As for the central area of the intersection, Schiller and Carvey merely give the following hint: "Presumably, the perception of lightness and darkness in those regions of the figure that contain no edges is produced largely by responses elicited in unoriented cells in VI that receive either ON or OFF inputs" (page 1389). Nevertheless, the fundamental question here is: why does one observe illusory spots in the middle of the intersections? Their explanation leaves this question unanswered, too.

On the basis of this analysis, it is clear that neither Baumgartner's, nor Schiller's propositions provide sufficient explanation for the phenomena occurring in the classical, unmodified Hermann grid.

3 Distorted grids

Although we have demonstrated two shortcomings of Baumgartner's explanatory principle, this alone is not sufficient for rejecting that account totally. One possible response to our argument could be, as noted by Sekuler and Blake in an answer to Wolfe's (1984) criticism, that, although criticism is justifiable, "the explanation offered here is probably basically correct" (Sekuler and Blake 1994, page 98).

Here, we shall present some distortions which will prove the untenability of Baumgartner's explanation. All these distortions are of the kind in which Baumgartner's hypothesis would still predict illusory spots; however, the illusory spots totally disappear in all cases. The common properties of the distorted grids are that the intersections remain right-angled, and only the straightness and/or the directions of the edges of the grid lines are varied. The most effective distortion is to substitute sinusoid curves for the straight lines. The result is shown in figure 2—the illusory spots have totally disappeared.

It is evident that the applied distortion has no impact on the response of concentric receptive fields (ie on the relationship between the image and the Mexican hat); therefore Baumgartner's explanation predicts the same illusory spots in the distorted grid as in the undistorted Hermann grid. However, as observers do not see illusory spots in the distorted grids, the prediction of Baumgartner's model is certainly discrepant from perception.

Now, by simple logic, we shall demonstrate that Baumgartner's explanatory principle on its own does not account for the illusory spots perceived in the Hermann grid (at least in the versions that have been originally formulated, cited, and frequently described). To specify the conditions of the original explanatory hypothesis, let us consider the citation below:

"The subjective brightening and darkening effects at the crossing of a grid may be explained by relative difference of lateral inhibition and activation. A neurone of the B-system 'looking' at an intersection receives more light in its receptive field surround and produces more lateral inhibition than when it is stimulated by a bar." (Jung 1972, page 223)

This citation implies that the increment in the surround stimulation of the receptive field is a sufficient condition for the illusion if the central stimulation is constant. Accordingly, no other conditions are required by Baumgartner's explanation than the different ratio of centre/surround stimulation. Hence, the straightness, continuity, and homogeneity of the lines are not required by his hypothesis, nor is collinearity of the intersections demanded. But, although we have not changed any conditions of the

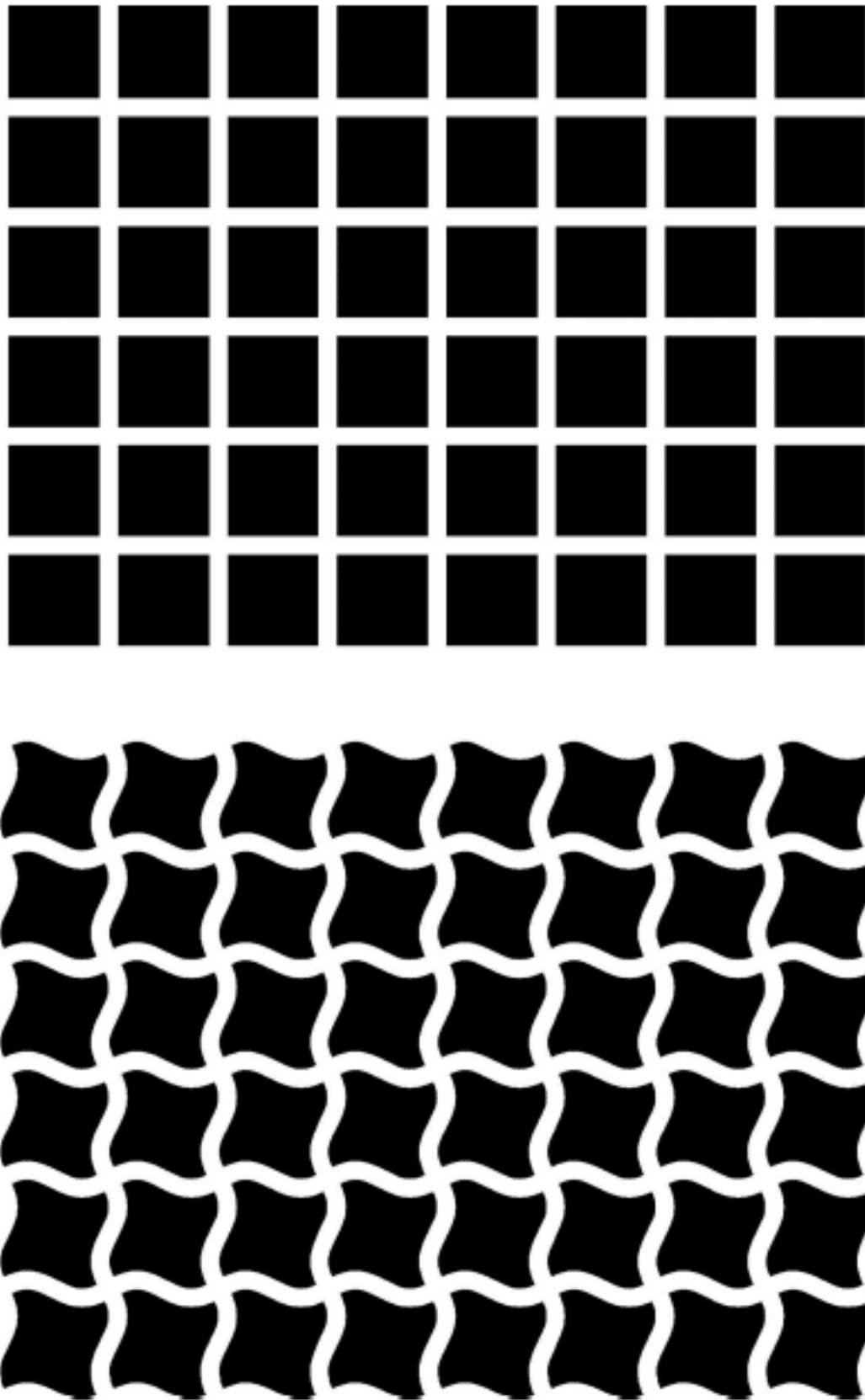


Figure 2. The classical Hermann grid (above) and the sinusoid grid (below). In the case of straight grid lines, illusory spots are seen in the intersections, but they totally disappear in the case of the curved grid lines. The amplitude of sine curve is less than 10% of its wavelength.

original explanation, the spots have disappeared in the sinusoid grid (figure 3). This line of evidence undermines Baumgartner's hypothesis as an account of the illusory spots in the Hermann grid. Thus, Baumgartner's hypothesis should be either supplemented by further conditions, or declined as a whole.

To demonstrate the foregoing, let us have a look at figure 4, in which the output image of the sinusoid grid is displayed, filtered by the Mexican-hat weighting function. The line widths and distances of this sinusoid grid are identical to those of figure 1a. The size of Mexican-hat function applied here is $\sigma = 8$, which is the same as the 'optimal' one shown in figure 1c. It is obvious that the Mexican-hat simulation is not sensitive to the curvature of the grid lines: the output spots are exactly like those in figure 1c, which corresponds to the prediction of Baumgartner's explanatory principle. This entirely contradicts perception.

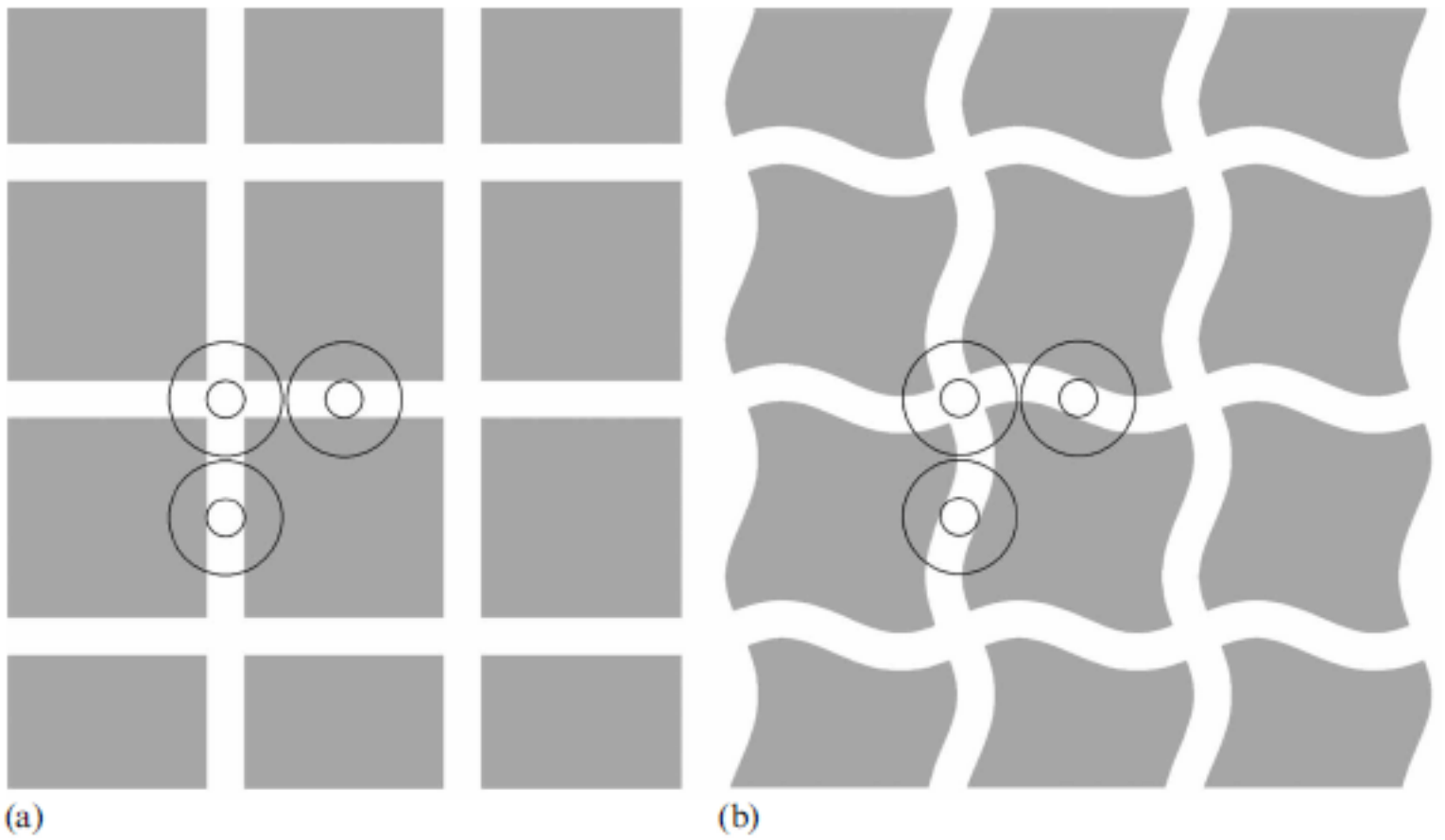


Figure 3. (a) A usual explanatory image of Baumgartner's hypothesis [a similar one is in Spillmann (1994), page 693, figure 1]. According to this account, to observe illusory spots, it is sufficient to inhibit the lateral ring of the receptive fields located at the intersection twice as much as those located in the grid-line sections, while the stimulation of the centres remains constant. Though these conditions are totally fulfilled by the sinusoid grid (b), no illusory spots are perceived at line intersections. If double lateral inhibition were sufficient in itself to elicit the illusory effect, spots would appear in both images. However, they do not. Thus, the question arises whether Baumgartner's hypothesis could be extended to be a satisfactory account of the illusion by including the straightness of the lines as a condition, or should it be rejected totally.

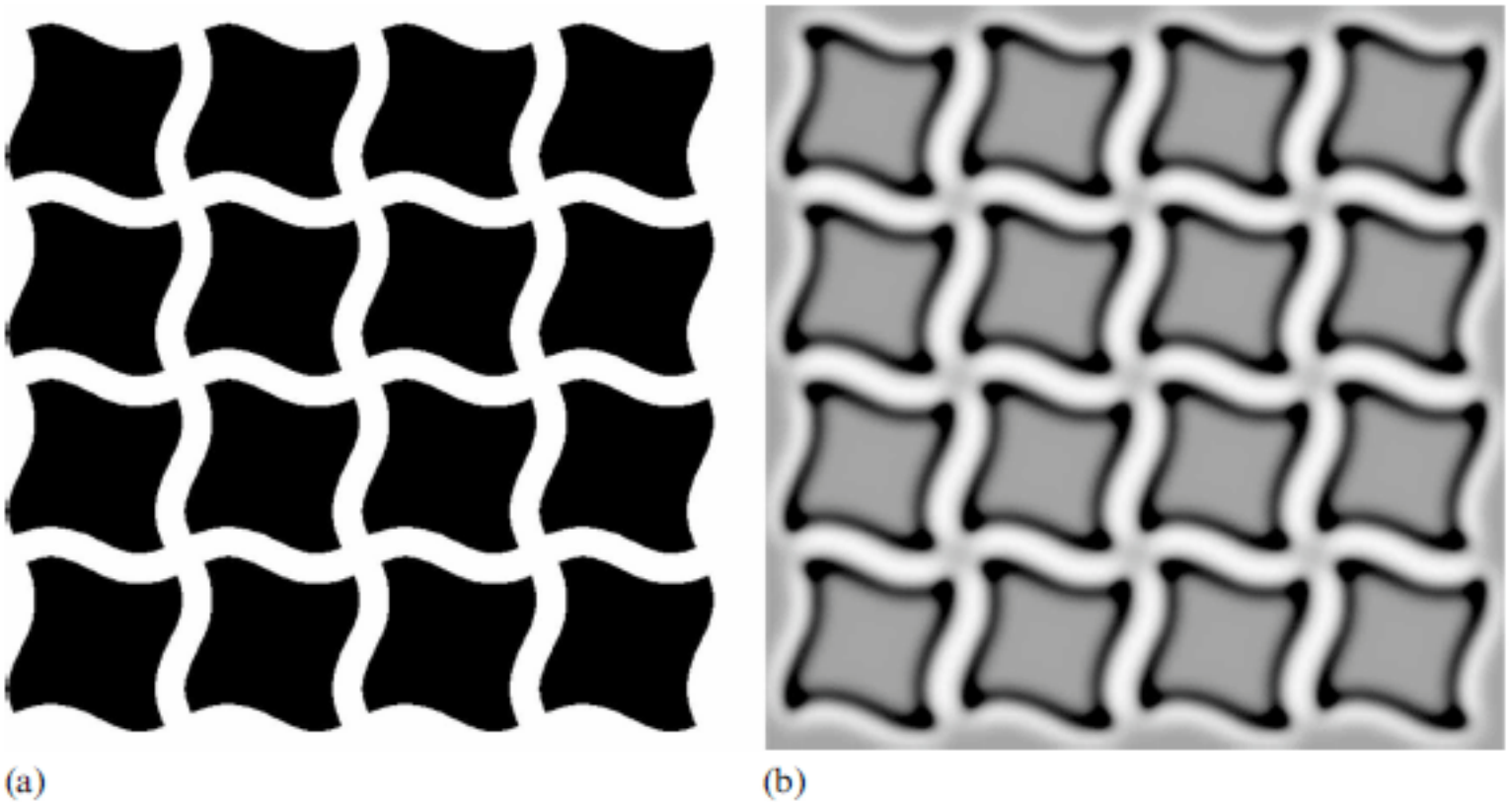


Figure 4. Sinusoid grid (a) and its output image by the Mexican-hat computer simulation at $\sigma = 8$ (b). It is noticeable that the simulation predicts the same spots at the intersections as in (a). The curvature has no effect. This result corresponds to Baumgartner's conception; however, it contradicts human perception.

3.1 Possible solutions

Theoretically, there are two possible ways to resolve the strong contradictions between human perception and the predictions of Baumgartner's hypothesis. The first is to find an extension that provides an answer to the question: if it is the concentric receptive fields that produce the illusory spots in the unmodified Hermann grid, what is the reason for their disappearance in the distorted grids? The second one is to reject Baumgartner's hypothesis as an explanation of the Hermann spots.

Taking into consideration the unresolved questions and problems raised by Baumgartner's classical explanation, our opinion is that it should be totally rejected: it is not the ON and OFF centred receptive fields that underlie the phenomenon of illusory spots in the Hermann grid. However, as long as Baumgartner's hypothesis is not supplemented by further conditions to explain the difference between the cases of the classical and the distorted Hermann grids, the grounds of this explanatory principle seem to be problematic.

In saying this, we do not deny the role of ON and OFF centred receptive fields in the visual process in general, but we consider the explanation to be more complex than that proposed in Baumgartner's hypothesis. Perhaps ON and OFF systems play an important role in the background, but their effect does not manifest itself directly in the perceptual sensation.

4 Experiment

Here the question emerges what the 'right' explanation could be. In order to develop a new theory, one should get to know the principles of the appearance and disappearance of the illusion. Our experiment was planned in order to reveal the effects of distortions on the illusion, which might provide a viable basis of a new model. The experiment here was a tool to provide an answer to the basic question: what is the rationale for the illusory spots in the Hermann grid?

Earlier experiments concerning the Hermann grid illusion were based on asking the subjects how intensively they perceived the illusory spots (eg Wolfe 1984). However, since we can eliminate the illusion completely, it seems more plausible to pose a much more objective question: when does the illusion disappear? Determining the limit when the spots are no longer visible is an even more reliable method than rating the subjective intensity on a scale.

We define the term 'distortion tolerance' as the degree of distortion at which the illusory spots disappear. Potentially, the distortion tolerance may depend on the distortion type, grid-line width, or on the individual subject. Our aim was to reveal, by means of empirical data, what distortion tolerance depended on, and whether it would differ significantly in the case of different distortion types.

4.1 Selection of the applied distortion types

In addition to the sine curves, further distortion types were used (figure 5).

4.1.1 *Wavy grid* is introduced for testing the role of the collinearity of the intersections. If collinearity plays a role in the presence of spots, there should be significant differences in the means of the distortion tolerance of the sinusoid grid and wavy grid.

4.1.2 *Knotted grid* is introduced for testing the role of the (white and black) area sizes, which is a crucial point of Baumgartner's model. Increasing the light intensity only at the OFF surrounds of the receptive fields, while leaving the stimulation of the centre constant, allowed us to examine the role of the proportion of white and black areas.

4.1.3 *Half-sided humped grid and an asymmetrical humped grid* were introduced in order to verify whether straight grid-line edges play an essential role. The half-sided humped grid was generated from the humped grid by replacing the lower curve of the latter

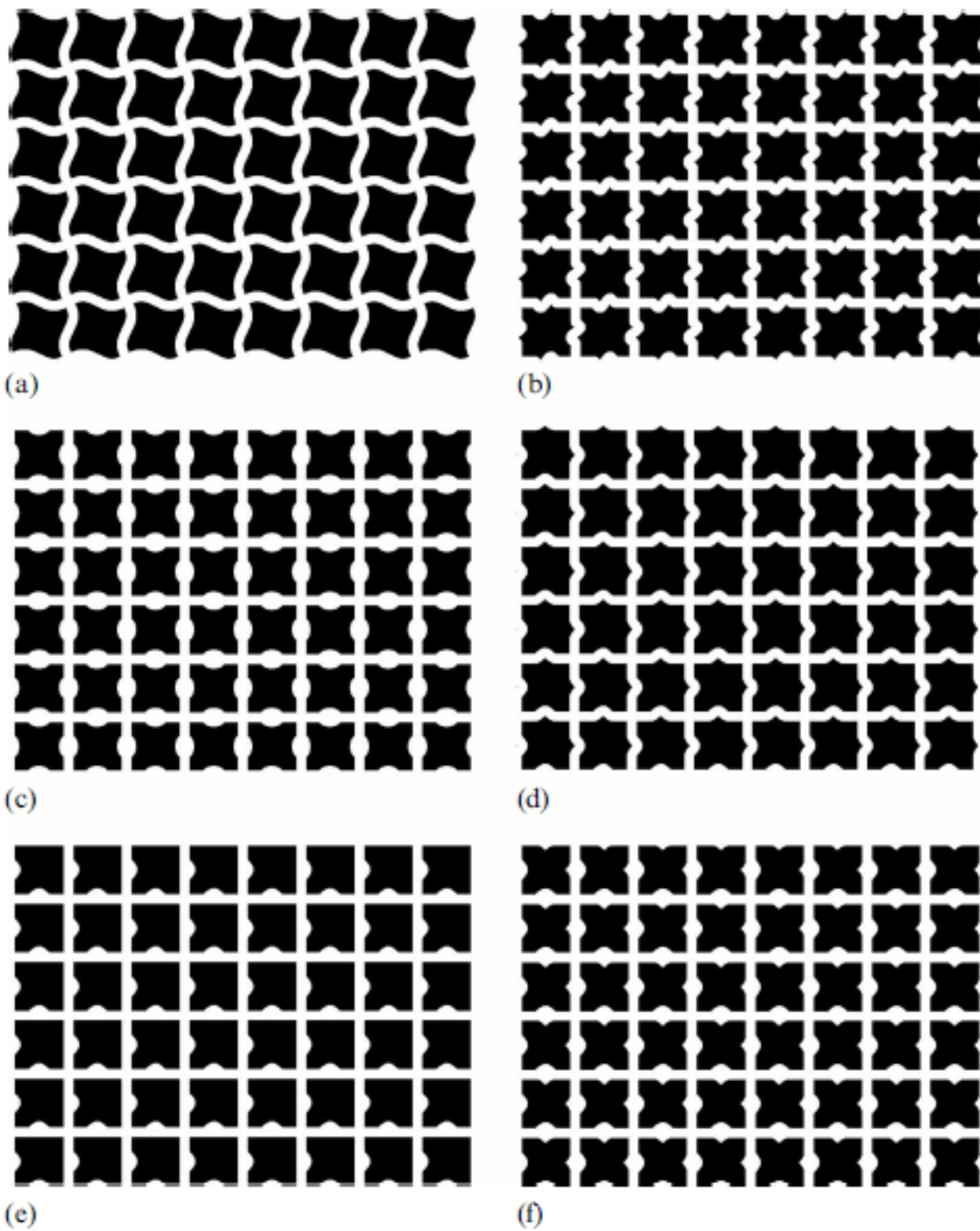


Figure 5. The six distortion types used in our experiment: (a) sinus, (b) wave, (c) knot, (d) hump, (e) half-sided hump, (f) asymmetrical hump. The magnitude of the distortion was set by the subject by pressing the arrow buttons of the computer keyboard until the illusion disappeared. These images were presented with three different line widths (11, 17, and 23 pixels; the resolution of the monitor was 1024×768 pixels), but the distance of the lines was identical in all cases (102 pixels between the left sides of the lines). In this figure, only the images of 17 pixel line width are presented.

by a straight edge segment. The asymmetrical humped grid was also derived from the humped grid, by flipping its lower curve vertically along the edge of the grid line, so that the lower curves of the line edges were identical; the only difference was the proportion of the black and white areas.

4.2 *Modifying grid-line widths*

In the light of our earlier experiments (Geier et al 2004, 2005), we assumed that grid-line width does not significantly affect the degree of distortion tolerance. This assumption corresponds to the well-known fact that the illusion is independent of grid-line width within a wide range. However, by introducing the concept of distortion tolerance a more reliable experimental method has been devised.

In order to investigate the role of grid-line width, we displayed all the six grid types in three versions of line width: the lines of the grids were 11, 17, and 23 pixels wide. This is quite a wide range, since the largest width is more than twice the smallest one.

4.3 Method of the experiment

The dependent variable was the distortion tolerance; the independent variables were the distortion type and the line width. Stimuli were shown in random order on a 15 inch wide computer monitor: screen size = 1024 × 768 pixels; viewing distance = 60 cm.

Distorted Hermann grids included 7 × 5 white lines on a black background, with constant line spacing of 102 pixels. There were six categories of distortion type: sinusoid, waved, knotted, humped, half-sided humped, and asymmetrical humped. Three categories of line width were used: 11 pixels, 17 pixels, and 23 pixels. There were twenty-two subjects.

The task of the subjects was to set the amplitude of the given type of curves by pressing the arrow keys of the computer keyboard when they could no longer see the illusory spots. The starting point of all distortions was the classical Hermann grid. If the subject overshoot the limit at which the illusion disappeared, he could backtrack the previous setting and could adjust it until he re-established the right amplitude. After each grid, masking stimuli consisting of random squares were shown for 3 s. The type of distortion and the width of the lines were randomly generated by the computer program.

4.4 Results of the experiments

The distortion tolerance (figure 6) was analysed by a 3 (line width) × 6 (distortion type) repeated-measures ANOVA and by Bonferroni pairwise comparison. The ANOVA showed for the main effect of grid-line width: $F_{2,42} = 0.649$, $p > 0.05$; for the main effect of distortion type: $F_{5,105} = 15.708$, $p < 0.01$; and for their interaction: $F_{10,210} = 1.163$, $p > 0.05$. One can see that the only significant effect is the distortion type. The Bonferroni pairwise comparison showed that the mean difference between the pairs of sinusoid/wavy, sinusoid/knotted, and wavy/knotted is not significant; the mean difference between the pairs of hump/asymmetrical hump is not significant; but the mean difference between the half-sided hump and all the others is highly significant.

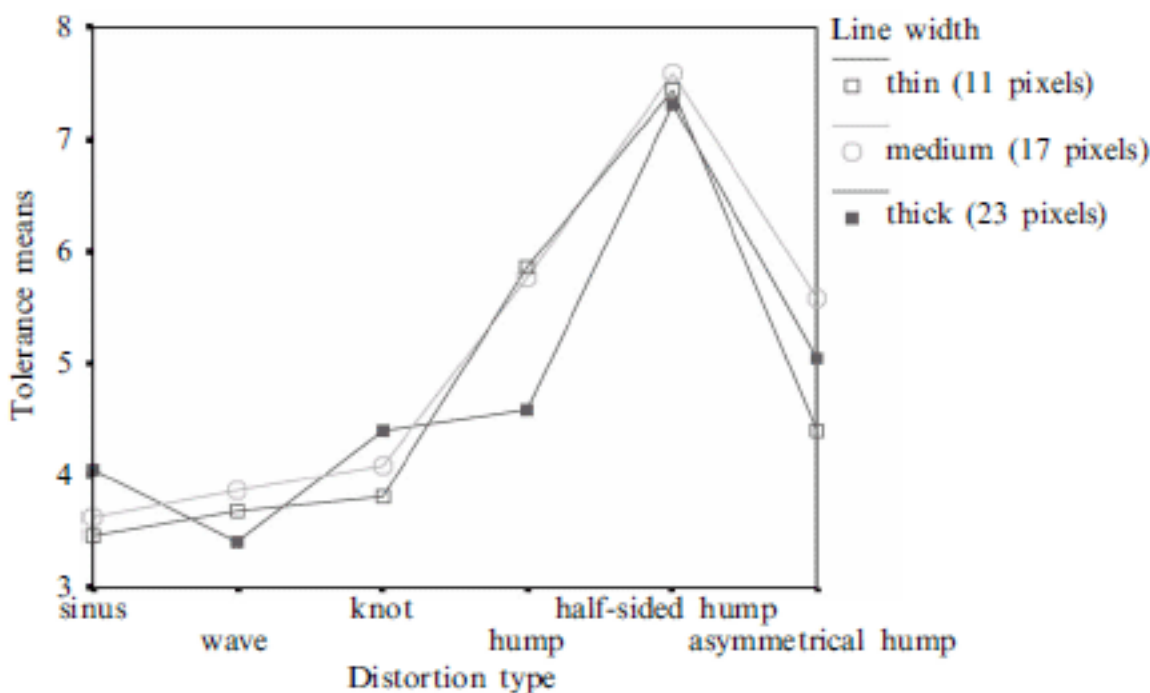


Figure 6. Experimental results. The horizontal axis illustrates the six distortion types, while the vertical axis represents the means of the distortion tolerance of twenty-two subjects. The three lines, representing three line widths, are nearly parallel to each other, which implies that the distortion tolerance is independent of line width. The distortion tolerance of the half-sided hump is seen to be much greater than that of the others.

The fact that the main effect of the grid-line width in the ANOVA is not significant confirms our assumption that grid-line width does not play a significant role in the perception of the Hermann grid illusion. The significant main effect of distortion type in the ANOVA, in addition to the results of the Bonferroni pairwise comparison, demonstrates that the distortion tolerance of the half-sided hump distortion type is an exception; this contains the essence of our results. Since it is only the half-sided humped grid that includes straight grid-line edges, the conclusion is that the main cause of the Hermann grid illusion is the straightness of the black–white edges of the grid lines, but their width plays no significant role; also the collinearity of the intersections plays no significant role.

5 Towards a new theory

As expected, an essential principle emerged from the experiment. The straightness of the edges of the grid lines lies behind the perception of illusory spots. The basic idea of the theory presented in this paper stems from these findings.

Having analysed the distortion types and their effects, we can make an essential, but not trivial, remark: the location of the change in the illusion is far removed from the location of the physical change.

In all distortion types, the curving of line edges is applied exclusively to the middle part of each line section. Nonetheless, the appearance and the disappearance of the illusory spots take place at the intersections, where no physical change is applied. How does the change in the middle part of the grid-line sections get to the intersections, then?

Our answer is that, in fact, it does not even get there. We suggest that, instead of the spots being darker, it is the line segments that are perceived lighter than the intersections. On the basis of this assumption, we formulate the main hypothesis, as the axioms of our theory.

5.1 Radiating edge hypothesis:

- (a) *The short segments of white – black edges radiate ‘darkness’ on their dark side and ‘lightness’ on their light side.*
- (b) *The straighter a continuous edge is, the stronger is the radiation of its elemental segments.”*

The direction of the radiation is perpendicular to the orientation of the edges, and it disperses at a certain ‘fuzzy’ angle (see figure 7). The intensity of the radiation is strongest in two opposite directions perpendicular to the edge. The radiation diffuses all over the retinal points that are located in heading of the radiation, thereby affecting the perceived brightness at each point by producing an additive effect, whose weighted value decreases with distance.

These axioms allow us to bridge over our question by introducing a change of viewpoint: only at first sight does the location of change in the illusion seem distant from the location of the physical change. In fact, it is not distant at all, since according to point (a) the grid-line edge directly illuminates the section next to it. Consequently, the line sections will be much lighter than the intersections, as they are irradiated by the edge segments of the grid lines. On the other hand, the intersections are not affected by this radiation.

The analogy of the ‘illuminating’ or ‘radiating’ effect of straight lines is based on the study of electronics. It is known that the potential of electronic or magnetic dipoles decreases with distance [the exact rule is that the potential decreases as the reciprocal of third power ratio of the distance—see eg Feynman et al (1969)]. Let us now image the line edges of the Hermann grid consisting of dipoles placed next to each other (‘particles’ that are radiating black in one direction, and white in the opposite one).

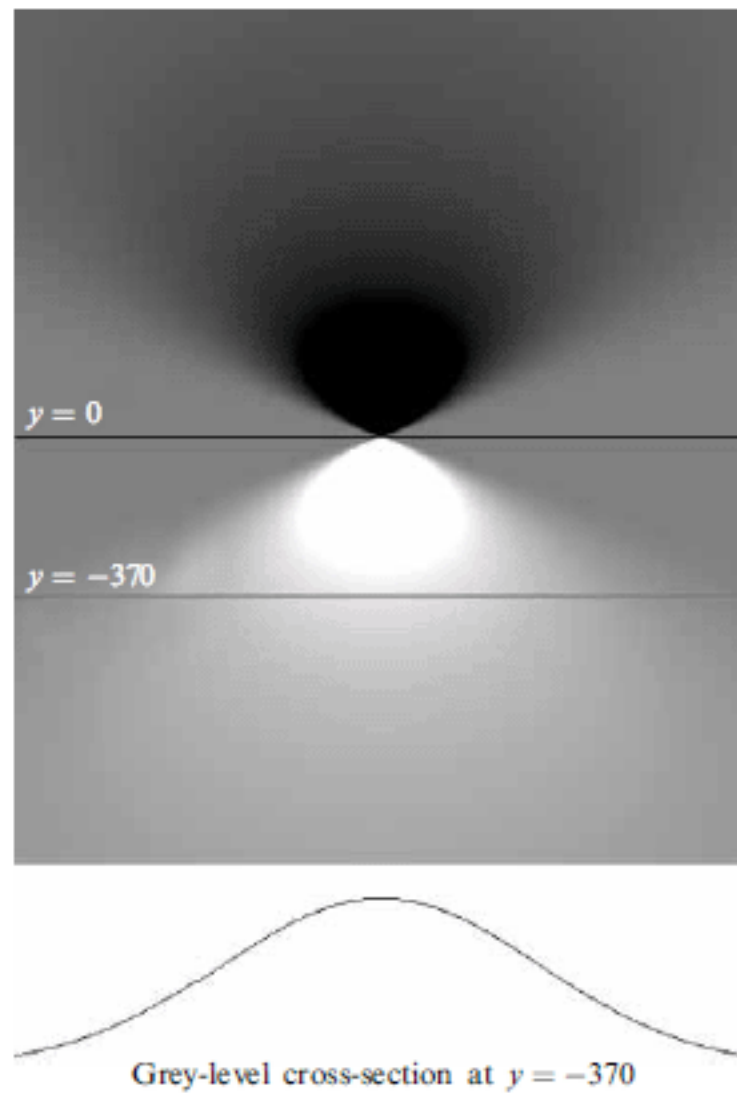


Figure 7. The radiation characteristics of a horizontally oriented edge segment. The intensity of the radiation is indicated by the grey-scale values. The value of medium grey is 0. Grey values lighter than 0 represent stimulation, darker values stand for inhibition. The edge segment of the sensor layer is a small fragment of the white–black edge crossing the $(x, y) = (0, 0)$ point horizontally (not indicated here). According to point (a) of the radiating edge hypothesis, the edge radiates ‘black’ in the upward direction and ‘white’ downwards. The cross-section of the radiation intensity is a Gaussian curve at any y value. The deviation of the Gaussian curve is proportional to the absolute value of y , and its magnitude is proportional to $1/y$. The cross-section of grey level at $y = -370$ is shown as an example.

These dipoles quasi-irradiate the line sections, and, of course, they irradiate the squares as well in the opposite direction by the opposite sign of radiation. Therefore, the light side of each segment radiates lightness while its dark side radiates darkness.

We take it that the radiating angle is not too large; therefore the radiation cannot reach the intersections. On the other hand, in the case of curved line edges, some oblique segments may irradiate the intersections as well. According to point (b) the segments of curved edges radiate much more weakly than the segments of straight edges. Therefore, the line sections enclosed by curved edges will receive much less lightness than those enclosed by straight edges.

Of course, the radiating edge hypothesis should be treated as an analogy. It is not the light reaching the retina that radiates. Yet, we believe that photosensitive cells in the retina and other neural structures (not only in the retina) connected to them transmit neural signals to each other in accordance with a pattern that is largely akin to the analogy of radiation.

5.2 A theoretical model based on the radiating edge hypothesis

The model consists of the following two-dimensional layers: sensor layer, edge-detector layer, and diffusion layer (see figure 8).

The sensor layer comprises photosensitive units which are directly equivalent to the retinal photosensitive neurons.

The edge-detector layer allocates the direction of the normal vector of any edge crossing any point in the area it monitors. This should not be confused with a receptive field; instead, it can be characterised as a unit comprising several receptive fields, which are sensitive to different directions. The inner processes of the edge-detector units select the receptive field which produces the most intensive response; the selected orientation will therefore be the output of the edge-detector unit. We propose that the diameters of the edge detectors are very small, since it is the derivatives that need to be computed here. In computer simulations, the so called Sobel filter of 3×3 pixel size is generally used.

The diffusion layer is a 'tissue' in which signals diffuse in accordance with the following rules. When a direction signal reaches a given point, two diffusion processes of opposite directions are set in motion. In the direction of the normal vector, the diffusing signal will be stimulating ('light'), whereas in the opposite direction it will be inhibitory ('dark').

The process of the radiation of edges described here is akin to the so-called standard diffusion process (Grossberg and Todorović 1988). This diffusion model uses a DOG filter as its first step. Thereafter, the model applies a heat diffusion process, constrained within the so-called 'boundary contours' (see the referred paper).

In contrast, in our theoretical model, the direction of the edges is specified by the first derivative of the edges. Then two opposite 'radiation' processes (which might be compared to Galton's board) start from the elemental edge segments perpendicularly, in two opposite directions. This radiation spreads through the entire image. The radiations that meet cross each other in accordance with the principle of superposition (as two waves do in water). We do not apply real or 'emerged' boundary contours. The theoretical radiation characteristics of an elemental edge segment is indicated in figure 7.

Point (b) suggests that the straightness of a continuous edge acts upon the radiation intensity of its elemental segments. This assumption is similar to the collector unit theory put forward by Morgan and Hotopf (1989). According to this theory, the Hermann grid is related to the pincushion-grid phenomenon. The basis of this explanation for the pincushion diagonals is that the output of the local long receptive fields adjoins one common unit, which integrates the signals of the local units connected to it. The stimuli of the local units are the corner pairs positioned diagonally relative to each other in the intersections.

In contrast, we do not postulate that such collector units would participate in the edge-detection process. Instead, we assume that units close to each other send to each other signals about orientation they have detected. The more similar these two orientations are, the more intensive amplification—and, as a consequence, the larger the signal—that both units will produce. The effect of interaction decreases with growing distance between the two points monitored by the two units.

Bearing in mind the foregoing, it is obvious that the interaction described above is an apt realisation of point (b). If a series of edge-detector units is placed along a straight edge, then neighbours located close to each other will amplify the signals of each other. This principle entails that each segment of a straight edge will radiate more intensively than those of a curved edge, where interaction is much weaker.

The model accounting for the background of the radiating edge hypothesis is illustrated in figure 8. A possible feature of the model is that it is sufficient to require short-range interactions, as long-range effects are a consequence of the diffusion of the short-range effect.

(vi) The distortion tolerances of the sinusoid and wavy versions are nearly equal; collinearity plays no significant role in it. Explanation: the decrease of the radiation effect depends exclusively on the curvature of the edge, where the direction plays no role.

(vii) In the case of inverse grids (ie black lines and white squares), the illusory spots are lighter at the intersections. Explanation: points (i)–(vi) are all valid even in this case, if the word ‘black’ is substituted for ‘white’ in those statements.

6 Discussion

In conclusion, it is now clear that the radiating edge hypothesis is a unifying principle, since it has accounted for the presence of spots in the classical Hermann grid, and also for their disappearance in the curved grids. It also provides an explanation for the higher distortion tolerance of the half-sided humped grid, in which one of the line sides remains straight.

Our model also manages to solve the old problem that the Hermann grid is very sensitive to the size of the receptive fields in modeling used generally, but scale-invariant in human perception. Our solution is that we do not use DOG filters of large diameters; instead, we use small edge detectors only. The cause of the spots is that less radiation gets into the intersections.

6.1 *Perspectives, further questions*

An alternative solution may perhaps be provided by applying multiscale models of other lightness/brightness illusions, eg Morrone’s local energy model (Morrone and Burr 1988), which may be suitable for modeling Hermann spots independently of line widths. Unfortunately, neither the above paper nor others show the applicability of a local energy model to modeling the Hermann spots. There is also some doubt whether the spots would disappear in the curved grids on applying this model.

At present, no such explicit alternative models are found in the literature that would serve specifically as the explanatory principle of the Hermann spots; it was only the DOG model that focused on this specific issue. As a matter of fact, in the paper of Grossberg and Todorović (1988), there is a Hermann spot simulation. However, its first step involves the application of the DOG filter, so it seems that the spots are caused by that filter, and not by the diffusion. For this reason, if Grossberg’s diffusion model were applied to the curved grids, the illusory spots would not disappear.

Though the Hermann grid is generally known for its illusory spots, little research has been devoted to another illusion inherent in it: when the Hermann grid is rotated by 45°, most people see diagonal lines of the same polarity as the squares that pass through the corners of the squares. Morgan and Hotopf (1989) consider this phenomenon to be related to the pincushion grid illusion.

The reason that little attention has been paid by researchers to the illusory diagonals may be due to the fact that only approximately 5%–10% of viewers see diagonal lines in a horizontally positioned Hermann grid (and this applies to most Hermann grids that have been drawn so far). In the 45° grid, however, almost everyone reports seeing the diagonals. In the case of 45° curved grids, the number of people seeing such diagonals strongly decreases. Future research is needed here.

Our paper was aiming at Marr’s 1st level: we have developed a theoretical computational theory on the basis of our empirical results. The computational algorithm (Marr’s 2nd level) and its corresponding neural background (implementation—Marr’s 3rd level) are to be elicited by future computer programming and physiological measurements. All the same, one can predict that if the underlying neural background processes of the radiating edge hypothesis are successfully derived in the future, the explanation will not be based on local neurons working independently of each other. Instead, the working principle here will probably reflect the information processing characteristics of the visual system.

Acknowledgments. We are grateful to Iлона Kovács and Esther Stocker who have made essential contributions to the publication of our idea at EVCP2004, Budapest. We wish to thank George N Bernath for his assistance in translating an earlier version of this paper.

References

- Baumgartner G, 1960 "Indirekte Größenbestimmung der rezeptiven Felder der Retina beim Menschen mittels der Hermannschen Gittertäuschung" *Pflügers Archiv für die gesamte Psychologie* **272** 21–22 (abstract)
- Feynman R P, Leighton R B, Sands M, 1969 *Feynman Lectures on Physics* volume 2, chapter 6 (Readings, MA: Addison-Wesley)
- Geier J, Séra L, Bernáth L, 2004 "Stopping the Hermann grid illusion by simple sine distortion" *Perception* **33** Supplement, 53
- Geier J, Séra L, Bernáth L, 2005 "Distortion tolerance of the Hermann grid" *Perception* **34** Supplement, 103
- Grossberg S, Todorović D, 1988 "Neural dynamics of 1-D and 2-D brightness perception: A unified model of classical and recent phenomena" *Perception & Psychophysics* **43** 241–277
- Jung R, 1972 "Neurophysiological and psychophysical correlates in vision research", in *Brain and Human Behavior* Eds A G Karczmar, J C Eccles (New York: Springer) pp 209–258
- Marr D, 1982 *Vision* (San Francisco, CA: W H Freeman)
- Morgan M J, Hotopf N A, 1989 "Perceived diagonals in grids and lattices" *Vision Research* **29** 1005–1015
- Morrone M C, Burr D C, 1988 "Feature detection in human vision: a phase dependent energy model" *Proceedings of the Royal Society of London, Series B* **235** 221–245
- Ninio J, Stevens K A, 2000 "Variations on Hermann grid: an extinction illusion" *Perception* **29** 1209–1217
- Schiller P H, Carvey C E, 2005 "The Hermann grid illusion revisited" *Perception* **34** 1375–1397
- Sekuler R, Blake R, 1994 *Perception* 3rd edition (New York: McGraw-Hill)
- Spillmann L, 1994 "The Hermann grid illusion: a tool for studying human perceptive field organization" *Perception* **23** 691–708
- Wolfe J, 1984 "Global factors in the Hermann grid illusion" *Perception* **13** 33–40

Changing the Chevreul Illusion by a Background Luminance Ramp: Lateral Inhibition Fails at Its Traditional Stronghold - A Psychophysical Refutation

János Geier^{1*}, Mariann Hudák^{2,3}

1 Stereo Vision Ltd., Budapest, Hungary, **2** Faculty of Natural Sciences, Department of Cognitive Science, Budapest University of Technology and Economics, Budapest, Hungary, **3** Hungarian Academy of Science-Budapest University of Technology and Economics Research Group of Cognitive Science, Budapest, Hungary

Abstract

The Chevreul illusion is a well-known 19th century brightness illusion, comprising adjacent homogeneous grey bands of different luminance, which are perceived as inhomogeneous. It is generally explained by lateral inhibition, according to which brighter areas projected to the retina inhibit the sensitivity of neighbouring retinal areas. Lateral inhibition has been considered the foundation-stone of early vision for a century, upon which several computational models of brightness perception are built. One of the last strongholds of lateral inhibition is the Chevreul illusion, which is often illustrated even in current textbooks. Here we prove that lateral inhibition is insufficient to explain the Chevreul illusion. For this aim, we placed the Chevreul staircase in a luminance ramp background, which noticeably changed the illusion. In our psychophysical experiments, all 23 observers reported a strong illusion, when the direction of the ramp was identical to that of the staircase, and all reported homogeneous steps (no illusion) when its direction was the opposite. When the background of the staircase was uniform, 14 saw the illusion, and 9 saw no illusion. To see whether the change of the entire background area or that of the staircase boundary edges were more important, we placed another ramp around the staircase, whose direction was opposite to that of the original, larger ramp. The result is that though the inner ramp is rather narrow (mean = 0.51 deg, SD = 0.48 deg, N = 23), it still dominates perception. Since all conditions of the lateral inhibition account were untouched within the staircase, lateral inhibition fails to model these perceptual changes. Area ratios seem insignificant; the role of boundary edges seems crucial. We suggest that long range interactions between boundary edges and areas enclosed by them, such that diffusion-based models describe, provide a much more plausible account for these brightness phenomena, and local models are insufficient.

Citation: Geier J, Hudák M (2011) Changing the Chevreul Illusion by a Background Luminance Ramp: Lateral Inhibition Fails at Its Traditional Stronghold - A Psychophysical Refutation. PLoS ONE 6(10): e26062. doi:10.1371/journal.pone.0026062

Editor: Steven Barnes, Dalhousie University, Canada

Received: April 19, 2011; **Accepted:** September 19, 2011; **Published:** October 13, 2011

Copyright: © 2011 Geier, Hudák. This is an open-access article distributed under the terms of the Creative Commons Attribution License, which permits unrestricted use, distribution, and reproduction in any medium, provided the original author and source are credited.

Funding: This study was funded by Stereo Vision Ltd. through the directorship and 50% ownership of János Geier, who designed the experiments, contributed to the analysis and wrote the paper.

Competing Interests: This study was funded by Stereo Vision Ltd. through the directorship and 50% ownership of János Geier. There are no patents, products in development or marketed products to declare. This does not alter the authors' adherence to all the PLoS ONE policies on sharing data and materials, as detailed online in the guide for authors.

* E-mail: janos@geier.hu

Introduction

The Chevreul illusion comprises spatially uniform grey bands of different luminance, which seem inhomogeneous, as if they were crimped: each band looks darker on one side and brighter on the other (see Figure 1). This illusion is attributed to Michel Eugène Chevreul (1786–1889), who, on developing his theory of colour, placed spatially uniform bands of gradually increasing luminance next to each other, whereby he discovered the illusion. Since the physical luminance-cross section profile of this image looks like a staircase, we will use the term 'staircase' in this paper for the series of bands, while the bands themselves will be termed as 'steps'.

Traditionally, the Chevreul illusion has been explained in terms of lateral inhibition, which means that brighter areas projected to the retina inhibit the sensitivity of neighbouring retinal areas. In neurological terms, "cells in one region inhibit cells in adjacent regions" ([1] p2042). In line with this classical principle, the reason for the perceived inhomogeneity in the physically homogeneous steps is that the side of each step neighbouring a lighter one receives more inhibition than its other side.

Lateral inhibition not only serves as the explanatory principle for the Chevreul illusion, but it has long been considered as the basic mechanism of early vision [2]. It stems back as early as the 19th century, since it seemed to explain many of the then known brightness illusions, such as the Hermann grid illusion [3], Mach bands [2,4], or the simultaneous brightness contrast.

By the 1950s, neuroscientists were searching for lateral inhibition in the visual system of animals, embodied by the circularly symmetric antagonistic (on/off or off/on) retinal receptive fields [5,6]. Antagonistic circular receptive fields implementing lateral inhibition in the retina are described mathematically by the DoG (Difference of Gaussians) model [7].

By the 1960s, lateral inhibition was considered as a general working principle of sensation in the nervous system [4], and was not limited to visual perception. The principle of lateral inhibition was also adopted by textbooks, and is included in even current ones e.g. [8,9]. Textbooks demonstrate lateral inhibition as "the working mechanism" of early vision. They illustrate lateral inhibition or the DoG model by means of two classical illusions, the Hermann grid illusion and the Chevreul illusion.



Figure 1. The classical Chevreul illusion. The steps adjacent to each other are physically homogeneous; however, they seem inhomogeneous (crimped). The side of each step adjoining a brighter step seems darker than its other side. The physical luminance cross-section of the midline of the staircase is displayed in the bottom part of the figure.

doi:10.1371/journal.pone.0026062.g001

It has to be noted here that many textbooks e.g. [8,9] misdescribe the Chevreul illusion as Mach bands. The inferential reason for this misdescription is that Mach produced various images by means of quickly rotating disks [2,4]. Among these figures, there was one that comprised spatially uniform concentric rings of gradually increasing luminance. Although that figure could be regarded as the concentric disk-shaped counterpart of the Chevreul illusion, this, according to Ratliff or von Békésy [2,4], was not the main image that Mach created. According to these two resources, Mach bands are seen when the linearity of the luminance ramp, which progresses from the centre of a disk towards its edge, breaks. The investigation of Mach bands is

not subject of this paper; it has been mentioned only to clarify the terminology misused in some textbooks.

Several current multiscale spatial filtering models of brightness perception also build upon the DoG model with more or less supplementation, retaining its local nature. These theories consider the illusion as a direct consequence of the convolution of the input image with a series of certain DoG-like weight functions e.g. [10–12]. All these models vary the DoG principle so that they either use series of DoG filters or their variants, with an elongated shape (ODOG), of various spatial frequencies.

The above-mentioned group of brightness phenomena, which are traditionally explained by lateral inhibition, are also termed contrast phenomena. The basis of this term is that in these images, the perceived contrast is enhanced compared to the physical contrast, as it can be experienced e.g. in the Chevreul illusion at the edges of the steps.

Nonetheless, the Bezold illusion [13], for example, is known already since the 19th century, which cannot be explained by the classical lateral inhibition principle. (The Bezold effect is defined by Gilchrist ([14], p114) as follows “... von Bezold (1874) described and illustrated an effect in which a colored surface appears lighter when overlaid with by thin white lines or small white dots and appears darker if the lines or dots are black.”) The fact that lateral inhibition cannot be considered as the only principal mechanism of early vision is shown more unequivocally by the White effect [15] published in 1979. This illusory effect decisively contradicts the classical lateral inhibition account. In White’s figure, grey areas that are surrounded by more white seem brighter than those surrounded by more black, though physically they are of equal luminance. Such phenomena have been termed assimilation in the literature, in order to distinguish them from contrast phenomena. (The term ‘reverse contrast’ is occasionally used as a synonym of the term ‘assimilation’, see for example [16]).

Attempts are found in the literature to capture these two different types of phenomena within a unified computational model framework [11,12], combining output images of DoG-like local filters. Another attempt for the resolution of this issue is to trace assimilation phenomena back to contrast phenomena by applying certain gestalt grouping principles [17].

In addition to the assimilation phenomena, further images were created to challenge the lateral inhibition account [1,18]. These novel images were presented to show the role of mid-level mechanisms, involving contours, junctions and grouping in brightness perception [19]. In those studies, novel illusory images were designed in which some parts could be perceived as a dark, semi-transparent smoked glass, shadow or as clouds. The conclusion of these studies was that in the images they presented, identically bright grey areas seemed different because one grey area was interpreted as being located in a shaded area or behind a smoked glass, while the other was perceived as being in a better-lit environment; or as dark disks behind white clouds and vice versa. These authors rejected the lateral inhibition account.

Despite all these counter-examples and arguments, lateral inhibition still persists as a basic explanatory principle. Presumably, theorists of lateral inhibition succeeded in avoiding confrontation with the contradictory phenomena because the mentioned previous studies, that aimed to overthrow the concept that brightness illusions were manifestations of lateral inhibition, applied different illusory images from those that were traditionally explained so. Therefore the idea could still hold true. Most classical illusions known since the 19th century were still in agreement with lateral inhibition-based accounts.

Our general aim is to prove that lateral inhibition (and thus any DoG-based convolution model) is untenable even for the classical illusions. We recently refuted that such models were suitable to explain the Hermann grid illusion (Geier, Sera, Bernath, 2004, *Perception* 33, supplement 53); [20], which, besides the Chevreul illusion, had been considered one of the last strongholds of the lateral inhibition account.

We now show that such local models building upon lateral inhibition fail to explain the Chevreul illusion, too.

Results and Discussion

A decisive challenge for the lateral inhibition as an explanatory principle for the Chevreul illusion is aimed at by means of the images and phenomena presented below.

Chevreul staircase surrounded by a luminance ramp background

We placed the Chevreul staircase in a gradually increasing luminance ramp background. (This background is termed as ‘ramp’, since its physical luminance cross-section looks like a ramp.)

Our first main result is that this modification considerably affected the illusion: the illusion significantly increases or decreases, depending on the progression of the ramp relative to the staircase. When the progression of the staircase is identical to that of the ramp, the illusion is enhanced, whereas when the staircase and the ramp progress in opposite directions, the illusion ceases.

This phenomenon can be experienced directly by the reader of this paper on looking at Figure 2, where we placed two physically identical staircases of opposite progressions in a luminance ramp background. Note that the change in the illusory effect is equally strong through the entire area of the staircase; it is not limited to the immediate neighbourhood of the upper and lower edges of the steps, where they adjoin the ramp.

The placement of the staircases into a luminance ramp can also be conceived as replacing the originally uniform background (which usually is a white paper) with a luminance ramp background, leaving the staircases themselves physically untouched.

The luminance ramp background was created so that the luminance of the ramp equals the luminance of each step at its

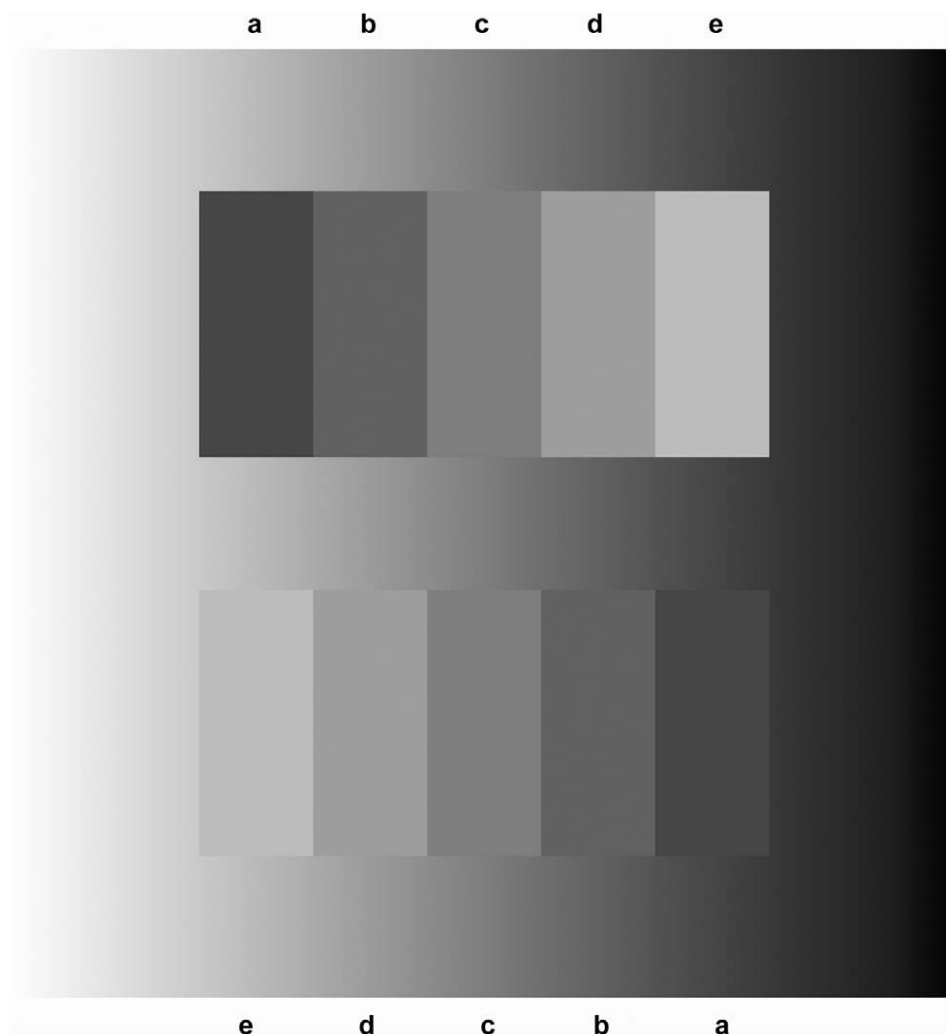


Figure 2. The effect of the luminance ramp background. Two physically identical Chevreul staircases of opposite progression were placed in a luminance ramp background. (Identical letters indicate the steps of physically identical luminance). It can be seen that due to the ramp, the illusion has significantly changed: The illusion ceases if the progression of the staircase is opposite to that of the ramp (upper staircase), while it is strongly enhanced when the progressions of the ramp and that of the staircase are identical (lower staircase).

doi:10.1371/journal.pone.0026062.g002

vertical midline, whereby the sign of the upper and lower boundary changes along its length. This was adjusted empirically, since the change of illusion was strongest with such parameters. Here we are not aiming to investigate in detail the case when the progression of the ramp is identical to that of the staircase but it is matched to the steps in a different way. We cover this issue only to the extent that we include some such variations in Figure S1).

For the sake of a more exact analysis, we conducted psychophysical experiments with 23 participants. Stimuli used in our experiment are illustrated in Movie S1 and are described in the Materials and Methods section in detail. In the first part of our experiment, we asked the observers whether they saw the steps as crimped (inhomogeneous) or uniform (homogeneous). When the background was homogeneous grey (similarly to the classical demonstration of the Chevreul illusion, as in Figure 1.) 14 observers reported the steps of the staircase as looking crimped, while 9 reported them as uniform. In comparison, when the staircase was surrounded by a ramp of identical progression, all 23 observers reported seeing the steps as crimped. However, when the progression of the ramp was in the opposite direction to that of the staircase, all observers saw the steps as uniform.

Our first conclusion is that if classical lateral inhibition-based explanations were tenable, then the perception within the steps should not have been changed by the ramp. Note that the replacement of the original white background with a luminance ramp background causes physical luminance change exclusively *outside* the area of the staircase, while no physical change has occurred within the staircase. Classical lateral inhibition-based explanations [2,8,9], however, build exclusively upon luminance relations of the steps *within* the staircase. This is in contradiction with the phenomenon that the perception has changed through the entire vertical height of the staircase merely due to the surrounding luminance ramp.

The ramp effect can neither be explained by the mentioned theories of mid-level mechanisms [1,18], since no physical brightness change occurred within the staircase that could be interpreted as a smoked glass or shadow, nor can any gestalt idea be applied, which could account for the perceptual difference between the two identical staircases of opposite direction in the same ramp background.

Chevreul staircase surrounded by a double luminance ramp background

If we aim to find a new explanatory principle for these phenomena, we have to notice that due to placing the ramp around the staircases, not only the area outside the staircases has been changed physically, but their boundary edges, too. To decide which of these plays more important role in the change of the Chevreul illusion, we placed another, narrow ramp around the staircase, whose direction was opposite to that of the original, larger ramp.

The result of this modification involving a double luminance ramp can directly be observed in Figure 3. It can be seen there that although the area of the inner ramp is significantly smaller than that of the outer ramp, still the inner one governs the change in the Chevreul illusion. If the inner ramp is replaced by a homogeneous rectangle, then two perceptually identical classical Chevreul staircases will be obtained, progressing in opposite directions, and the outer ramp will have no effect.

For the sake of a quantitative analysis, we supported the effect of the double ramp background by psychophysical experiments. Subjects had to adjust the size of the inner ramp until they found the ramp height at which the steps turned inhomogeneous, if they were uniform at the beginning, or vice versa (see Procedure in

Materials and Methods). The changeover occurred at an average height of 0.51 deg above and below the borders of the staircase (SD = 0.48 deg). So, we found that even when the inner ramp is rather narrow, it is still the inner ramp which determines the perceptual experience, whether the steps are seen as strongly inhomogeneous or totally uniform.

This result supports that the upper and lower boundary edges of the staircase control the perceptual experience, and not the area size of the ramp, since such a narrow ramp as half a degree can prevail against the effect of the much larger outer ramp. Therefore, we conclude that it is the boundary edges in the image that govern perceptual experience instead of the large background areas, and long-range interactions should be supposed between edges and the areas enclosed by them.

We summarise the description of these perceptual phenomena as follows:

- *Result 1:* In a Chevreul staircase with a homogeneous background, most observers (roughly two-third of the 23 subjects in our experiment) see the steps as crimped.
- *Result 2:* On placing the staircase in a luminance ramp background of opposite direction, the illusion ceases, while on placing it into a ramp of identical progression, the illusion is significantly enhanced. This was the case for all our 23 observers without exception.
- *Result 3:* When the staircase is placed in a double luminance ramp, the inner one governs the perceptual experience even when its area is rather small compared to the outer one (mean: 0,51 deg), and Result 1–2 also holds here for the perceptual experience.
- *Result 4:* Regardless of the variant of the Chevreul staircase being observed (either the classical one with a homogeneous background or the single or double ramped versions enhancing or ceasing the effect), the extent of the perceived homogeneity (or the inhomogeneity) of each step is equal within the entire height of the staircase. The illusion is of the same magnitude near the upper or the lower boundaries, as well as in the midline of the staircase.

Lateral inhibition and DoG models

Prior to discussing our criticism in more detail, the concept of lateral inhibition should be further clarified.

On reviewing the relevant literature, two different, but functionally equivalent definitions can be found. One of them has already been used by Ernest Mach: the stimulated neural area inhibits the activity of the neighbouring area. This is termed reciprocal effect by Mach: "...the phenomena discussed can only be explained on the basis of a reciprocal action (Wechselwirkung) of neighbouring areas of the retina" ([2], p97). Mach, for obvious reasons, inferred this on a theoretical basis. The discoverer of lateral inhibition, Haldan Keffer Hartline provided a similar definition ([21], p85), and analogous definitions can also be found in current literature (e.g. [1], p2042).

The other phrasing of the definition emerged presumably after the followers of Hartline (e.g. [6]): a receptive field is associated with each retinal point (or ganglion cell), comprising a stimulating (on) centre and an inhibitory (off) surround. The circularly symmetric on-centre, off-surround DoG (or the Mexican hat) weight function is obtained by the abstraction of physiological measurements [7]. Ratliff ([2] p122) lists the weight functions contrived by six different authors, including the one by Mach himself. Ratliff regards these weight functions fundamentally equivalent. By varying the diameter and the ratio of the

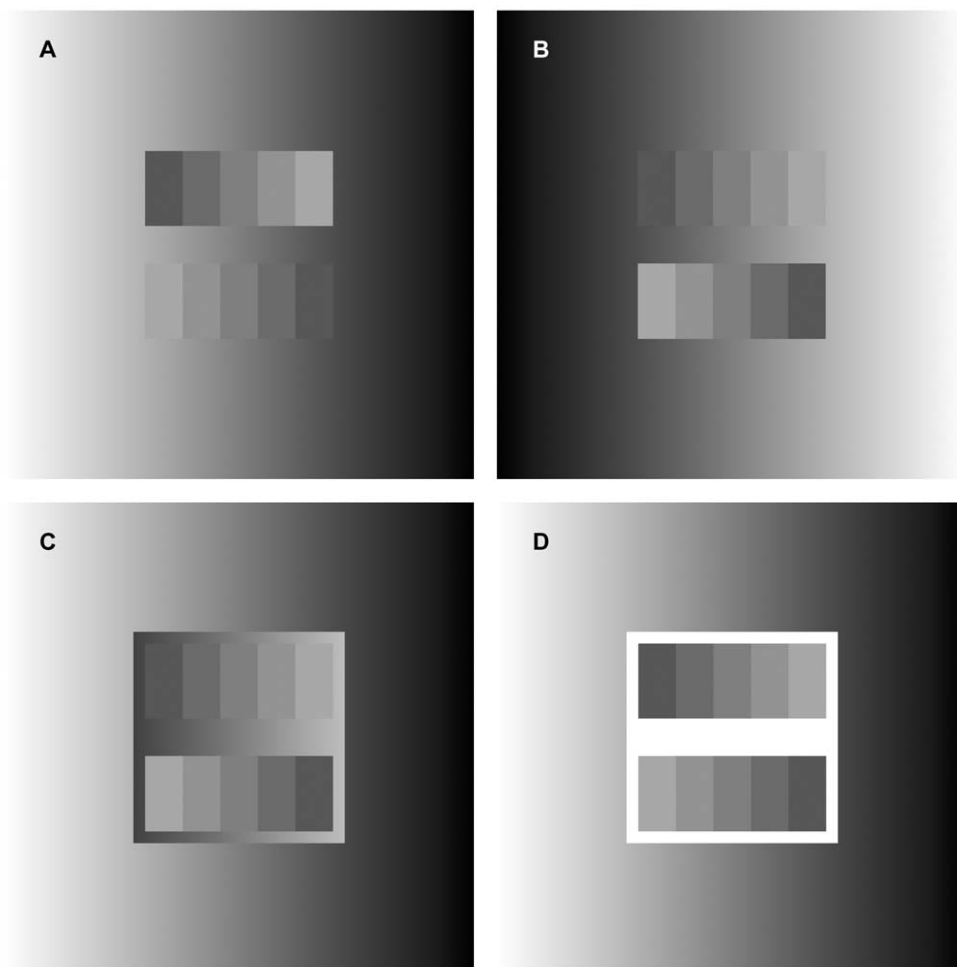


Figure 3. The effect of a double ramp background. The staircase-pairs in the four images are physically identical; the upper and lower staircases in each image are also identical except for their progression to opposite directions. On comparing Fig. 4. A and B, it can be seen that a ramp of opposite direction causes opposite effects. On comparing Figure C with A and B, it can be seen that the illusion in C is identical with that in B. This is so, although the large outer ramp in Fig C is identical with the one in A. Therefore the small inner ramp dominates perception, whose direction is homogeneous white rectangle is what dominates. doi:10.1371/journal.pone.0026062.g003

stimulating centre and the inhibitory surround, weight functions of different shapes can be produced.

If it is assumed that the decay of lateral inhibition is equal in all directions (isotropy), then the two definitions are practically equivalent. A slight difference between them is that the first phrasing of the definition allows that each retinal point is inhibited by its immediate neighbour, whereas in case of the most widely used DoG filters, this principle is contradicted by the large stimulating centres. Multiscale models attempt to overcome this difficulty by including DoG filters of small diameter.

On this basis, in line with the terminology found in the literature, *we will hereafter identify the concept of lateral inhibition with models using DoG-like filters*, including multiscale models [10,12,22,23] and models using elongated filters [11] as well as any qualitative explanations referring to such, e.g. the classical textbook-explanation.

The aim of the DoG model (as well as other models of brightness perception) is to reproduce the brightness (perceived luminance) distribution from the physical luminance distribution of an image. The input of such a model is an image corresponding to the physical luminance distribution, while another image is

expected as output, in which the intensities correspond to human perception.

The main point of DoG-based models is the convolution between the points of the input image and a particular weight function. In other words, the output image is generated by the algorithm from the input image so that each P point of the input image is replaced by the weighted average of the intensities of the neighbouring points of P. The weight function is the given DoG filter, whose central point is allocated at P. In case of multiscale models, a series of DoG (or ODOG) functions are applied, ranging from small to large diameters. Here the output image is the weighted sum of the outputs of individual (O)DoG filters [10–12,22,23]. Another characteristic of DoG models is that they are local, which means (among other things) that there is no interaction between DoGs (receptive fields) whose centres are located at different points.

Why is lateral inhibition insufficient here?

The main point of our criticism, as mentioned above, is that the classical lateral inhibition account of the Chevreul illusion considers merely the neighbouring steps as the local surround of

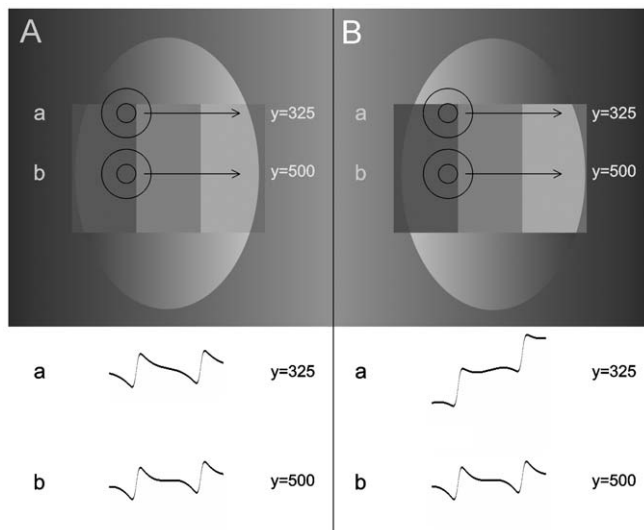


Figure 4. The output of the DoG model for steps in ramps of opposite directions. The middle step of two staircases surrounded by ramps of opposite progressions are enlarged in the upper part of A and B. If the DoG filters are moved along the horizontal direction, as shown by the arrows, they will predict the brightness values shown in the brightness cross-section diagrams *a* and *b* below the image. The luminance cross-sections produced by our simulation of the DoG filter at $y=325$ and $y=500$ (*a* and *b*) are shown below the enlarged steps, respectively. On the one hand, the prediction of DoG filter (*a*) is somewhat similar to human perception, since it predicts a steeper slope in A. On the other hand, though the step in B is seen as totally flat, DoG filter (*a*) still predicts scalloping there. In addition, in the midline of the two staircases, no difference is predicted between A and B by DoG filter (*b*), contradictory to human perception, according to which the steps in A and B look largely different. Moreover, the predictions of (*a*) and (*b*) within each staircase shows different brightness cross-sections, although the illusion is equally strong through the entire height of the staircase. (The cross-section diagrams were produced by our computer simulation). doi:10.1371/journal.pone.0026062.g004

each step, and thus it cannot take the effect of the ramp outside the staircase into account. Let us analyze this in more detail.

DoG filters corresponding to the classical explanation are illustrated in the inner area and near the upper boundary edges of the staircases in Figure 4. By comparing the cross-section diagrams of the responses of DoG filters, two contradictions can be found with human perception. If the cross sections *a* and *b* are compared with each other either within Figure 4A or within Figure 4B, it can be seen that they are significantly different from each other, which contradicts Result 4 (the change of the illusion is equally strong through the entire height of the staircase). Moreover, it can also be seen that the cross-sections *b* of Figure 4A and B are identical, which contradicts Result 2 (ramps of opposite progressions cause opposite effects on the illusion). The cross section diagrams of Figure 4A and B differ only near the horizontal boundary edges of the staircases, showing some similarity to human perception only there: the cross section diagram *a* is steeper in A compared to the one in B. Nonetheless, cross section *a* in B is still crimped, although the steps in B are perceived as uniform.

These contradictions are not surprising, since a significant portion of the inhibitory surrounds of DoGs near the boundary edges (*b*) reach into the ramp. In contrast, the entire area of DoG filters located in the inner part of the staircase (position (*a*)) falls only within the staircase, and is not influenced by the ramp.

Another side-effect of such a simple DoG filtering is the blur of the step edges, as it can be seen in the cross-section diagrams. Multiscale models attempt to handle this problem by applying DoG filters of small diameters to avoid blurring, as well as very large ones to ensure that remote points can influence inner parts of large homogeneous areas (e.g. in the ODOG model, the largest filter diameter is 36 deg including the surround). Therefore, it could be reasonable to think that multiscale models can predict the phenomena presented in our images. However, we are going to

show below that multiscale filters fail to predict our double-ramped variants for inherent theoretical reasons.

In Figure 5, DoG filters of different diameters are illustrated. In accordance with what was described regarding Figure 4, it can be seen that small DoG filters near the upper and lower boundary edges can produce more or less similar predictions to human perception, since their areas reach into the inner ramp, and do not exceed into the outer one. The small filters in the inner areas of the staircase (Figure 5 D-F DoG *b*), however, produce identical results in A, B and C. Therefore, all in all, the output of small filters contradicts human perception.

If now DoGs of large diameters are considered (Figure 5 D-F DoG *a*), whose inhibitory surrounds extend beyond the staircase into the ramp, it is obvious that these inhibitory surrounds will extend also beyond the narrow inner ramp in Figure 5F into the outer one. Therefore, the stimulation of such large DoG filters in Figure 5F(*a*) will be much more similar to that of E(*a*) than to that of D(*a*). Consequently, outputs of large DoGs will reflect a stronger influence of the far surround (outer ramp) than the near surround (inner ramp) in these images.

Nonetheless, the staircases both in A and in C look crimped, whereas the one in B looks flat. Therefore, it is the near surround (inner ramp) that dominates human perception. Consequently, the output of large DoG filters will also be in contradiction with human perception. It also can be questioned whether such large antagonistic, circularly symmetric receptive fields exist.

Since multiscale models use DoGs of diameters ranging from small to large, however, neither small, nor large filters can model the perception of the ramped versions of the Chevreul illusion, the sum of the output images of different scales will also fail to model human perception, irrespective of the averaging method.

The ODOG model [11] must also be mentioned here. In this model, ODOG filters of different orientations are included, whose inhibitory surrounds can roughly be described as elongated

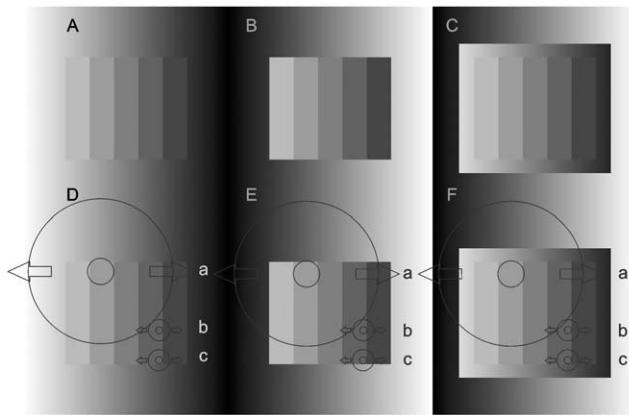


Figure 5. Perceptual experience vs. the stimulation of DoG filters of different spatial scales. The staircases are physically identical in all the six panels. The steps in B are perceived as spatially uniform, while steps in A and C are both perceived as crimped, i.e. the inner ramp dominates in C. Panels D, E and F correspond to A, B and C respectively, illustrating larger and smaller DoG filters at critical locations. A portion of the inhibitory surrounds of small DoG filters near the upper and lower boundary edges of the staircases (c) reaches into the ramp, therefore if they are moved along the horizontal direction, their output will be somewhat similar to human perception due to the change of the intensity of the ramp along the horizontal direction. However, if the small DoG filters are moved within the inner area of the staircase (b), they do not reach into the ramp, therefore they provide identical outputs for all images, contradictory to human perception. The effect of the ramp background can manifest in the DoG filter outputs in the midline of the staircase if and only if the diameter of the DoG filter is larger than the height of the staircase. Following the same logic as above, DoGs of such large diameters (a) might predict the different perception of A and B. Nonetheless, such large filters exceed significantly beyond the inner ramp in F(a). As a consequence, the stimulation of DoG filter F(a) is much more similar to that of E(a) compared to D(a). This is in contradiction with human perception, since the perception of A and C are crimped, while B is perceived as flat. doi:10.1371/journal.pone.0026062.g005

ellipses. However, from our point of view, the same criticism stands for elongated ellipses as for circularly symmetric filters: if they are small, then they are insensitive to the ramp in the midline of the staircase while if they are large, then they extend beyond the inner ramp into the outer one, causing it to dominate the simulation results, contradictory to human perception. In conclusion, neither can the ODOG model be expected to predict the perceptual changes in the Chevreul illusion properly.

In the light of the foregoing, it can be stated that DoG models fail to model the novel phenomena. The basic reason of this is that the sensitivity of each DoG filter is limited to the particular area that it covers, however, these critical areas are so various in our images, as it was shown above, that neither small, nor large filters are able to capture these changes, irrespective of whether they are circularly symmetric or elongated.

Conclusions

On the basis of our results, our conclusions are the following:

- *Conclusion 1:* It is the edges that play the most significant role in the change of the illusion.
- *Conclusion 2:* The edges also obstruct effects coming from farther edges (here the outer edge of the inner ramp prevents the effects coming from the direction of the outer ramp from spreading into the staircase).

- *Conclusion 3:* There is a long range interaction between edges and areas enclosed by them.

These conclusions might extend beyond the Chevreul illusion embedded in background ramp(s). We regard these conclusions generally valid to brightness perception, not being limited to brightness phenomena introduced here.

As it has been shown above in detail, DoG models fail to give a unified explanation to these phenomena. Such models are built on the weighted sum (convolution) of areas covered by single DoG filters, therefore they are essentially sensitive to appropriately weighted average intensities of larger or smaller portions of the image. The accentuated role of edges in the generation of the illusion is not included in DoG models, nor is their segmenting role included. Finally, DoG models do not apply any interaction between filters remotely located from each other.

Let us not be misled by the fact that the DoG model quasi ‘detects’ edges. This is only a consequence of the DoG model: on the two sides of each edge, areas of two different intensities are found, and the DoG models are in fact sensitive to that. The main point of the concept of lateral inhibition, as it can be found in the definitions of relevant literature, is the reciprocal interaction of neighbouring areas. In these definitions, the role of edges or their effect on larger areas is not even mentioned.

When the principle of lateral inhibition is applied to account for particular illusions, we tend to select areas - that will inhibit each other in accordance with the principle of lateral inhibition - along certain well-discernible edges. Nevertheless, this is a rule that wound its way implicitly to such explanations, which is not contained explicitly by any lateral inhibition model. It is not even forbidden by lateral inhibition models that - ad absurdum - a rectangle is selected mentally without any cue in a uniform white paper, in which case an intriguing contradiction is met: the mentally selected white rectangle should be inhibited by its white surround, implying that the remaining area of the white paper darkens its own inner portion.

By means of the foregoing, we proved directly ‘only’ that the ramped versions of the Chevreul illusion cannot be accounted for by the DoG model. It could be argued against this that the DoG model is still suitable to explain the classical Chevreul illusion presented on a white background. Nonetheless, let us consider the following: by the introduction of the variations with luminance ramp backgrounds, the classical white-background version has become merely a special case of the broader range of the Chevreul phenomena (i.e. here the slope of the background ramp is 0). It has been shown that the DoG model fails to provide a unified account for the ramped versions, therefore, a new model should be sought. To our knowledge, no such model exists at present in the literature. However, it is certain that if once such a model is developed, it should obviously be able to capture both the ramped versions and the classical Chevreul illusion as well.

If the prediction of a model is more or less agrees with the perceptual facts, it is useful. However, it is not sufficient in itself, since it might happen that this agreement is only apparent, occurring only in a special case. What can be expected from a good model in principle is that it should capture the essence of the modelled process. This is the reason for developing models at all: to understand processes and phenomena better. The DoG model failed to capture the ramped versions, therefore it is clear that it

fails to capture the essence of these phenomena. Why would one think therefore that it captures the essence in the classical uniform-background case?

Therefore, we base our claim that the lateral inhibition-based models are refuted by the ramped versions on the basis of this line of thought. The principle of lateral inhibition is unable to capture the Chevreul illusion since it fails to capture the essence of the broader range of phenomena of which the classical Chevreul illusion is a special case.

Here it is important to note that we do not consider the presence of edges in general a necessary condition for brightness illusions to occur. In other words, if there are edges in an image, then they certainly operate as described in our conclusions. However, this does not exclude the possibility of other brightness illusions, which do not include edges, or if they do, the illusion is influenced by another factor. One example for the latter is Logvinenko's illusion [24], where the effect is caused not by the edges but the sinusoid luminance grating located between the edges. What is certain is that the second derivative of the sinusoid grating is not zero, which is also true for edges. If a model (either an existing one or a future one) captures non-zero second derivatives appropriately, it should also capture edges, as special cases, appropriately.

Where do we go from here?

Therefore, we are in want of a model that can universally handle the points we claimed in our conclusions. The most suitable candidates for this are the filling-in type of models. The prototype of such models (the 'standard diffusion model') is what Cohen and Grossberg [25] applied in one dimension, and after them, Grossberg and Todorović [26] extended it to two dimensions. This 'CGT' model was further developed by others, but as it turns out from Gilchrist's review ([14] p106, p206-207), its basic principle is practically unchanged even until nowadays.

The main point of the CGT model in short is that after the allocation of the edges, the areas enclosed by the edges are filled in by a diffusion process. At the same time, edges are also assigned an obstructive role. These principles are fully in line with our conclusions: it is the edges what govern the process; they also have an obstructive role; and the basis of the long range interactions between the edges and the areas enclosed by them is the diffusion process.

However, Gilchrist's comment ([14] p207), that the CGT model is unable to handle the staircase luminance pattern (i.e. the Chevreul illusion) should be taken into account. Here he exposes the following note by Pessoa et al ([27] p2202) on the CGT model: 'Perhaps an even greater challenge to filling-in models is a luminance staircase distribution. The "steps" of the staircase presumably block diffusion, and it is not evident how a filling-in model can predict that different steps appear with different brightnesses (since "border contrast" is the same everywhere).'

Therefore, the CGT model is in the need of an essential correction: the issue of the brightness of areas separated by edges should be solved. Hopefully, this correction will sooner or later be achieved by someone. (For instance, this candidate could try adding the contrast of the elementary edge segments to the brightness of the points in the neighbouring area in a skilful way...).

Materials and Methods

Ethical statement

The experimental procedure was approved by the Budapest University of Technology and Economics Institutional Review

Board #1 – Behavioural and Biomedical. Oral informed consent was obtained from all participants after the nature of the experiment was explained both in written format on the application form and orally before the experiment. The reason for not collecting written consent from each subject is that our experiment had no risk at all and caused no harm. People only had to look at an image displayed on a computer screen and were free to rest or leave anytime, and they were informed so beforehand. The process was documented by our experimental software: name of the subject, age, gender, and type of vision (normal, or wearing glasses or contact lenses). The documented measure was a parameter of the viewed image that the subject set for herself (the height of the inner ramp at which the illusion turned over for her). Only the two researchers have access to the data, which was processed anonymously. The institutional ethics committee approved this process.

Subjects

23 observers (12 males, 11 females), aged 18-32 years, with normal (20) or corrected-to-normal (3) vision, participated.

Stimuli

A staircase luminance profile of 3.68*7.38 deg, consisting of 6 steps, was used for a stimulus. Steps were 1.23 deg wide and had luminances of 18.3, 13.9, 10.0, 7.4, 4.5, and 2.5 cd/m². In the first part of the experiment, the staircase was surrounded by (i) a uniformly grey background of 7.3 cd/m²; (ii) a smooth luminance ramp ranging from 30.3 – 0.1 cd/m² and progressing either in the same or (iii) in the opposite direction as the staircase. All backgrounds subtended 12.27*12.27 deg. In the second part, a background, consisting of an outer ramp and an inner ramp of opposite progression, surrounded the staircase. The inner ramp was 9.81 deg wide (luminances as stated above (ii)). Four stimuli were used: the staircase progressed either (i) from high to low or (ii) low to high, thus its progression was either the same or the opposite to the inner ramp. Initially, the inner ramp either (iii) surrounded the Chevreul staircase extending by 2.5 deg above and below or (iv) was occluded by the staircase (0 deg visible above and below). Stimuli were presented on a calibrated CRT monitor (resolution 1024*768 pixels, 60 Hz) in a dimly lit room at a distance of 72 cm.

Procedure

In the first part of the experiment, we tested the effect of the various backgrounds on the Chevreul illusion. Observers were asked whether the individual steps of the staircase appeared either darker on one side and lighter on the other (crimped), or uniform. In the second part, they adjusted the initial size of the inner ramp, until the percept of the steps in the staircase changed from crimped to uniform, or vice versa. The aim was to measure the minimal size of the inner ramp at which it still prevailed over the effect of the outer ramp, in order to determine whether area size proportions or boundary edges were more important. After familiarization with the task, stimuli were presented in a random order, followed by a mask of black-and-white dots exposed for 2500 ms.

Supporting Information

Figure S1 The demonstration of the case when the sign of the elementary edge segments changes along the upper and lower boundary edges of the staircase (A3) and the cases when it does not (A1, A2, A4, A5). The luminance cross-sections of the horizontal midline of the staircases

are displayed below each ramped Chevreul image. The three staircases are physically identical within each row. The intensities of the staircases increase from row 1 to 6, whereas the background ramps are identical in all rows. Rows: A1: the intensity of the steps is lower than that of the background ramp. A2: the left side of the steps is fitted to the ramp. A3: the vertical midline of the steps is fitted to the ramp. A4: the right side of the steps is fitted to the ramp. A5: the intensity of the steps is higher than that of the ramp. Columns: A: the progression of the ramp is identical to that of the staircase. B: the progression of the ramp is opposite to that of the staircase. C: white background. It can be seen that it is column A in which the steps are crimped to the highest extent; the illusion is weakest in column B, while the magnitude of the illusion in C is in between that in A and B. It can be seen that the crimping effect of the ramp is strongest in A3, but it is also not negligible even in the other rows. This fact deserves attention particularly because the intensity of the staircases run below the intensity of the ramp in A1, and above it in A5, while the ramp still changes the crimping of the steps. This implies that the change of the sign along the

upper and lower boundary edges of the staircase is not a necessary condition for the ramp effect to occur.

(TIF)

Movie S1 Illustration of our experimental stimuli.

(SWF)

Acknowledgments

We would like to thank Ilona Kovács, Xavier Otazu, Lothar Spillmann and Michael White for their valuable comments on earlier versions of this manuscript. We thank Barbara Blakeslee and Mark McCourt for their assistance in interpreting the relation of the ODOG model to our images by providing us with simulation results.

Author Contributions

Conceived and designed the experiments: JG MH. Performed the experiments: MH. Analyzed the data: MH. Contributed reagents/materials/analysis tools: JG MH. Wrote the paper: JG MH. Invented the effect: JG. Wrote the experimental program: JG. Wrote the supporting Flash demo: MH.

References

- Adelson EH (1993) Perceptual organization and the judgment of brightness. *Science* 262: 2042–2044.
- Ratliff F (1965) *Mach Bands: Quantitative studies on neural networks on the retina*. San Francisco/Amsterdam, London: Holden-Day Inc. 365 p.
- Spillmann L (1994) The Hermann Grid Illusion: a Tool for Studying Human Perceptive Field Organization. *Perception* 23: 691–708.
- von Békésy G (1967) *Sensory inhibition*. New Jersey, Princeton: Princeton University Press. 277 p.
- Hartline HK, Wagner HG, Ratliff F (1956) Inhibition in the eye of *Limulus*. *J Gen Physiol* 39(5): 651–673.
- Kuffler SW (1953) Discharge patterns and functional organization of mammalian retina. *J Neurophysiol* 16: 57–68.
- Rodieck RW (1965) Quantitative analysis of cat retinal ganglion cell response to visual stimuli. *Vis Res* 5: 583–601.
- Goldstein EB (2009) *Sensation and perception*. Belmont: Wadsworth Cengage Learning. 496 p.
- Blake R, Sekuler R (2006) *Perception*, Boston: McGraw-Hill. 652 p.
- McArthur JA, Moulden B (1999) A two-dimensional model of brightness perception based on spatial filtering consistent with retinal processing. *Vis Res* 39: 1199–1219.
- Blakeslee B, McCourt ME (1999) A multiscale spatial filtering account of the White effect, simultaneous brightness contrast and grating induction, *Vis Res* 39: 4361–4377.
- Otazu X, Vanrell M, Párraga A (2008) Multiresolution wavelet framework models brightness induction effects. *Vis Res* 48: 733–751.
- von Bezold W (1874) *Die farbenlehre im Hinblick auf Kunst und Kuntsgewerbe*. Brunswick: Westermann. 326 p.
- Gilchrist A (2006) *Seeing Black and White*. Oxford: Oxford University Press. 430 p.
- White M (1979) A new effect of pattern on perceived lightness. *Perception* 8: 413–416.
- Jameson D, Hurvich LM (1975) From Contrast to Assimilation: in Art and in the Eye. *Leonardo* 9: 125–131.
- Anderson BL (1997) A theory of illusory lightness and transparency in monocular and binocular images: the role of contour junctions. *Perception* 26(4): 419–453.
- Anderson BL, Winawer J (2005) Image segmentation and lightness perception. *Nature* 434: 79–83.
- Adelson EH (2000) Lightness Perception and Lightness Illusions. In Gazzaniga M, ed. *The New Cognitive Neurosciences*. 2nd ed. CambridgeMA: MIT Press. pp 339–351.
- Geier J, Bernáth L, Hudák M, Séra L (2008) Straightness as the main factor of the Hermann grid illusion. *Perception* 37: 651–665.
- Hartline HK (1949) Inhibition of activity of visual receptors by illuminating nearby retinal areas in the *Limulus* eye. *Fed Proc* 8(1): 69–69.
- Kingdom F, Moulden G (1992) A multi-channel approach to brightness coding. *Vis Res* 32(8): 1565–1582.
- Watt J, Morgan MJ (1985) A Theory of the Primitive Spatial Code in Human Vision. *Vis Res* 25(11): 1661–1674.
- Logvinenko A (1999) Lightness induction revisited. *Perception* 28: 803–816.
- Cohen MA, Grossberg S (1984) Neural dynamics of brightness perception: features, boundaries, diffusion, and resonance. *Percept Psychophys* 36: 428–456.
- Grossberg S, Todorović D (1988) Neural dynamics of 1-D and 2-D brightness perception: A unified model of classical and recent phenomena. *Perception & Psychophysics* 43: 241–277.
- Pessoa L, Mignolla E, Neumann H (1994) A Contrast- and Luminance-driven Multiscale Network Model of Brightness Perception, *Vis Res* 35(15): 2201–2223.

SHORT AND SWEET**Afterimages from unseen stimuli**

Stuart Anstis

Department of Psychology UC San Diego La Jolla CA 92093, USA; e-mail: sanstis@ucsd.edu

Janos Geier

Stereo Vision Ltd, Nádasdy Kálmán utca 34, Budapest, Hungary; e-mail: janos@geier.hu

Mariann Hudak

Budapest University of Technology and Economics, Department of Cognitive Science, Egrý József utca 1, Budapest, Hungary; e-mail: mariann@stereovision.hu

Received 30 June 2012, in revised form 13 July 2012; published 31 July 2012.

Abstract. Observers adapted to a field of randomly coloured twinkling tiles, in which was embedded a faint, subthreshold green letter. Observers failed to discern this letter, but they readily reported its pink afterimage afterwards. This demonstrates a storage of changing colours over time; adaptation occurs for the average of each retinal point.

Keywords: afterimage, color vision, visual storage, subthreshold summation.

An afterimage is usually weaker than the stimulus that induces it, as well as being of opposite colour. But here we show that an invisible stimulus can give a visible afterimage. The inducer was a faint, subthreshold green letter, masked by twinkling colour noise, and its afterimage was a strong, pink perceived letter. All four movies are embodied in this Flash file:

Afterimages from unseen patterns - demo movies by S. Anstis, J. Geier and M. Hudák

- Movie1 Display grid at the end
 Movie2
 Movie3
 Movie4

Instructions for the Observer:

1. Select a movie from the list above by clicking the radiobutton next to it.
2. Fixate the red circle
3. Push the Play button and keep fixating
4. Keep fixating even when the movie ends.

What letter do you see?

Fixation time can be altered by the up/down arrows between 5..60 s. The movie can be stopped earlier by clicking the Stop button or by hitting the Shift button on the keyboard.

Stop ■ Fixation time (s)

Movie 4. The demo of the experimental stimulus.

The constantly changing colours in each letter tile were given a faint greenish statistical bias superimposed on their random values, and the colours of the background tiles were given a faint magenta bias. These biases gradually increased on every frame.

Movies 1–4. Please click image to play. Then use play button to start and stop.

The phenomenon is demonstrated in [Movie 1](#). To experience the illusion, just start the movie. (All movies are best viewed in a darkened room. If you do not see an afterimage on your first try, please increase the fixation time.) You will see coloured, flickering tiles. Fixate the centre for approximately 30 s. When the flickering stops, a homogeneous white background is presented. Most observers do not perceive any letter during the twinkling adapting phase, but afterwards they do see the pink afterimage of a capital letter. This letter is named at the end of the paper. The afterimages often take a few seconds to bloom gradually into view.

[Movie 1](#) was made with a 6×7 array of coloured square tiles, each subtending 1° angle. The R, G and B channels of each tile were randomly assigned a value of either 0 or 255, independently of each other. The frames of the display were refreshed at 10 Hz, producing coarsely pixelated dynamic random-dot noise. A letter was hidden in the centre of the display as follows: the probability that the R and B channels of the letter tiles were assigned the value of 255 was 25%, whereas on the G channel, the probability of 255 was 75%; and the probabilities for the background tiles were the opposite. This biased the probabilities in the letter tiles towards green, and, in the background tiles towards magenta. Therefore, the letter was not visible during the display, since physically no letter was presented in any of the frames. However, if all frames were averaged together, then there would be a green letter on a magenta background.

Did you have experience the magenta afterimage of a letter on a greenish background after watching the movie? This result is the same as if you had fixated a green letter on a magenta background. Therefore, it seems that you have adapted to the average of the frames while not seeing any letter in the meantime.

Black outlines are believed to facilitate the perception of any afterimages (Anstis, Van Lier, & Vergeer, manuscript submitted for publication; Daw, [1962](#); Hamburger, Geremek, & Spillmann, [2012](#); Van Lier, Vergeer, & Anstis, [2009](#); Van Boxtel & Koch, [2010](#)). By checking this option in the Movies, you can test whether the grid-like outline at the end of the movie helps you detect the letter.

The effect also works in a black-and-white version ([Movie 2](#)). In this movie, the probability of 255 (white) in the letter tiles is 75%, but only 25% in the background tiles. Moreover, a black-and-white after-effect can be elicited even by a chromatic flickering stimulus ([Movie 3](#)). Guess, how.

As for the chromatic version of the afterimage, the same result can also be obtained by a different algorithm, which can be experienced in [Movie 4](#). It was prepared as follows: in an array of 6×7 tiles, a letter-shaped subset of tiles was designated to spell a single capital letter. Each tile flickered at 10 Hz in independent, random colours, which were refreshed with new colours on every frame. The constantly changing colours in each letter tile were given a faint greenish statistical bias superimposed on their random values, and the colours of the background tiles were given a faint magenta bias. These biases gradually increased on every frame, in accordance with the following algorithm.

Let $y = \text{yes}$, $n = \text{no}$, and $f = \text{frame number}$, $y = 1 + f \times 0.005$, and $n = 1/y$. Note that $n < 1 < y$. R, G and B began as randomly chosen integers from a universal distribution between 0 and 255 and were independent for every tile and every frame. The letter tiles were reset on every frame to $R \times n$, $G \times y$, $B \times n$ (biased towards green) and the background tiles were set to $R \times y$, $G \times n$, $B \times y$ (biased towards magenta). Hereby, the average of both the letter and the background tiles was 127 at the beginning, but the letter tiles gradually shifted towards green, and the background tiles towards magenta. By means of the low slope value (0.005), we ensured that the letter always remained below perceptual threshold. Adapting to [Movie 4](#) for 20 s should suffice to give the pink afterimage of a letter. Watch [Movie 4](#) for 60 s if you wish to see the colour bias gradually becoming visible.

We showed [Movie 4](#) to 132 student participants. Following 45 s of adaptation to the twinkling random coloured tiles shown in [Movie 4](#), with strict fixation on a central point, the display was switched to a congruent 6×7 test array of white tiles outlined in black, which was intended to facilitate the perception of the afterimage.

Participants viewed the stimulus from a great variety of distances and angles. Each student held a Clicker, which is a device like a TV remote, with five buttons labelled A through E. Students were told: 'You may see a shadowy letter, A, B, C, D or E, either during the flickering or the white phase of the stimulus. If you do, or think you do, please press the corresponding button on your clicker. If in doubt, feel free to guess.' All button pushes were detected and recorded by a central receiver at the front of the lecture hall, from which they were recorded for later analysis.

During the flickering adapting phase, 11 (8.3%) of the observers correctly reported a camouflaged letter (an 'E'). During the white test phase, 79 (59.8%) correctly identified the pink afterimage of the

letter. Thus, observers were seven times as likely to identify the letter from its afterimage as from the original adapting stimulus.

Although most observers did not perceive these biases during the adaptation, they clearly saw their resulting afterimages. Thus, during adaptation, the target letters had a different mean colour from the background, but the deliberately high variance kept the signal/noise ratio of the bias below the observer's visual threshold—its *d*-prime was too low. Detecting the letter target in the twinkling display would require the visual system to act as a statistician, isolating the difference in the means while hindered by the variance. The afterimage, however, emerges from the sum and discards the variance. Nearly all observers saw the afterimage without ever discriminating the twinkling target that caused it and this shows that the formation of afterimages has a longer integrating time than perception does. Thus, the visual system stores and averages the stimulus colours over time.

Incidentally, the afterimage letters in [Movies 1–4](#) were, respectively, H, E, L, P.

Acknowledgments. M.H. was supported by grant TAMOP 4.2.1/B-09/1/KMR-2010–0002 and S.A. by a grant from the Department of Psychology, UC San Diego. The authors thank Sean Deering, Neal Dykman, Doreen Hsu, Katherine Hsueh, and Esther Strom for their assistance; and Beth Norman for granting access to her class of 132 students with clickers.

References

- Anstis, S., Van Lier, R., & Vergeer, M. *Luminance contours can gate afterimage colors and 'real' colors*. Manuscript submitted for publication. ◀
- Daw, N. (1962). Why afterimages are not seen in normal circumstances. *Nature*, *196*, 1143–1145. [doi:10.1038/1961143a0](https://doi.org/10.1038/1961143a0).
- Hamburger, K., Geremek, A., & Spillmann, L. (2012). Perceptual filling-in of negative coloured afterimages. *Perception*, *41*, 50–56. [doi:10.1068/p7066](https://doi.org/10.1068/p7066).
- Van Boxtel, J.J.A., & Koch, C. (2010). Perceptual organization: Contours and 2D form: Boundary information and filling-in in afterimage perception. *Journal of Vision*, *10*(7), 1159.
- Van Lier, R., Vergeer, M., & Anstis, S. (2009). Filling-in afterimage colors between the lines. *Current Biology*, *19*, R323–R324. [doi:10.1016/j.cub.2009.03.010](https://doi.org/10.1016/j.cub.2009.03.010).



Stuart Anstis took his Ph.D. in experimental psychology at the University of Cambridge under Richard Gregory. He then taught at the University of Bristol, then at York University in Toronto, Canada. For the last 20 years he has taught at UC San Diego. For more information visit http://psy2.ucsd.edu/~sanstis/Stuart_Anstis/Welcome.html.



János Geier (1950-) mathematician, independent visual researcher. He took his MA in mathematics at Eötvös Loránd University, Budapest, after which he taught mathematics and statistics to students of psychology for 25 years there. He has dealt with visual science from the early 1990s; he visited Julesz Béla's laboratory and ARVO conferences numerous times. For the past 8 years, he has earned his bread from "teaching" the computer to recognize letters, within his private enterprise. His main interest is investigating the regularities of visual illusions, and modelling them mathematically-computationally. He considers mathematical models, which are general in theoretical physics, important in visual science, too.



Mariann Hudák (1983-) took her MA in psychology and English at Eötvös Loránd University, Budapest, where she got involved into János Geier's work on the Hermann grid and other brightness illusions. She investigates the regularities of these "errors" by means of psychophysical experiments, which aim to provide new ideas to develop a unified theoretical model for all known low-level brightness phenomena, including contrast and assimilation illusions. From 2009 on, she has been taking her PhD under Ilona Kovács at the Budapest University of Technology and Economics, investigating developmental issues of vision, adaptation and binocular rivalry, besides continuing the work on lightness-brightness perception.



Increased readiness for adaptation and faster alternation rates under binocular rivalry in children

Mariann Hudak^{1,2}, Patricia Gervan^{1,2,3}, Björn Friedrich⁴, Alexander Pastukhov⁴, Jochen Braun⁴ and Ilona Kovacs^{1,2,3}*

¹ Hungarian Academy of Sciences, Budapest, Hungary

² Research Group of Cognitive Science, Budapest University of Technology and Economics, Budapest, Hungary

³ Department of Cognitive Science, Budapest University of Technology and Economics, Budapest, Hungary

⁴ Cognitive Biology, University of Magdeburg, Magdeburg, Germany

Edited by:

Alexander Maier, Vanderbilt University, USA

Reviewed by:

Sidney R. Lehky, The Salk Institute, USA

Jan Brascamp, Vanderbilt University, USA

*Correspondence:

Ilona Kovacs, Department of Cognitive Science, Budapest University of Technology and Economics, Egry J. u. 1, T 503, Budapest 1111, Hungary.
e-mail: ikovacs@cogsci.bme.hu

Binocular rivalry in childhood has been poorly investigated in the past. Information is scarce with respect to infancy, and there is a complete lack of data on the development of binocular rivalry beyond the first 5–6 years of age. In this study, we are attempting to fill this gap by investigating the developmental trends in binocular rivalry in pre-puberty. We employ a classic behavioral paradigm with orthogonal gratings, and introduce novel statistical measures (after Pastukhov and Braun) to analyze the data. These novel measures provide a sensitive tool to estimate the impact of the history of perceptual dominance on future alternations. We found that the cumulative history of perceptual alternations has an impact on future percepts, and that this impact is significantly stronger and faster in children than in adults. Assessment of the “cumulative history” and its characteristic time-constant helps us to take a look at the adaptive states of the visual system under multi-stable perception, and brings us closer to establishing a possible developmental scenario of binocular rivalry: a greater and faster relative contribution of neural adaptation is found in children, and this increased readiness for adaption seems to be associated with faster alternation rates.

Keywords: multi-stable perception, binocular rivalry, human development, adaptation, cumulative history, dominance time

INTRODUCTION

Binocular vision or stereopsis provides precise depth perception by aligning the two eyes' views. Under the eye-specific stimulation of binocular rivalry, the mature visual system enters into a continuous fluctuation between two or more perceptual states, not yielding stereopsis. While cortical binocularity in humans seems to have a relatively abrupt onset (at around 3.5 months) during ontogeny (Braddick et al., 1980; Petrig et al., 1981), driven by experience-dependent mechanisms (Kovacs et al., 2011), little is known about the onset time of binocular rivalry and its further development. Here we review information with respect to the human development of binocular rivalry, and make an attempt to assess its maturity before puberty in a behavioral experiment. We interpret our data in the wider framework of neural adaptation.

The nature of binocular vision of human infants before the occurrence of binocular 3D perception has been debated. This issue was mainly investigated in preferential looking paradigms, employing stimuli that induce binocularly rivalry in adults. Shimojo et al. (1986) found that infants younger than 3.5 months of age preferred to look at the dichoptic (interocularly orthogonal) pattern. However, at an average age of 3.5 months, a sudden shift of preference occurred from the rivalrous pattern to the fusible stimulus. They interpret this result as a preference for a blended stimulus, resulting in a grid-like pattern, which is more complex than the monocularly projected simple lines. However, from the time by which binocular functions have further developed

(3.5 months of age), the two patterns begin to oscillate, which might be aversive for infants. This would account for the shift in the preference for binocularly fusible stimuli, and would suggest that pre-stereoscopic vision blends those images that are rivalrous for adults. However, these results could not be replicated (Brown and Miracle, 2003). Nor did Brown et al. (1999) find any physiological evidence for binocular rivalry using a visually evoked potential paradigm with 5- to 15-month-old infants. They attribute their result to the immaturity of dichoptic suppression.

Even less data have accumulated so far concerning the development of rivalry following infancy. In a study that aimed to compare binocular interactions of children aged 6–14 years to normal and amblyopic adults, it was found that binocular summation decreased with age in a dichoptic visual acuity task (Vedamurthy et al., 2007). The acuity of the dominant eye did not improve significantly in children in the dichoptic viewing condition compared to the monocular condition. In this respect, the performance of children was similar to that of adults. However, they found a significant negative correlation with age in the improvement of acuity of the non-dominant eye in the dichoptic condition compared to the monocular one, indicating that developmental trends in binocular interactions are present after infancy, until at least pre-puberty.

The development of binocular rivalry was investigated in 5- to 6-year-old children (Kovacs and Eisenberg, 2005). They found that children alternated significantly more quickly than adults. Verbal reports of the subjects also indicated that children perceived a

patchwork of the two images more frequently than adults. On this basis, the conclusion was drawn that the visual system of 5- to 6-year-old children is not sufficiently mature to integrate entire images spatially, thus they experience more piecemeal rivalry than adults. This is in line with their earlier findings in contour integration (Kovacs et al., 1999; Kovacs, 2000) and spatial integration (Káldy and Kovacs, 2003).

Binocular rivalry shares several features with the perception of ambiguous figures, such as the Necker cube. Common features are gamma distribution of the dominance times of each percept, the high inter-subject variability of the frequency of reversals, the significant influence of stimulus properties on reversal rates, or the fact that both can be influenced by the voluntary control of the subject (see Kornmeier and Bach, 2005).

According to the findings reviewed by Leopold and Logothetis (1999), stimulus properties, such as brightness, contrast, and spatial-frequency content can have a significant impact on the balance of dominance and suppression. In addition, high-level properties of the stimuli can also modify dominance periods in multi-stable perception. Such properties include recognizability or semantic content. For instance, if a recognizable figure is inverted, then its perceptual dominance might significantly be altered in both figure/ground stimuli and binocular rivalry.

Voluntary control is another modifying factor of multi-stable perception. The influence of voluntary control of the subject was found to be stronger in the case of ambiguous figures than for binocularly presented rivalrous stimuli (van Ee et al., 2005). Taddei-Ferretti et al. (2008) also point out that the rivalry between the two possible percepts of an ambiguous figure is less automatic than the competition between two different images presented binocularly. An additional common feature of binocular rivalry and ambiguous figures that Taddei-Ferretti et al. (2008) mention is that both are influenced by eye movements (Ellis and Stark, 1978; Sabrin and Kertesz, 1980). Leopold and Logothetis (1999) consider exclusivity, inevitability, and randomness as the three most fundamental common features of multi-stable perception including binocular rivalry and ambiguous figures. Exclusivity means that only one percept is present at one time, while inevitability implies that “perception can never become ‘locked’ onto a single solution” (p. 261); perceptual hypotheses are constantly changing concerning the presented stimuli. These attributes are characteristics of both binocular rivalry and ambiguous figures.

Reese and Ford's (1962) pioneering study intended to investigate developmental aspects of ambiguous figure perception. Nursery-school children were shown a series of six pictures of either animals or human faces. Their task was to name each. After that, they were asked to state an expectancy about the next picture. The result was that when they were shown the Bugelski rat-man ambiguous figure, it was easier for them to provide the “animal” interpretation than the “human face” interpretation, which means that the animal interpretation was easier to prime by the previously shown pictures. This might be considered evidence of stimulus-dependency even at such an early age. However, 3- to 5-year-old children also show significant performance differences even in this short age range. Doherty and Wimmer (2005) found that 3-year-old children cannot even report both interpretations of such

ambiguous images as the duck–rabbit or the man–mouse figures. However, 4-year-old children can easily interpret the ambiguous figures in both ways. Nonetheless, spontaneous reversals occurred only at the age of 5. The conclusion of this study is that understanding that the perception of the same physical image might reverse is not sufficient for spontaneous reversals to occur.

The foregoing review of the literature indicates that binocular rivalry in childhood has been poorly investigated in the past, and the case is similar concerning the broader sense of bistable or multi-stable perception. Some studies focused on changes in binocular rivalry during adulthood. In these studies, it was found that domination times became longer with age. Jalavisto (1964) for instance, investigated binocular oscillations in the age range of 40–93. It was found that the frequency of oscillation decreased with age in a regular manner, and a total lack of change became prevalent in the oldest age classes. In a more recent study, similar results were obtained (Ukai et al., 2003), in which the alternation rates in three age-groups were compared: 20–34, 35–49, and 50–64-year-old subjects were investigated. In line with the results of Jalavisto (1964), they found a prolongation in alternation time as a function of age. Information is still scarce with respect to infancy, and there is a complete lack of data on the development of binocular rivalry beyond the first 5–6 years of life in childhood. In this study, we are attempting to fill this gap by investigating the developmental trends in binocular rivalry in pre-puberty. We employ a classic behavioral paradigm with orthogonal gratings, and introduce novel statistical measures to analyze the data. These novel measures were developed by Pastukhov and Braun (2011), and they provide a sensitive tool to estimate the impact of the history of perceptual dominance on future percept durations. The Pastukhov and Braun (2011) method used here reveals a significant correlation between past perceptual history and future dominance duration, which does not become evident with conventional measures such as sequential correlations of dominance durations (Fox and Herrmann, 1967; Borsellino et al., 1972; Walker, 1975; Lehky, 1995). Assessment of the “cumulative history” and its characteristic time-constant helps us to take a look at the adaptive states of the visual system under multi-stable perception, and brings us closer to establishing a possible developmental scenario for binocular rivalry.

MATERIALS AND METHODS

SUBJECTS

A total of 59 observers participated in the experiment: 9-year-olds ($n = 23$; mean age = 116.4 months; $SD = 4.6$); 12-year-olds ($n = 19$; mean age = 151.4 months; $SD = 4.4$); 21-year-olds ($n = 17$; mean age = 249.1 months; $SD = 27.9$). All subjects had normal or corrected-to-normal vision and were naive to the purpose of the experiment. Approval of the Budapest University of Technology and Economics (Faculty of Economics and Social Sciences) Ethical Board was obtained. Informed consent was obtained from adult participants or from the parent/caregiver of the child. Observers were not paid for their contribution.

APPARATUS

Stimuli were generated in real-time and displayed on a 15" LCD screen, with a spatial resolution of 1366×768 pixels and a refresh

rate of 60 Hz. The viewing distance was 60 cm, so that each pixel subtended approximately 0.024° . Anaglyph glasses (red/green) were used for the dichoptic presentation. Responses were obtained by means of a joystick, whose tilt was recorded by a MATLAB program controlling the experiment.

STIMULI

The binocular rivalry stimulus consisted of two gratings presented dichoptically: radius, 3° ; spatial frequency 0.6 cycles/degree; contrast 50%. One grating was tilted leftward by 45° and the other rightward by 45° . To minimize inter-block effects, tilt for left and right eye was exchanged in every block, and grating-phase was changed by 180° in every second block (Figure 1A).

PROCEDURE

Data were collected in a normally lit, quiet room. Initially, subjects were provided anaglyph glasses and invited to view the computer screen with the rivalrous gratings. When asked about their percept, all subjects reported alternating percepts. After this introduction to the stimulus, observers reported their perceptual state continuously using a joystick. The joystick allowed them to report three different percepts (leftward tilt, rightward tilt, and mixed), and in the case of dominant gratings with a particular tilt, the degree of dominance was indicated by the degree of movement. Dominant gratings were indicated by tilting the joystick in the corresponding direction, while subjects were asked to keep the joystick at the center in the case of a mixed percept. The experimental program recorded the joystick tilt at 50 Hz sampling frequency. The experiment comprised five blocks; each block lasted 5 min. Each block

was followed by a 1-min interval, during which subjects were asked to rest (Figure 1B).

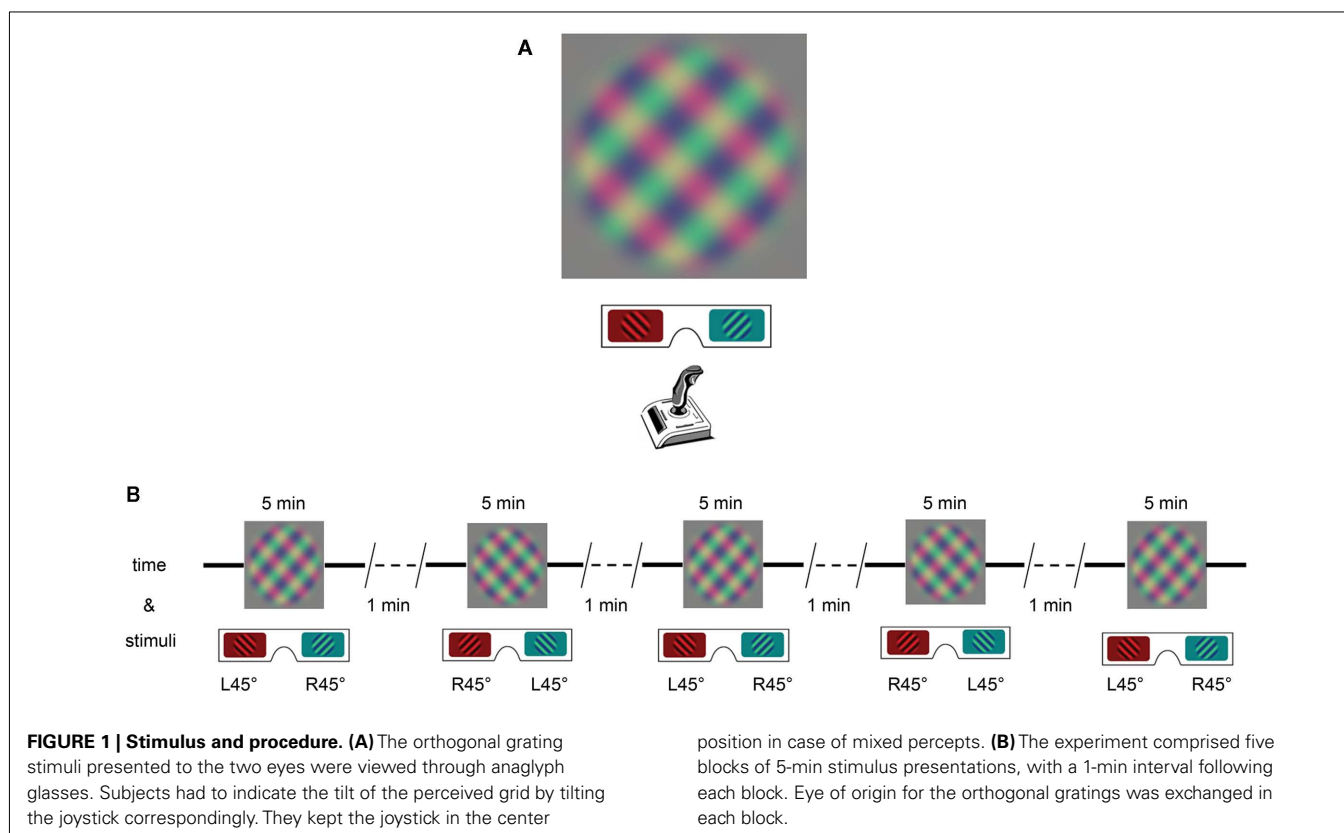
STATISTICAL ANALYSIS

In order to extract perceptual dominance phases from sampled continuous responses, inputs were discretized into left and right percepts using 75% threshold of maximal joystick tilt (i.e., a percept was labeled as left if joystick was over -75% and it was labeled as right if it was over $+75\%$ of horizontal tilt). Mean dominance time (T_{dom}) was computed from the sequence of discrete dominance periods T_i .

As a measure of history dependence for multi-stable displays we have used a coefficient of correlation with cumulative history c_H (Pastukhov and Braun, 2011), which was computed as follows. Let $S_x(t)$ be a record of perceptual experience x as a function of time t , defined as unity while percept x dominates, 0.5 during a mixed or patchy percept, and zero when percept x is suppressed. The cumulative history $H_x(t)$ computed using a leaky integrator (Tuckwell, 2006) is then given by

$$H_x(t) \approx \frac{1}{\tau_H} \int_0^t S_x(t') \cdot e^{-\frac{(t-t')}{\tau_H}} dt' \quad (1)$$

where $x \in \{\text{red/green}\}$ denotes a uniform percept and τ_H is a time-constant to be determined empirically. This assumes that the contribution of prior experience decays exponentially, multiple contributions of same percept combine additively, and there is no contribution from competing percept (see Figure 2 for an



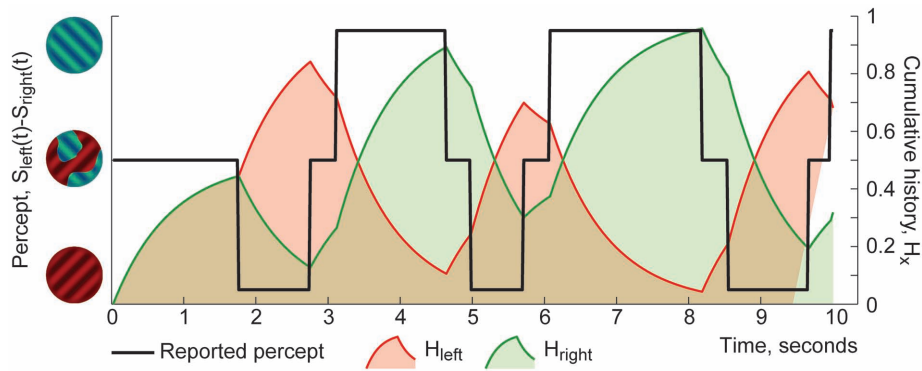


FIGURE 2 | Example of cumulative history traces for series of dominance phases of visual appearances (9 years old). Black trace indicates reported visual appearance (“green/left eye,” “red/right eye,” or “patchy”). Color traces

illustrate hypothetical cumulative histories (correspondingly, green for “green/left eye” percepts and red for “red/right eye”), computed with $\tau_H = 0.5 \cdot T_{\text{dom}}$.

illustration on cumulative history computed from a sequence of perceptual dominance phases).

After computing the cumulative histories H_{left} and H_{right} for two alternative percepts from a sequence of dominance periods up to time t , we computed linear correlation coefficients with the immediately following dominance period T_i ($H_{\text{left}} \times T^{\text{left}}$, $H_{\text{left}} \times T^{\text{right}}$, $H_{\text{right}} \times T^{\text{left}}$, and $H_{\text{right}} \times T^{\text{right}}$). Specifically, we computed linear correlations between logarithm of its normalized duration and cumulative history for the same and opposite percept, e.g., when left eye is dominant, $S_{\text{left}}(t) = 1$; $c_H^{\text{same}} = r(\ln(T_i/T_{\text{dom}}), H_{\text{left}})$ and $c_H^{\text{diff}} = r(\ln(T_i/T_{\text{dom}}), H_{\text{right}})$. Note that cumulative histories of two competing percepts approach unity ($H_{\text{left}} + H_{\text{right}} \approx 1$) only in the absence of “patchy” percepts, we have used both to compute an average absolute correlation:

$$c_H = \frac{|c_H^{\text{diff}}| + |c_H^{\text{same}}|}{2} \quad (2)$$

To determine the characteristic time-constant (τ_H), we computed average absolute correlations for values of τ ranging from 0.01 to 60 s. The maximal correlation obtained was taken as the value of c_H , and the τ yielding this maximal correlation was taken as the value of τ_H . In sum, c_H stands for the measure of adaptation taking into account the entire stimulus presentation up to time t , while τ_H indicates how fast the adaptation is built up. Note that for small τ_H cumulative history assumes intermediate values only after one or more short dominance periods. The higher the τ_H value is, the slower the subject adapts to each percept; while a higher c_H value indicates a larger extent of adaptation.

After computing the above-mentioned variables, outliers were excluded from each group. The criterion for exclusion was identical for each group. The SD of each subject was computed for each variable across the blocks. The mean SD of each group was also computed from the individual SDs. The individual SDs here indicate the reliability of the perceptual reports of the particular subject: the responses of subjects who show a high SD among a given observable, can be considered as inconsistent, which might be due to either lack of attention or fatigue. Therefore, subjects, whose SD along any of the investigated variables approached the

4 SD distance from the average SD of the group, were excluded from the analysis. This criterion was re-checked following each exclusion. A total of eight subjects were excluded.

After removing extreme outliers, independent sample t -tests were conducted between all groups for all the five variables, and correlations were computed between age-groups and observables.

RESULTS

The t -test yielded a marginally significant difference in average dominance times (T_{dom}) between 9-year-olds and adults (for means and t -values see **Figure 3A**). Each percept tends to persist for a longer period in adults than in 9-year-old children (**Figure 3B**). There was no significant difference between 9- and 12-year-olds, and between 12-year-olds and adults. However, the developmental trend in **Figure 3B** seems to be clear: dominance times increase with age. The same tendency was found earlier in 5- to 6-year-olds as compared with adults (Kovacs and Eisenberg, 2005).

The c_H value is significantly higher in 9-year-olds than adults, i.e., the length of the subsequent dominance period of a particular percept shows a higher correlation with the previous dominance time ratio of the other percept in 9-year-olds than in adults (**Figures 3A,C**). This means that 9-year-olds and adults show a significant difference in their extent of adaptation to each percept. There was no significant difference between 9- and 12-year-olds, and between 12-year-olds and adults.

The time-constant of the build-up of the adaptation (τ_H) produced significant differences both between 9-year-olds and adults as well as 12-year-olds and adults (**Figures 3A,D**). There was no significant difference between 9- and 12-year-olds. The τ_H value of adults is significantly higher than that of 9- and 12-year-old children, showing that the build-up of adaptation is slower in adults.

These differences were also indicated by correlations between age-groups and the observables (see **Table 1**).

DISCUSSION

Our results indicate that 9-year-old children are not exactly adult-like in terms of alternation rate which is a conventional measure

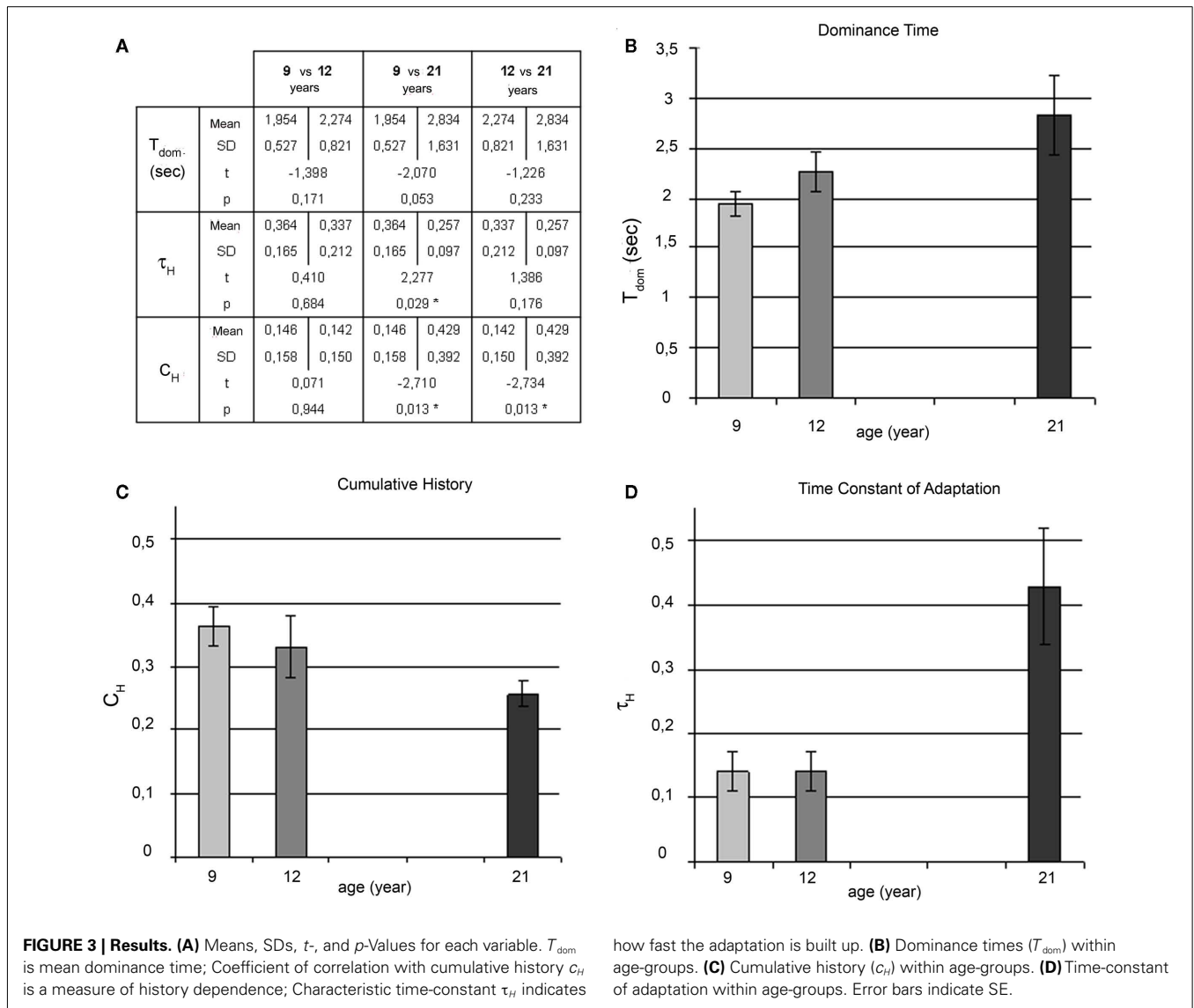


Table 1 | Correlations between age-groups and the investigated observables.

Correlations	T_{dom}	τ_H	c_H
AGE-GROUP			
Pearson correlation	0.329	0.457	-0.273
Sig. (two-tailed)	0.018	0.001	0.053
N	51	51	51

of binocular rivalry. Children seem to have shorter average dominance times than adults. This is consistent with an earlier study by Kovacs and Eisenberg (2005) that showed that 5- to 6-year-old children are alternating very quickly. Our findings are also in line with the results of Jalavisto (1964) and Ukai et al. (2003), who found that alternation rate decreased with age in adulthood. Although the developmental curve is not complete yet, and there are several further age-groups to be tested, it can be concluded

that the development of binocular rivalry, as measured by its most salient feature, is not complete by the end of the first decade in life. That draws a conspicuously slow developmental trajectory which is not yet supported by explanatory anatomical or physiological data.

In addition, we have applied two novel measures of the effect of neural adaptation, recently suggested by Pastukhov and Braun (2011). The first such measure (c_H) was the correlation between dominance times and accumulated prior dominance history and the second (τ_H) was the effective time-constant of this accumulation. To appreciate the import (and limitations) of these measures, one has to consider that perceptual reversals may have several contributing causes (Wolfe, 1984; Nawrot and Blake, 1989; Peter-sik, 2002; van Ee, 2009; Alais et al., 2010; Kang and Blake, 2010; Pastukhov and Braun, 2011).

Firstly, neural adaptation of the dominant representation is thought to progressively destabilize the dominant percept by both the adaptation of the dominant percept, and the recovery from

adaptation of the suppressed percept. Secondly, spontaneous activity fluctuations in perceptual representations as well as external transients such as eye movements or eye blinks curtail the duration of dominance periods. Thirdly, internal transients such as shifts in attention or in other volitional processes may trigger reversals. The measure c_H is a correlative measure and estimates only the relative contribution of neural adaptation to reversal timing, that is, relative to all other possible factors. We emphasize that it should not be taken to estimate the absolute strength of neural adaptation.

Specifically, our finding that dominance durations are more correlated with prior history in children than in adults, implies simply a greater relative contribution of neural adaptation. This could either be because adaptation is more pronounced, or because other factors (e.g., neural noise, attention shifts) are less pronounced in children. Our observations that shorter dominance phase duration in children are accompanied by shorter time-constants of reconstructed neural adaptation are consistent with predictions of models of multi-stable perception (Wilson, 2007; Shpiro et al., 2009), where mean dominance duration is directly

proportional to the adaptation time-constant. A related possibility is that, due to the generally shorter dominance times of children, stochastic factors such as neural noise or attention shifts simply have fewer opportunities for triggering a perceptual reversal. Voluntary control over binocular rivalry is limited (Chong et al., 2005; Hancock and Andrews, 2007) and in fact less than for other bistable displays (Meng and Tong, 2004). Rivalrous displays undergo perceptual reversals even when attention is diverted (Lee et al., 2007). Nevertheless, we cannot rule out the possibility that our findings reflect differences in attentional characteristics between children and adults.

Although our study provides the first articulate view on the human developmental trajectory of binocular rivalry, more age-groups, and the underlying factors behind the protracted developmental curve need to be further investigated.

ACKNOWLEDGMENTS

We thank János Geier and Anett Szabó for helpful discussions on the statistics. This work was supported by TÁMOP – 4.2.2.B-10/1-2010-0009.

REFERENCES

- Alais, D., Cass, J., O'Shea, R. P., and Blake, R. (2010). Visual sensitivity underlying changes in visual consciousness. *Curr. Biol.* 20, 1362–1367.
- Borsellino, A., De Marco, A., Allazetta, A., Rinesi, S., and Bartolini, B. (1972). Reversal time distribution in the perception of visual ambiguous stimuli. *Kybernetik* 10, 139–144.
- Braddick, O., Atkinson, J., Julesz, B., Kropfl, W., Bodis-Wollner, I., and Raab, E. (1980). Cortical binocularity in infants. *Nature* 288, 363–365.
- Brown, A. M., and Miracle, J. A. (2003). Early binocular vision in human infants: limitations. *Vision Res.* 43, 1563–1574.
- Brown, R. J., Candy, T. R., and Norcia, A. M. (1999). Development of rivalry and dichoptic masking in human infants. *Invest. Ophthalmol. Vis. Sci.* 40, 3324–3333.
- Chong, S. C., Tadin, D., and Blake, R. (2005). Endogenous attention prolongs dominance durations in binocular rivalry. *J. Vis.* 5, 1004–1012.
- Doherty, M. J., and Wimmer, M. C. (2005). Children's understanding of ambiguous figures: which cognitive developments are necessary to experience reversal? *Cogn. Dev.* 20, 407–421.
- Ellis, S. R., and Stark, L. (1978). Eye movements during the viewing of Necker cubes. *Perception* 7, 575–581.
- Fox, R., and Herrmann, J. (1967). Stochastic properties of binocular rivalry alternations. *Percept. Psychophys.* 2, 432–446.
- Hancock, S., and Andrews, T. J. (2007). The role of voluntary and involuntary attention in selecting perceptual dominance during binocular rivalry. *Perception* 36, 288–298.
- Jalavisto, E. (1964). The phenomenon of retinal rivalry in the aged. *Gerontologia* 9, 1–8.
- Káldy, Z., and Kovacs, I. (2003). Visual context integration is not fully developed in 4-year-old children. *Perception* 32, 657–666.
- Kang, M.-S., and Blake, R. (2010). What causes alternations in dominance during binocular rivalry? *Atten. Percept. Psychophys.* 72, 179–186.
- Kornmeier, J., and Bach, M. (2005). The Necker cube – an ambiguous figure disambiguated in early visual processing. *Vision Res.* 45, 955–960.
- Kovacs, E., Mikó-Baráth, K., Markó, K., Hollódy, B., and Török, G. J. (2011). Ready to experience: binocular function is turned on earlier in preterm infants. *Society for Neuroscience Annual Meeting*, Washington.
- Kovacs, I. (2000). Human development of perceptual organization. *Vision Res.* 40, 1301–1310.
- Kovacs, I., and Eisenberg, M. (2005). "Human development of binocular rivalry," in *Binocular Rivalry*, eds D. Alais and R. Blake (Cambridge: MIT Press), 101–116.
- Kovacs, I., Kozma, P., Fehér, Á., and Benedek, G. (1999). Late maturation of visual spatial integration in humans. *Proc. Natl. Acad. Sci. U.S.A.* 96, 12204–12209.
- Lee, S.-H., Blake, R., and Heeger, D. J. (2007). Hierarchy of cortical responses underlying binocular rivalry. *Nat. Neurosci.* 10, 1048–1054.
- Lehky, S. R. (1995). Binocular rivalry is not chaotic. *Proc. Biol. Sci.* 259, 71–76.
- Leopold, D. A., and Logothetis, N. K. (1999). Multistable phenomena: changing views in perception. *Trends Cogn. Sci. (Regul. Ed.)* 3, 254–264.
- Meng, M., and Tong, F. (2004). Can attention selectively bias bistable perception? Differences between binocular rivalry and ambiguous figures. *J. Vis.* 4, 539–551.
- Nawrot, M., and Blake, R. (1989). Neural integration of information specifying structure from stereopsis and motion. *Science* 244, 716–718.
- Pastukhov, A., and Braun, J. (2011). Cumulative history quantifies the role of neural adaptation in multistable perception. *J. Vis.* 11, 12.
- Petersik, J. T. (2002). Buildup and decay of a three-dimensional rotational aftereffect obtained with a three dimensional figure. *Perception* 31, 825–836.
- Petrig, B., Julesz, B., Kropfl, W., Baumgartner, G., and Anliker, M. (1981). Development of stereopsis and cortical binocularity in human infants: electro-physiological evidence. *Science* 213, 1402–1404.
- Reese, H. W., and Ford, L. R. Jr. (1962). Expectancy and perception of an ambiguous figure in preschool children. *J. Verbal Learn. Verbal Behav.* 1, 188–191.
- Sabrin, H. W., and Kertesz, A. E. (1980). Microsaccadic eye movements and binocular rivalry. *Percept. Psychophys.* 28, 150–154.
- Shimojo, S., Bauer, J. Jr., O'Connell, K. M., and Held, R. (1986). Pre-stereoptic binocular vision in infants. *Vis. Res.* 26, 501–510.
- Shpiro, A., Moreno-Bote, R., Rubin, N., and Rinzel, J. (2009). Balance between noise and adaptation in competition models of perceptual bistability. *J. Comput. Neurosci.* 27, 37–54.
- Taddei-Ferretti, C., Radilovac, J., Musioa, C., Santilloa, S., Cibellib, E., Cotugnoa, A., and Radilc, T. (2008). The effects of pattern shape, subliminal stimulation, and voluntary control on multistable visual perception. *Brain Res.* 1225, 163–170.
- Tuckwell, H. C. (2006). *Introduction to theoretical neurobiology: linear cable theory and dendritic structure*. Cambridge: Cambridge University Press, 1.
- Ukai, K., Ando, H., and Kuze, J. (2003). Binocular rivalry alternation rate declines with age. *Percept. Mot. Skills* 97, 393–397.
- van Ee, R. (2009). Stochastic variations in sensory awareness are driven by noisy neuronal adaptation: evidence from serial correlations in perceptual bistability. *J. Opt. Soc. Am. A. Opt. Image Sci. Vis.* 26, 2612–2622.
- van Ee, R., van Dam, L. C. J., and Brouwer, G. J. (2005). Voluntary control and the dynamics of perceptual bi-stability. *Vision Res.* 45, 41–55.

- Vedamurthy, I., Suttle, C. M., Alexander, J., and Asper, R. J. (2007). Interocular interactions during acuity measurement in children and adults, and in adults with amblyopia. *Vision Res.* 47, 179–188.
- Walker, P. (1975). Stochastic properties of binocular-rivalry alternations. *Percept. Psychophys.* 18, 467–473.
- Wilson, H. R. (2007). Minimal physiological conditions for binocular rivalry and rivalry memory. *Vision Res.* 47, 2741–2750.
- Wolfe, J. M. (1984). Reversing ocular dominance and suppression in a single flash. *Vision Res.* 24, 471–488.
- Conflict of Interest Statement:** The authors declare that the research was conducted in the absence of any commercial or financial relationships that could be construed as a potential conflict of interest.
- Received: 06 July 2011; accepted: 17 October 2011; published online: 04 November 2011.*
- Citation: Hudak M, Gervan P, Friedrich B, Pastukhov A, Braun J and Kovacs I (2011) Increased readiness for adaptation and faster alternation rates under binocular rivalry in children. Front. Hum. Neurosci. 5:128. doi: 10.3389/fnhum.2011.00128*
- Copyright © 2011 Hudak, Gervan, Friedrich, Pastukhov, Braun and Kovacs. This is an open-access article subject to a non-exclusive license between the authors and Frontiers Media SA, which permits use, distribution and reproduction in other forums, provided the original authors and source are credited and other Frontiers conditions are complied with.*